10-16-2009

Sensitivity analysis and calibration of the alligator cracking model in the mechanistic-empirical pavement design guide using regional data

Vivek Jha
Rowan University

SENSITIVITY ANALYSIS AND CALIBRATION OF THE ALLIGATOR CRACKING MODEL IN THE MECHANISTIC-EMPIRICAL PAVEMENT DESIGN GUIDE USING REGIONAL DATA

by
Vivek Jha

A Thesis

Submitted in partial fulfillment of the requirements of the
Master of Science in Engineering Degree
Of
The Graduate School
at
Rowan University
October 16, 2009

Thesis Chair: Yusuf Mehta, Ph.D., P.E.

Dedicated to:
Di
Maa
Dad
Dr. Yusuf Mehta
Prashant Shirodkar
All my friends who helped me in every way possible
And My Lord

ABSTRACT

Vivek Jha

Sensitivity Analysis and Calibration of the Alligator Cracking Model in the Mechanistic-Empirical Pavement Design Guide Using Regional Data

2008/09

Yusuf Mehta, Ph.D., P.E.
Master of Science in Civil Engineering

The models used in the mechanistic-empirical pavement design guide (M-EPDG) were calibrated using the data from all across the United States. The alligator cracking model uses traffic, material and structural data along with local and global calibration factors to calculate the number of axles to failure and the damage index. Both of which are further used to calculate the fatigue cracking in the pavement with the help of regression coefficients and calibration constants. However, as these coefficients and constants were developed using the national database, the model might not predict the fatigue behavior of the pavement accurately for a particular state. This problem arises from the fact that there were limited sections of LTPP in every state and the model was calibrated on the average value using the national database.

The verification of M-EPDG with level 2 and 3 inputs for the State of New Jersey did not yield satisfactory results with respect to alligator cracking for 25 sections analyzed in one of the studies. The reasons for the difference between the predicted and measured results might be due to inaccurate inputs or error in the calibration factors or regression coefficients in the prediction models. As the accuracy of the input data was confirmed by using multiple resources, the confidence level with respect to the input data was very high. Thus the error might be due to error in the calibration factors or regression coefficients in the prediction model that was calculated based on the national average.

The main focus of this study is to use the twenty five sections evaluated in the above mentioned study and four more NJDOT sections to understand the physical impact of these regression constants on pavement performance and their variability with different pavement properties and parameters. The final aim of this study is to calibrate and validate the alligator cracking model for the state of New Jersey using these twenty nine sections spread across the State.

ACKNOWLEGMENTS

Mr. Robert Blight
Dr. Yusuf Mehta
Dr. William Riddell
Dr. Beena Sukumaran
Nusrat Siraj
Keicha Murial
Alan Norton
Christopher Tomlinson

TABLE OF CONTENTS

List of Figures

List of Tables

Chapter 1 Introduction

1.1 Background

The principal design procedures adopted by all the state agencies across the United States are based primarily on the 1993 American Association of State Highway and Transportation Officials (AASHTO) Guide for Design of Pavement Structures. These empirical design procedures were based on the regression equation developed during the extensive road test carried out in the late 1950's and early 1960's in Ottawa, Illinois (Huang, 2004). The 1993 AASHTO guide was updated first in 1986 and then in 1993. Even with the revisions, the empirical design procedure based on the 1993 AASHTO guide had served limitations with respect to the range of climate, traffic, and material it encompassed. The National Cooperative Highway Research Program (NCHRP) pointed out these shortcomings (NCHRP, 2004) and decided to move from the empirical to the mechanistic-empirical (M-E) design procedure. The first step toward this move was the implementation of NCHRP 1-37A Mechanistic Empirical Pavement Design Guide (M-EPDG).

The mechanistic aspect of M-EPDG arises from the fact that it predicts pavement performance based on the stresses and strains calculated from the material properties measured in the laboratory. The empirical part of the M-EPDG consists of using the prediction models that are based on the statistical relationship between the measured distress and the mechanical responses. The statistical relationships developed were based on the national database. The M-EPDG requires the users to input the materials, traffic, environment, and pavement structure data. The mechanical responses are then calculated using the Design Guide software and the pavement performance is predicted using the damage models that correlate mechanical response to pavement performance. The calculated design life is determined by comparing the predicted performance to the

predefined failure criteria. The models that are used in the M-EPDG to predict the pavement performance were calibrated using the Long Term Pavement Performance (LTPP) database collected from all over the United States. Thus, to implement the M-EPDG in any state successfully, the prediction models must be verified and if required, re-calibrated so that accurate predictions can be obtained based on local database. The data in local databases might differ from the national database, which was used to develop the failure models. The local and national databases differ with respect to material properties and amount of failure observed (statistical relationships were developed based on the average amount of failure observed).

The verification of M-EPDG using level 2 and level 3 data for the State of New Jersey was done by Nusrat Siraj at Rowan University as part of her Master of Science (M.S) thesis (Siraj, 2008). An effort was made to verify all the distress such as rutting, thermal cracking, alligator cracking, longitudinal cracking, and international roughness index (IRI) for the state by comparing the predicted performance to the measured field distresses. One of the important findings that came out of the study was that alligator cracking could not be verified statistically for the State of New Jersey. Since, the measured and the predicted value of alligator cracking were far below the design limit; it was not looked into much detail with respect to finding the cause of difference in the two values. However, there were few sections (in all 7 sections) in the study that showed a large difference between the predicted and measured alligator cracking.

1.2 Problem Statement

The models used in the M-EPDG were calibrated using the data from all across the United States (NCHRP, 2007). The alligator cracking model uses traffic, material and structural data along with local and global calibration factors to calculate the number of axles to failure and the damage index. Both of which are further used to calculate the fatigue cracking in the pavement with the help of transfer functions. However, as the constants were developed using the national database, the model might not predict the fatigue behavior of the pavement accurately for a particular state. This problem arises

from the fact that there were limited sections of LTPP in every state and the model was calibrated on the average value using the national database.

The verification of M-EPDG with level 2 and 3 inputs for the State of New Jersey did not yield satisfactory results with respect to alligator cracking. The reasons for the difference between the predicted and measured results might be due to inaccurate inputs or error in the transfer function in the prediction models. As the accuracy of the input data was confirmed by using multiple resources, the confidence level with respect to the input data was very high. Thus the error might be due to error in the transfer function in the prediction model that was calculated based on the national average.

The accuracy of the predicted performance using any prediction models depends on the inputs and the coefficients established that correlates the predicted performance to the measured field performance. The alligator cracking prediction model as stated earlier, uses the traffic data, material data, structural data, critical tensile strain, local and global calibration constants and coefficients to predict the percent of alligator cracking in the pavement. The accuracy of output with respect to input for a specific project depends on the accuracy of the data collected, which can be improved. The calibration factors and the coefficients however were determined from the national database based on statistical relationship between the measured distress and the predicted performance. The form of the prediction model may be predicting the cracking performance accurately. However as the coefficients used in the prediction model were developed based on national database, there arises a need to understand the impact of these coefficients on the predicted distress. This information is critical in obtaining realistic values while calibrating performance data using regional database.

1.3 Hypothesis

I. Simulating the M-EPDG model by means of a spreadsheet can be used to study the effect of individual parameter on alligator cracking performance.

II. The alligator cracking model can be calibrated by using state specific data.

1.4 Objectives

The objectives of the study are

For hypothesis I and II:

1. Understanding the effect of the regression coefficients present in the model on the predicted performance.
2. Create a Microsoft Excel sheet to understand the effect of each parameter and the overall working of the Design Guide.
3. Compare the alligator cracking prediction from M-EPDG with the measured field data for the State of New Jersey.
4. Calibrate the alligator cracking model by changing the coefficients by using state specific data to match measured field performance.
5. Validate the changes made in the model using sections that were not used in the calibration process.

1.5 Research Approach

To meet the objectives outlined above, the research approach was divided into the following five tasks.

1.5.1 Task I: Literature Review

Review past studies related to the prediction models for alligator cracking performance. Also review past studies that deal with formation and calibration of alligator cracking model in the M-EPDG by other researchers to find which parameters were altered to minimize the difference between the predicted performances to the measured field performance.

1.5.2 Task II: Understand impact of constants and coefficients used

Understand the physical significance of the calibration constants and regression coefficients with respect to its impact on pavement properties, thickness and the predicted distress.

1.5.3 *Task III: Calibration of alligator cracking model*

Calibrate the alligator cracking model by changing the constants so that the difference between the predicted and the measured cracking performance are as close as possible.

1.5.4 *Task IV: Validation of the new values in the model*

Validate the new model, with the help of data sets that were not used during the calibration process. Figure 1.1 schematically depicts the research approach adopted during this study. The figure illustrates that the first step in this study was to review literature related to fatigue cracking and models that have been used to predict it. The next section of this study deals with in-depth literature review with regard to fatigue cracking.

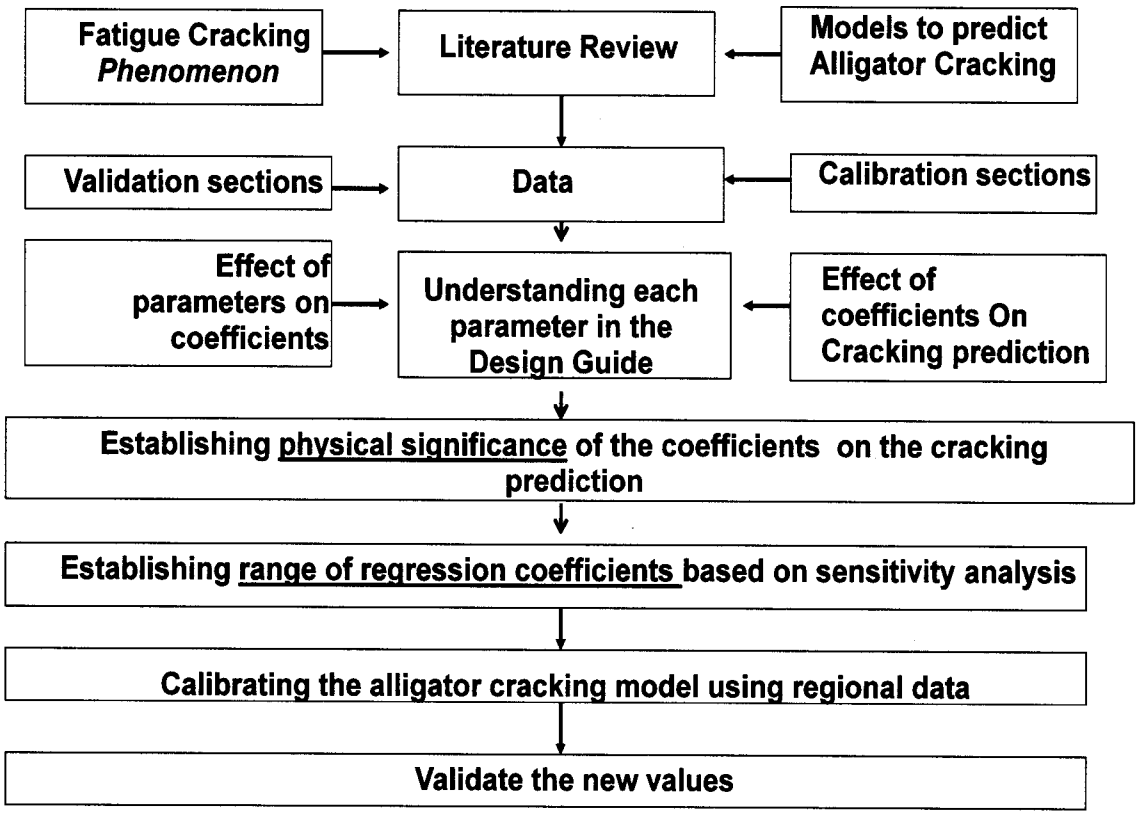

Figure 1.1 Flowchart showing the research approach adopted in this study

1.6 Summary

This chapter presented a brief introduction of the Design Guide and the reason for this study in the form of the problem statement. The hypothesis of this study was also presented in this chapter. Along with the hypothesis the objectives for each hypothesis was presented. Finally the research approach adopted for this study was presented. The approach adopted was based on the objectives outlined. The next chapter presents an in depth literature review that was conducted to allow better understanding of the Design Guide in general and alligator cracking prediction in particular.

Chapter 2 Literature Review

2.1 Background of fatigue cracking

Fatigue cracking in a pavement takes place due to the bending of the pavement under the load which leads to the development of tensile stresses at the bottom of the asphalt layer which leads to crack formation as shown in Figure 2.1. When the load is applied to the pavement the strain at the bottom of the asphalt layer has two components, elastic ($\varepsilon_{elastic}$) and residual ($\varepsilon_{residual}$) strains. The elastic strain is the one that come backs to its original position after the load is removed. However the residual strain, which is the smaller of the two components does not come back and starts accumulating. Even though the elastic strain comes back to its original position, due to the accumulation of the residual strain the peak of total strain ($\varepsilon_{residual} + \varepsilon_{elastic}$) keeps on increasing with every new load repetition. When the peak total strain for any load repetition exceeds the strain at failure ($\varepsilon_{failure}$) crack formation takes place.

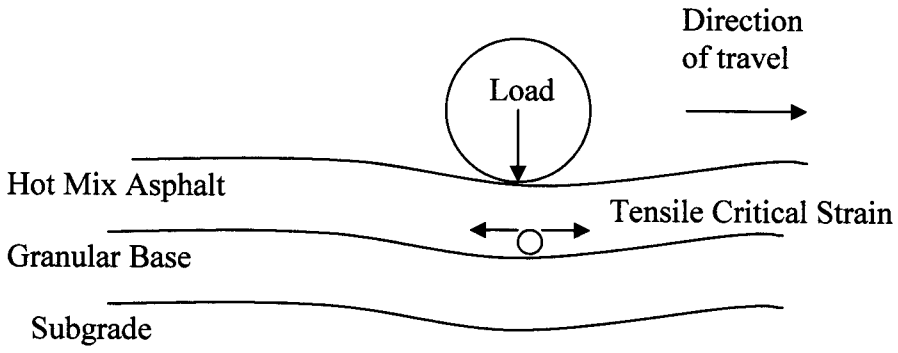

Figure 2.1 Location of tensile strain in the pavement structure

2.1.1 Types of fatigue cracking

Fatigue cracking was previously believed to originate only from the bottom of asphalt layer and propagate towards the top as described above and is known as alligator

cracking. However, recent studies have shown that critical stress/ strain may develop at the pavement surface and crack propagation towards the bottom of the asphalt layer could take place (NCHRP, 2004). This type of fatigue cracking is known as longitudinal cracking. Few of the possible factors which could lead to longitudinal cracking are listed below.

1. Extremely high tire pressure cause high surface horizontal (perpendicular to the direction of traffic) tensile stresses.
2. Aging of asphalt binder also results in high thermal stresses in the HMA, and
3. Lower stiffness of the surface layer results in high tensile stresses on application of load.

This study deals only with alligator cracking. Hence further literature review only deals with prediction models related to alligator cracking. Alligator cracking as described above is affected by many parameters. The effects of each of those parameters are described in the next section in detail.

One of the other factors that are important to be considered while evaluating alligator cracking is to ensure that it is not confused with block cracking. Block cracking is not dependent upon load coming on the pavement as in the case of alligator cracking. It is caused due to shrinkage of asphalt pavement due to temperature cycles and is top down cracking. Block cracking is series of large rectangular crack on the surface pavement and is many times confused with alligator cracking. Hence the field data should be analyzed carefully to distinguish between these two types of cracking.

2.2 Factors affecting alligator cracking

Alligator cracking, as described in the above sections is caused due to the increase in the residual strain which ultimately exceeds the total strain on failure. The incremental increase in strain which leads to the crack formation can be seen in Figure 2.2. It can also be observed that elastic component of the strain remains the same for every load application (if the load is constant). Figure 2.2 also shows the mechanism of crack formation with respect to time. The principle of incremental increase in the residual strain was used in the Asphalt Institute (AI) method to develop fatigue cracking models

which is discussed later in detail. Cracking can also be caused if the load coming on the pavement on its first repetition induces strain at failure. However this is not commonly observed as the pavements are designed with sufficient thickness and stiffness.

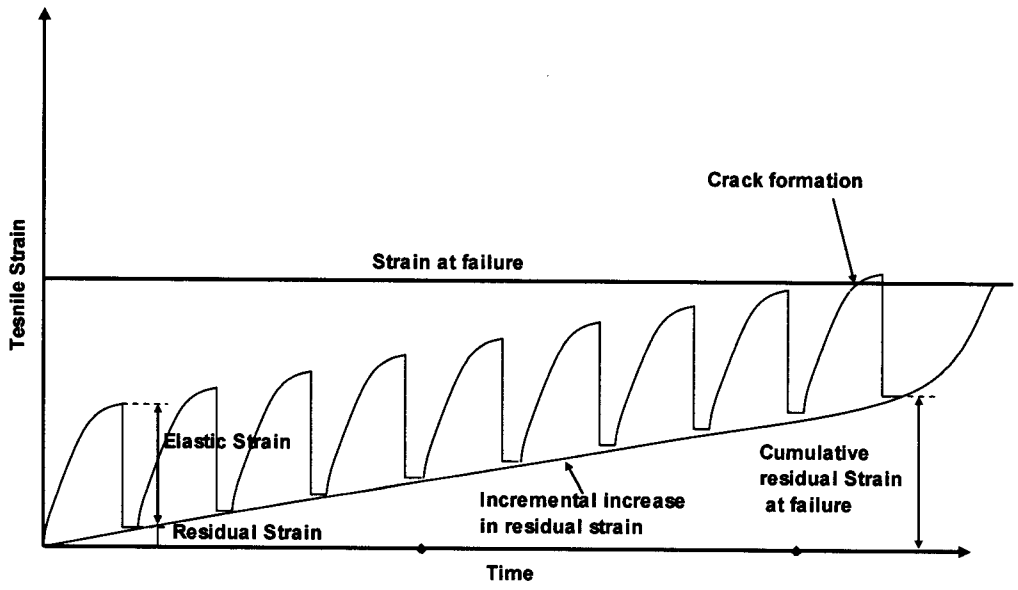

Figure 2.2 A Schematic of Incremental increase in residual strain leading to failure

From Figure 2.2 it can be observed that to restrict fatigue cracking the total strain in the asphalt layer should be as low as possible. The factors which affect the increase in the strain are described below.

2.2.1 *Stiffness of the mix*

Alligator cracking takes place between a certain ranges of stiffness value of the mix. If the stiffness of the mix is too high approaching cement concrete then alligator cracking is not observed. If the stiffness of the mix is too low, then load is taken by the stiffness of the layer below. However for intermediate stiffness values, the lower the stiffness value the lower is fatigue cracking. This is due to the fact that as the mix is not very stiff it easily dissipates the energy, hence the residual strain is very small, which prevents early cracking in the pavement. However the increase or decrease of stiffness and its result on fatigue cracking also depends on the thickness of the HMA layer

provided (Santucci, 1998). For thick HMA layer (greater than 4 inches) increase in stiffness reduces fatigue cracking. While the opposite is true for thinner HMA layer (less than 4 inches), decrease in stiffness decreases the strain which in turn decreases cracking.

2.2.2 *Strain*

Figure 2.2 clearly illustrates that increase in residual strain leads to fatigue cracking. Fatigue cracking can also take place in the pavement if the load coming on the pavement is so high that on its first application induces strain at failure. Thus strain becomes one of the most important parameter on which fatigue cracking depends. Jha, et al. 2009, found that if the critical tensile strain was kept below 90 microstrains for certain conditions (reference temperature in the study was 46°F) then the cracking in the pavement can be controlled. Thus by limiting the strain induced in the pavement cracking can be minimized.

2.2.3 *Thickness*

Thicker the HMA layer, lower is the alligator cracking. As the point of reference moves away from the load, cracking in the pavement is considerably reduced. Alligator cracking is mostly observed when pavement thickness ranges from 3-5 inches (NCHRP, 2004). Below 3 inches the pavement thickness is too small hence most of the load is taken by the layers below. This results in minimum fatigue cracking beneath the surface layer. If the thickness is more than 5 inches, due to this high thickness the cracking observed beneath the surface is comparatively low.

2.2.4 *Load*

Higher the load, higher is the alligator cracking in the pavement. As the load intensity increases, the strain induced in the pavement increase which causes cracking in the pavement. One of the study (Wang, et al., 2008) found that by increasing axle load by 10% the fatigue damage increased by18 % and 37% for the two section studied having HMA thickness 16.5 and 5.5 inches respectively.

2.2.5 *Binder content*

With increase in binder content, the cracking reduces. As the binder content increases the flexibility of the pavement increases and it is able to dissipate energy better thus reducing cracking. One of the studies (Walubita, et al., 2005) found that by increasing the binder content from 4.6 % binder content by weight of the aggregate to 5.6% saw considerable increase in fatigue life. The number of repetition to failure for mix with 4.6% binder content was 3.11 million ESAL's as compared to 8.4 million ESAL's for mix with 5.6 % binder content. Other study (WSDOT, 2009) states that increase in binder content lubricates aggregate better making their rearrangement under load better. Thus decreasing cracking under the application of load.

2.2.6 *Air voids*

Fatigue performance of pavement is significantly affected by air voids present in the mix. It has been found that (Santucci, 1998) decreasing air voids from 10% to 5 % increases the fatigue resistance by 10 times. Air voids act as pseudo cracks which on application of load result in micro-crack and ultimately into cracks.

2.2.7 *Binder aging*

Binder aging implies the loss of organic component in the binder due to oxidation. As the binder loses its organic component it becomes stiffer, which leads to increase in fatigue cracking. A study conducted at Texas A & M University (Walubita, et al., 2005) found that mixture stiffens significantly in response to binder oxidative aging. The researcher also found that mixture fatigue life declines significantly when the binder stiffens due to oxidative aging. This decline in fatigue life had dramatic effect on the pavement life according to the study.

The seven factors listed are the most important factors that affect the cracking behavior of the pavement directly. Their sensitivity effects are described later in detail. Accurate prediction of fatigue cracking can be done only when all of the above factors are captured effectively in the prediction model used. The different models that have

been used to predict fatigue cracking are discussed in detail in the next section with respect to what factors are encompassed in those models.

2.3 Models to predict Fatigue Cracking

Two main models which have been commonly used in the past until now to predict fatigue cracking have been discussed in detail. Other models that have been used are also listed in this section.

2.3.1 Asphalt Institute (AI) Model

The AI method was one of the first methods that used the M-E approach in pavement design. There are two equations in the AI method to predict alligator cracking, one based on constant stress while the other is based on constant strain. The constant stress criterion is applicable for sections with asphalt thickness greater than 6 to 8 inches, while the constant strain criterion is applicable to sections with thickness of asphalt layer usually less than 2 inches (NCHRP, 2004).

The constant stress method is only applicable at higher thickness of pavement layer. At higher thickness, the stress experienced below the asphalt layer is almost constant for every load application as the point is very far from the load. However the residual strain increases in a similar manner as shown in Figure 2.2. The incremental increase in strain ultimately results in cracking as shown in Figure 2.3.

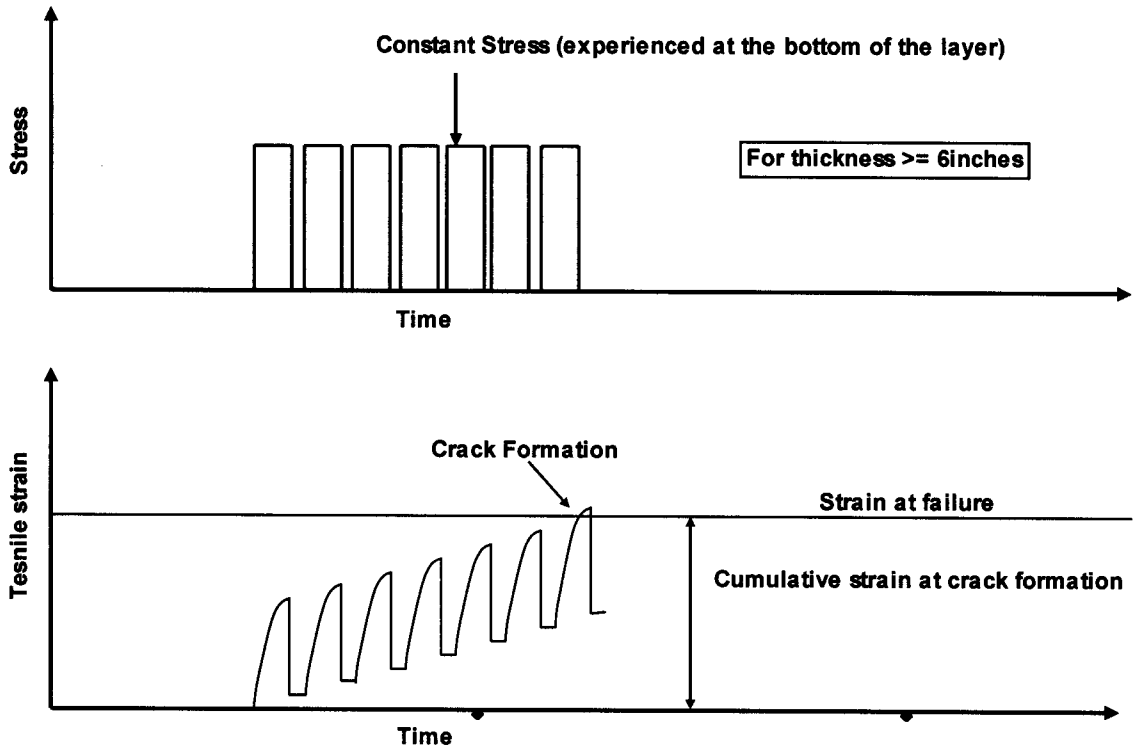

Figure 2.3 A Schematic of Incremental increase in Strain for a constant Stress method

The constant strain method is only applicable to lower thickness as the stress beneath the asphalt layer is the controlling criteria. When the thickness of the layer is very low, most of the load is taken by the layers below it, similar to a punch out effect. Punch out effect implies that the thickness of the layer was too small hence most of the load gets transferred to the layer below. Thus the strain at the bottom of the layer remains constant. However on application of load the stress increases till it finally result in cracking in the pavement after which relaxation takes which is observed by reduction in stress value. Crack formation takes place when the accumulated stress passes the stress at failure as shown in Figure 2.4.

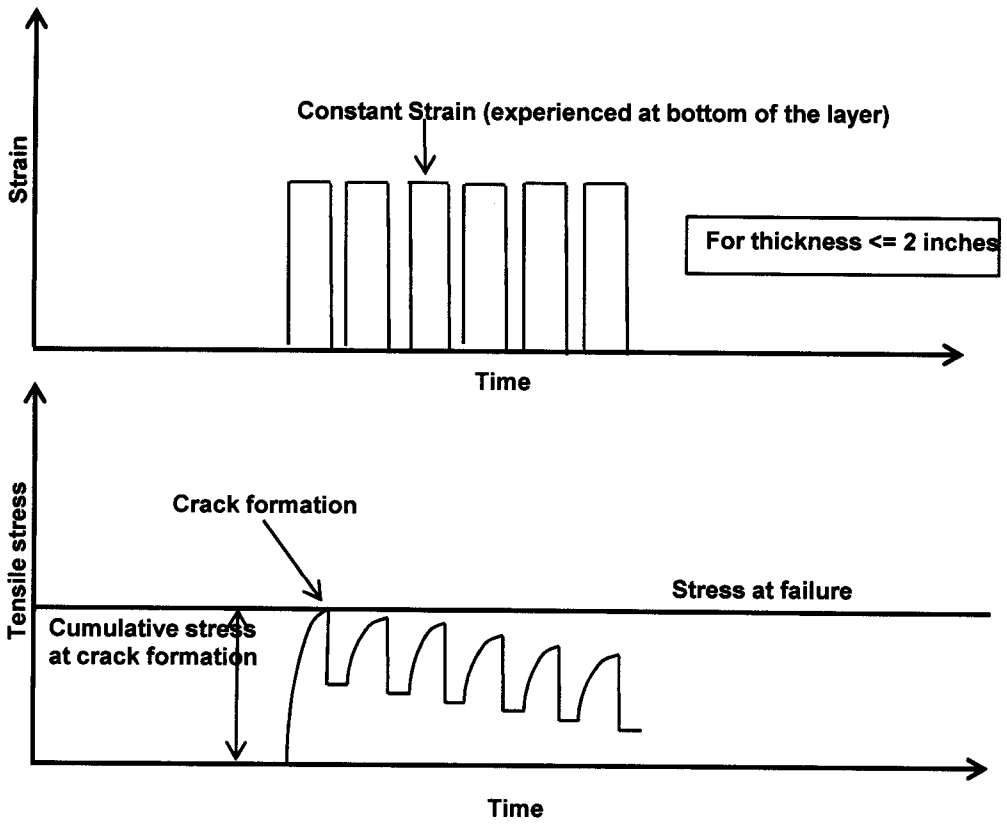

Figure 2.4 A Schematic of Incremental decrease in Stress for a constant Strain method

It was found that model based on the constant stress method was more accurate than one based on constant strain (Huang, 2004). The laboratory fatigue equation developed by the AI method based on constant stress criterion is shown in Equation 2.1. The N_f in Equation 2.1 corresponds to the stage just before the point of crack formation shown in Figure 2.4. The ε_t in Equation 2.1 is the total tensile strain as shown in Figure 2.3. The slope of curve of the residual strain in Figure is inversely related to the stiffness value of the mix, which is denoted as E^* in Equation 2.1.

$$N_f = 0.00432C\varepsilon_t^{-3.291}|E^*|^{-0.854} \tag{2.1}$$

Where

N_f = Allowable number of axle loads applications for a flexible pavements and flexible overlays

$$C = 10^{M} \tag{2.2}$$

$$M = 4.84\left(\frac{V_{be}}{V_a + V_{be}} - 0.69\right)$$

(2.3)

Where

V_{be} = Effective asphalt content by volume, %,

V_a = Percent air voids in the HMA mixture,

ε_t = Critical tensile strain, in. /in.

$|E^*|$ = Dynamic modulus of HMA, psi.

The model presented in Equation 2.1 was used in the development of the fatigue cracking model in the design guide. The model incorporates all the factors that lead to crack formation as discussed in the above section. The thickness effect is incorporated by the inclusion of strain and stiffness. However, it can be seen that the model given by Equation 2.1 only predicts the crack formation and does not include crack propagation through the layer and along the surface. Equation 2.1 also does not account for local conditions which might differ greatly from one region to another. Other models that have been developed and used in the past which give cracking in terms of number of repetition to failure are listed in Table 2.1.

Table 2.1 Models for Predicting Alligator Cracking

Model	Equation
Shell International Model (Shell, 1978)	$N_f = 0.0685\varepsilon_t^{-5.671}E^{-2.363}$
Probabilistic Distress model (Finn, et al., 1973) (Finn, et al., 1986)	$\log N_f\,(10\%) = 15.947 - 3.29\log\left(\frac{\varepsilon}{10^{-6}}\right) - 0.854log\left(\frac{E}{10^3}\right)$; for 10% load application to 10 % area fatigue cracking $\log N_f\,(45\%) = 16.086 - 3.29\log\left(\frac{\varepsilon}{10^{-6}}\right) - 0.854log\left(\frac{E}{10^3}\right)$; for 45% load application to 45 % area fatigue cracking
FHWA cost allocation study (Rauhut, et al., 1984a) (Rauhut, et al., 1984b)	$N_f = k_1\varepsilon_t^{k_2}$; $K_1 = K_{1R}\left(\frac{E_r}{E_{Rr}}\right)^{-4}$; $K_2 = 1.75 - 0.252[log(K_1)]$ Where: K_{1R}= Fatigue constant, E_r= Resilient modulus of the HMA layer using the indirect tensile test, psi, E_{Rr}= Reference resilient modulus of the HMA measured at the reference temperature, psi.
Asphalt Aggregate Mixture Analysis System (Von Quintus, et al., 1991)	$\log N_f\,(T_i) = 15.947 - K_r[\log\varepsilon_t(T_i)] - C_r\log E_r\,(T_i)$ Where: T_i= Total layer thickness, K_r= Fatigue constant
Virginia Research Council (Maupin, et al., 1976)	$N_f = K_1(\varepsilon_t)^{-n}$; $n = 0.0374\sigma_t - 0.744$; $logK_1 = 7.92 - 1.122\sigma_f$ Where: n= actual number of load application within a specific time period, σ_t= tensile stress at bottom of layer, σ_f= Indirect tensile strength measured at 70°F, psi
Transport and Road Research Laboratory (Powell, et al., 1984)	$N_f = 1.66 * 10^{-10}\varepsilon_t^{-4.32}$
Illinois (Thompson, 1987)	$N_f = 5.0 * 10^{-6}\varepsilon_t^{-3.0}$
Michigan (Baladi, 1987)	$\log(ESAL) = -2.544 + 0.154T_{AC} + 0.0694TB_{EQ} - 2.799log\delta_o - 0.216V_a + 0.917logE_{base} + 0.0000269M_R - 1.0964log\varepsilon_t + 1.173log\varepsilon_v - 0.001KV + 0.0064ANG$ Where: δ_0= surface deflection, in; V_a= percent air void in the mix; ε_v= compressive strain at bottom of HMA layer, in/in, ANG= aggregate angularity, TB_{EQ}= thickness of base material, in.

Equation 2.1 was developed in the early 1980's, since then the availabilty of computational resources has changed considerably and also the understanding of the fatigue behavior of the pavement. The model in M-EPDG makes an effort to reduce the gap between predicted and measured data by including parameters that account for local factors in Equation 2.1. However, the fundamentals behind the model remain the same.

A review of the alligator cracking model in the M-EPDG was conducted to get a better understanding of the inputs going in to the model and the factors which affected the prediction. The details of the model are explained in the following section.

2.3.2 Fatigue cracking Model in the M-EPDG

Fatigue cracking is caused by repeated loading of the pavement which induces tensile and shear stresses in the bound layers. The prediction of alligator cracking in the M-EPDG is done by using cumulative damage concept (NCHRP, 2004). The mechanism of alligator cracking can be divided into three phases:

1. Crack formation at the bottom of the asphalt layer
2. Propagation of crack to the surface
3. Propagation of crack longitudinally on the surface

Alligator cracking predictions in the M-EPDG were based on Miner's law for cumulative damage. The damage is calculated as the ratio of the actual number of traffic repetitions to the allowable number of load repetitions as shown in Equation 2.4. Damage occurs when the sum of the damage ratio reaches the value of 1. The damage calculated is used to predict the last two stages of alligator cracking.

$$\boldsymbol{D = \sum_{i=1}^{T} \frac{n_i}{N_{fi}}} \qquad (2.4)$$

Where

D= damage.

T= total number of periods.

n_i= actual traffic for period i.

N_{fi}= allowable failure repetitions under conditions prevailing in period i.

Number of axles to failure is calculated for each period and corresponding damage is calculated. The damage is used in the prediction model to predict the cracking performance at the end of that specified period. The total damage is calculated as a sum of all the damage at the end of the design life. Different equations used to calculate N_f, damage and percentage are described in detail below.

The fatigue model is divided into various parts consisting of calculation of allowable number of axle load, damage index and finally fatigue cracking in the pavement. The final equation that was used in the design guide to calculate the number of allowable ESAL's is given by Equation 2.5.

$$N_{f-HMA} = k_{f1}(C)(C_H)\beta_{f1}(\varepsilon_t)^{k_{f2}\beta_{f2}}(E_{HMA})^{k_{f3}\beta_{f3}} \tag{2.5}$$

Where

N_{f-HMA} = Allowable number of axle loads applications for a flexible pavements and flexible overlays

k_{f1}, k_{f2}, k_{f3} = Global field calibration parameters (from the NCHRP 1-40D recalibration; $k_{f1} = 0.007566, k_{f2} = -3.9492, k_{f3} = -1.281$)

$\beta_{f1}, \beta_{f2}, \beta_{f3}$ = Local or mixture specific field calibration constants; for the global calibration effort, these were set to 1.0

ε_t = Tensile strain at critical locations and calculated by the structural response model, in. / in

E_{HMA} = Dynamic modulus of the HMA measured in compression, psi.

$C = 10^M$

C_H = Thickness correction term, dependent on type of cracking.

N_f calculated from the above equation gives the number of axles to failure if the same load was coming on the pavement for same condition (both with respect to material and temperature). Thus for different axles load and different weather

condition for the same pavement section, N_f has to be calculated for each axle load coming on the pavement and for each weather condition. The tensile strain considered in the above equation is the total strain (sum of elastic and residual strain) just before crack formation.

For bottom up or alligator cracking

$$C_H = \frac{1}{0.000398 + \frac{0.00362}{1+e^{(11.02-3.49H_{HMA})}}} \quad (2.6)$$

Where

H_{HMA} = Total HMA thickness, in.

Equation 2.5, which calculates the number of axles to failure, is similar to Equation 2.1 if the field mixture and global calibration factors are removed. Equation 2.5 accounts for the first two stages of the alligator cracking; crack formation and crack propagation to the top of the surface. Crack propagation is accounted by field adjustment factor used in Equation 2.5 which is also present in Equation 2.1. However Equation 2.4 also has factors which accounts for mix and local conditions making it more accurate as compared to Equation 2.1. C_H takes into account the thickness of asphalt layer, as the critical strain criterion accounts for fatigue cracking for thinner section and critical stress criterion for thicker sections. The fatigue prediction in the design guide was based on constant stress criterion, to account for thinner sections C_H was introduced as a sigmoidal relationship between thick (thickness >= 8inches) and thin section (<= 2 inches) as well as all intermediate thickness (2 to 8 inches).

The allowable numbers of axles are used to calculate incremental damage index (ΔDI) (Equation 2.7), which is used to calculate the cumulative Damage Index (DI).

$$DI = \sum(\Delta DI)_{j,m,l,p,T} = \sum\left(\frac{n}{N_{f-HMA}}\right)_{j,m,l,p,T} \quad (2.7)$$

Where

n = actual number of axle load applications within a specific time period,

j = Axle load interval,

m = Axle load type (single, tandem, tridem, quad, or special axle configuration)

l = Truck type using the truck classification groups included in the MEPDG,

p = Month, and

T = Median temperature for the five temperatures intervals or quintiles used to subdivide each month, °F.

The area of alligator cracking from the total damage (DI) over time is given by Equation 2.8.

$$\mathbf{FC_{Bottom}} = \left(\frac{1}{60}\right)\left(\frac{C_4}{1+e^{\left(C_1C_1^*+C_2C_2^*\log(DI_{Bottom}*100)\right)}}\right) \quad (2.8)$$

Where

FC_{Bottom} = Area of alligator cracking that initiates at the bottom of the HMA layers, % of total area,

DI_{Bottom} = Cumulative damage index at the bottom of the HMA layers, and

$C_{1,2,4}$ = Transfer function regression constants; $C_4 = 6000; C_1 = C_2 = 1.00$

$$C_1^* = -2C_2^* \quad (2.9)$$

$$C_2^* = -2.40874 - 39.748(1 + H_{HMA})^{-2.856} \quad (2.10)$$

The 6000 in the alligator damage function is the total lane area (12 feet wide and 500 feet length). The value of (1/60) is a conversion to obtain the cracking in percentage, not in square feet. From Equations 2.8, 2.9 and 2.10 it can be observed that, only C_1 and C_2 are independent of any parameters that affect predicted performance. Both C_1 and C_2 were introduced as regression constants to reduce the gap between the predicted and measured distress in the transfer function.

The coefficients in the models were introduced to reduce the gap between predicted and measured distress as a part of the model development process. Some of the constants were introduced to account for specific field condition, such as propagation of

cracking through asphalt layer which accounts for the thickness of the layer (β_{f1}), while some of the constants were introduced as regression constants (C_1 and C_2). Thus it becomes essential to identify the physical significance of each of these parameters with respect to pavement performance before changing these constants. The standard error S_e (standard deviation of the residual errors) for alligator cracking prediction is given by Equation 2.11.

$$S_{e(Alligator)} = 32.7 + \frac{995.1}{1 + e^{2-2Log(FC_{Bottom+0.0001})}} \tag{2.11}$$

Based on the above literature review it can be concluded that, the model used in the design guide encompass all possible parameters that would affect the cracking behavior. It can also be observed that the β_{f2} and β_{f3} in Equation 2.5 and regression constants C_1 and C_2 in Equation 2.8 are the variables independent of any input parameters. The next section of literature review focuses on how the ranges of these constants were determined.

2.4 Range of constants used in the fatigue cracking model

The calibration factor (β_{fi}) in Equation 2.5 was introduced for each coefficient factor (k_{fi}) to eliminate the bias and the scatter in the predictions. The Design Guide specifies that it is these calibration factors which were used to calibrate the fatigue cracking model to actual field performance during the calibration process. The different values that were used during the calibration process for calibration factor on the strain (β_{f2}) were 0.8, 1.0 and 1.2 while that for modulus calibration factor (β_{f3}) were 0.8, 1.5 and 2.5 (NCHRP, 2004). The regression coefficients C_1 and C_2 used in the transfer function in Equation 8 were selected using optimization routine using Microsoft solver for coefficients C_1 and C_2. The optimization was done by selecting an initial value of C_1 and C_2 in Equation 2.8. This is followed by calculating the sum of the square of errors between the measured cracking and predicted cracking. The solver was then run to minimize the error till the solution converged to the minimum total sum of squared error was obtained.

The β_{f1} factor is a calibration factor for layer thickness. Thus for low thickness of AC layer (less than 4 inches), β_{fi} might have to be calibrated. Thus the alligator cracking calibration can be summarized as follows

1. Collection of input data.
2. Estimation of β_{f2} and β_{f3}.
3. Estimation of the alligator fatigue cracking-damage transfer function by minimizing the error to get a final of C_1 and C_2.
4. Calibration of β_{f1} if thin sections are present (less than 4 inches).

Accurate cracking prediction depends on the accuracy of the input data as well other properties and parameters which are internally calculated in the Design Guide. The next section deals with the calculation of stiffness and strain value in the Design Guide. The strain at the bottom of the bond layer is one of the critical parameter that has to be considered for accurate prediction of cracking.

2.5 *Stiffness and Strain Calculation in M-EPDG*

In a layered pavement structure critical strains are calculated using pavement response model. The number of cases depends on the damage increment. The following increments are considered in the Design Guide.

- Pavement age – by year
- Season – by month or semi month
- Load configuration – axle type
- Load level – discrete load levels in 1000 to 3000 lb increments depending on axle type.
- Temperature – pavement temperature for the HMA dynamic modulus.

The location of critical points in the pavement system has to be guessed as specified by the Design Guide (NCHRP, 2004). Thus identifying these critical points becomes a difficult and long process to solve. Design Guide uses different axle

configuration instead of single ESAL values. Thus for several different combination of axle configuration, it is not possible to specify one location that will result in maximum damage. To overcome this problem and to insure that the critical location is utilized in the damage analysis, the program internally specifies computational points depending upon axle type. The predefined analysis locations depend on the types of axle and traffic mix. Once these locations are defined the incremental damage is calculated at these locations for performance prediction within each computational analysis period to estimate maximum damage. Figure 2.5 shows the predefined analysis point for damage computation.

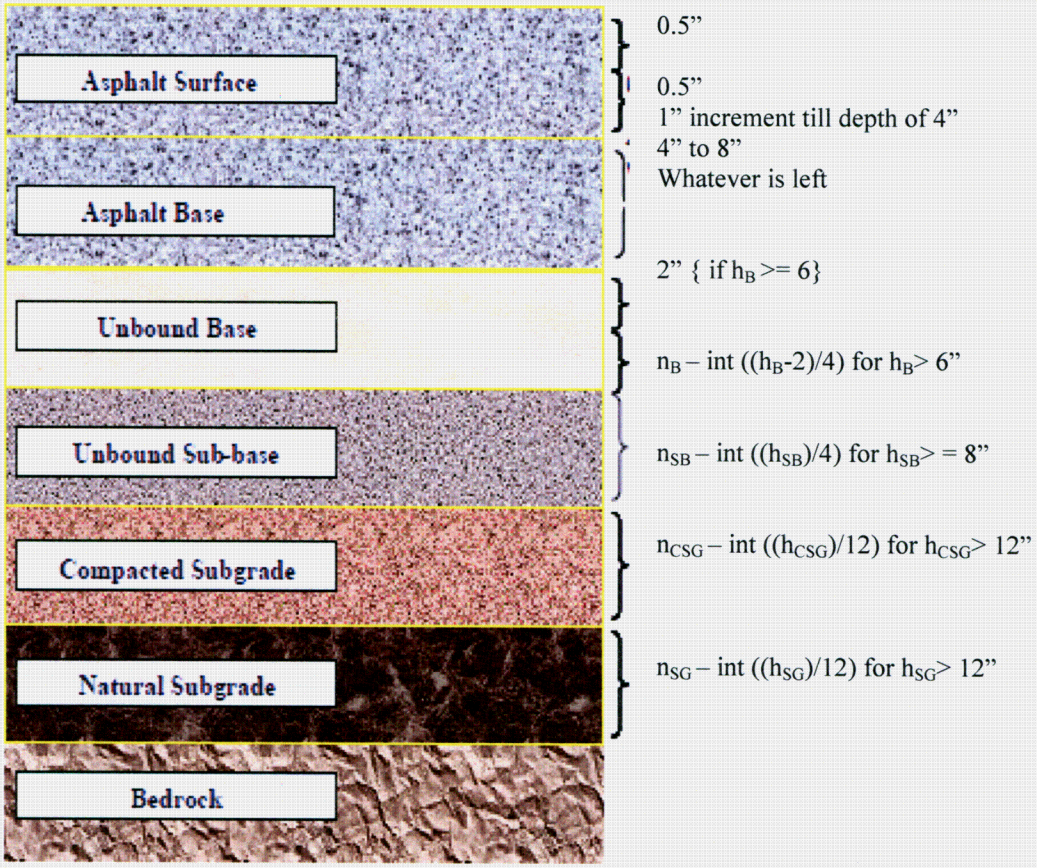

Figure 2.5 Layered pavement cross section for flexible pavement system (NCHRP, 2004).

The elastic layer analysis in the design guide was done using JULEA (NCHRP, 2004). For layered elastic analysis, the principle of superposition is used to account for

axles within specific axle type (single, tandem, tridem or quad). For any axle type, the response is only obtained for dual wheels on the single axle configuration and the effects of other wheels within the axle configuration are obtained by superposition.

The Design Guide has a total of 70 analysis points (10 X-locations with 7 Y-locations) for 4 axle types. These analysis locations are used for the determination of the critical stresses / strains for the damage calculations for fatigue crack prediction. The response is measured along these points to determine the critical value. The critical location is the one at which the response (strain) is maximum. The locations of responses are as shown in Figure 2.6.

X-Axis Locations

X1 = 0.0 {center of dual tires/tire spacing}
X2 = ((T$_{spacing}$/2) - T$_{radius}$)/2 {T$_{spacing}$ = tire spacing; T$_{radius}$ = tire contact
X3 = (T$_{spacing}$/2) - T$_{radius}$
X4 = T$_{spacing}$/2
X5 = (T$_{spacing}$/2) + T$_{radius}$
X6 = (T$_{spacing}$/2) + T$_{radius}$ + 4 in
X7 = (T$_{spacing}$/2) + T$_{radius}$ + 8 in
X8 = (T$_{spacing}$/2) + T$_{radius}$ + 16 in
X9 = (T$_{spacing}$/2) + T$_{radius}$ + 24 in
X10 = (T$_{spacing}$/2) + T$_{radius}$ + 32 in

Y-Axis Locations

Y1: y = 0.0 {center of dual tires/tire spacing}
Y2: y = S$_{tandem}$ {tandem axle spacing}
Y3: y = S$_{tandem}$/2
Y4: y = S$_{tridem}$ {tridem/quad axle spacing)
Y5: y = S$_{tridem}$/2
Y6: y = S$_{tridem}$3/2
Y7: y = S$_{tridem}$4/2

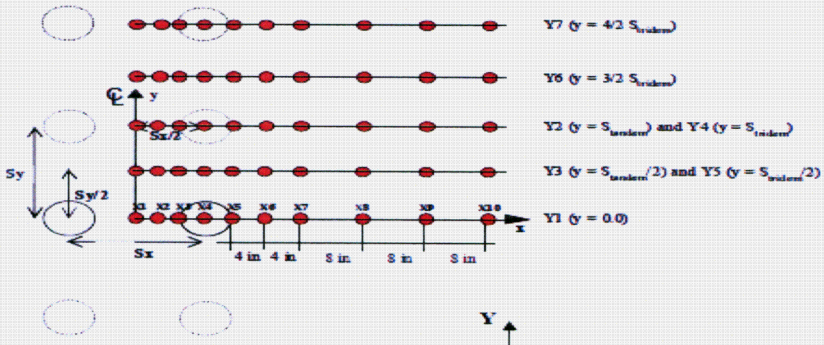

Computed Responses

- Single
  - Response 1 = Y1
- Tandem
  - Response 1 = Y1 + Y2
  - Response 2 = 2 * Y3
- Tridem
  - Response 1 = Y1 + 2 * Y4
  - Response 2 = 2 * Y5 + Y6
- Quad
  - Response 1 = Y1 + 2 * Y4 + Y7
  - Response 2 = 2 * Y5 + 2 * Y6

Figure 2.6 Schematics for horizontal analysis location having regular traffic (NCHRP, 2004).

The above discussion only related to the analysis location in the x-y plane. At these locations critical responses are also determined at several depths. The locations of these points are as shown in Figure. One of the most complex properties of HMA is the

dynamic modulus. The dynamic modulus varies considerably with temperature; this aspect is captured in the Design Guide with the help of a master curve. The method by which master curve is constructed in the design guide is explained in the next section.

2.6 Master Curve and Shift Factors

The complex dynamic modulus of asphalt mixtures are accounted in the Design Guide via a master curve. Thus, E* (same as in Equation 2.5) is expressed as a function of the mix properties, temperature and time of the load pulse. Asphalt is highly sensitive to temperature and the rate of loading. Asphalt being a viscoelastic –plastic material, the dynamic modulus of asphalt may approach that of an unbound material at high temperature and long loading rates. The process of plotting and shifting of master curve is described in detail below.

Master curves are constructed using the principle of superposition. First a standard reference temperature is selected. Next data at various points are shifted with respect to time until the curves merge into a single smooth function. The standard temperature or reference temperature in the Design Guide is taken as 70°F (NCHRP, 2004). The master curve of modulus formed in this manner describes the time dependency of the material. The temperature dependency of the material is given by the amount of shifting at each temperature.

The dynamic modulus master curve can be represented by the sigmoidal function described by Equation 2.12. Equation 2.12 enables determination of the dynamic modulus at any temperature if the mix properties are known.

$$log(E^*) = \delta + \frac{\alpha}{1+e^{\beta+\gamma(log\, t_r)}} \tag{2.12}$$

Where

E* = Dynamic modulus

t_r = time of loading at reference temperature

δ, α = fitting parameters, for a given set of data, δ represents the minimum value of E* and $\delta + \alpha$ represents maximum value of E*.

β, γ = parameters describing the shape of the sigmoidal function.

γ = 0.313351

$$\delta = 3.750063 + 0.02932\rho_{200} - 0.001767(\rho_{200})^2 - 0.002841\rho_4 - 0.05809V_a - 0.802208\left[\frac{V_{beff}}{V_{beff}+V_a}\right] \quad (2.13)$$

Where

ρ_{200} = %passing the No. 200 sieve

ρ_4 = cumulative %retained on the No. 4 sieve

V_{beff} = effective bitumen content, % by volume

V_a = air void content, %

$$\propto = 3.871977 - 0.0021\rho_4 + 0.003958\rho_{38} - 0.000017{\rho_{38}}^2 + 0.005470\rho_{34} \quad (2.14)$$

$$\beta = -0.603313 - 0.393532\log(\eta_{T_r}) \quad (2.15)$$

$$\log(t_r) = \log(t) - c(\log(\eta) - \log(\eta_{T_r})) \quad (2.16)$$

Where

c = 1.255882

ρ_{38} = cumulative % retained on the 3/8 in sieve

ρ_{34} = cumulative % retained on the 3/4 in sieve

η = binder viscosity, poise

The shift factor, which describes the temperature dependency of the modulus is given by Equation 2.17 and 2.18.

$$t_r = \frac{t}{a(T)} \tag{2.17}$$

$$\log(t_r) = \log(t) - \log[a(T)] \tag{2.18}$$

Where

t_r = time of loading at the reference temperature

t = time of loading at a given temperature of interest

a(T) = shift factor as a function of temperature

T = temperature of interest

The above mentioned equations can be used to develop master curve for any mix. The binder viscosity at any temperature of interest can be calculated using Equation 2.19.

$$\log\log\eta = A + VTS\log T_R \tag{2.19}$$

Where

η= viscosity, cP

T_R= temperature, Rankine

A =regression intercept

VTS= regression slope of viscosity temperature susceptibility

The dynamic modulus can also be calculated using Equation 2.20 (NCHRP, 2004). The dynamic modulus equation uses the gradation, the binder content and the percent air void. Equation 2.20 is similar to Equation 2.12, except that Equation 2.12 gives the relationship with respect to temperature while Equation 2.19 gives the relationship with respect to viscosity and frequency.

$$\log E^* = 3.750063 + 0.02932\rho_{200} - 0.001767(\rho_{200})^2 - 0.002841\rho_4 - 0.05809V_a - 0.802208\left[\frac{V_{beff}}{V_{beff}+V_a}\right] + \frac{3.871977 - 0.0021\rho_4 + 0.003958\rho_{38} - 0.000017\rho_{38}^2 + 0.005470\rho_{34}}{1+e^{(-0.603313 - 0.313351\log(f) - 0.3933532\log(\eta))}} \tag{2.20}$$

Equations 2.12 and 2.20 determine the stiffness of the mix and master curve respectively. These factors and properties have to be determined for the given binder for level 1 analysis. However for level 3 analyses, default values can be assumed, which are already input in the Design Guide based on LTPP data collected from all over the country. Design Guide plots the master curve for different asphalt layer for a particular section inputted into it. The master curve helps in finding out the time – temperature relationship as well as the temperature dependency of the mix. The range of temperature and frequency at which the stiffness of the mix is calculated ranges from 0 to 130 °F and 0.1 to 25 Hz respectively. The Design Guide outputs stiffness value based on Equation 2.19 at five different temperatures using the master curve obtained from Equation 2.11. However the value at 70 °F was used in the Design Guide as the stiffness value for calculating the critical strain value at the interfaces.

With time, the organic components in the binder get oxidized, which makes the asphalt binder brittle and thus increasing cracking (Walubita, et al., 2005). As explained earlier, binder aging is an important factor that affects fatigue cracking. Thus it becomes important to know how asphalt aging in incorporated in the Design Guide. The inclusion of aging component of asphalt binder is explained in the following section in detail.

2.7 Aging of Asphalt Binder

The effect of aging is incorporated into the determination of dynamic modulus using Global Aging System (NCHRP, 2004). This system provides models that describe the change in viscosity that occurs during mixing and compaction, as well as long-term in-situ aging. The Global Aging System includes four models.

- Original to mix/lay-down model.
- Surface aging model
- Air void adjustment
- Viscosity-depth model

The original to mix/lay-down model accounts for short-term aging that occurs during mixing and compaction. The surface aging model then predicts the viscosity of

the binder at the surface of the pavement after any period of time using the viscosity at mix/lay-down. If warranted, the surface viscosity from the surface aging model can be adjusted for different air void contents using the air void adjustment model. Finally, the viscosity as a function of depth is determined using the viscosity from the surface aging model or the air void adjusted model along with the viscosity-depth model. The entire above mentioned model forms an integrated part of the Design Guide dynamic modulus calculation.

Cracking prediction in the Design Guide depends on a variety of input parameters. It is thus essential to know the effect of these parameters on the cracking predicted. Sensitivity analysis provided in the Design Guide and by other researchers is described in the section below.

2.8 Sensitivity of input parameters on Fatigue cracking predictions

The Design guide provides the sensitivity analysis with respect to different input parameters on the alligator cracking. The effects of each parameter on the alligator cracking in the AC layer are listed in Table 2.2. Four of the twelve input parameters listed do not significantly affect the cracking prediction. Air void, AC thickness (3-5 inches), AADTT and binder content have a significant effect on cracking prediction. Air void and AADTT are listed as extremely sensitive parameters.

Sensitivity analyses were carried out by many other researchers to analyze the effect of variation of input parameters on the predicted fatigue cracking. Study done at University of Texas, Austin (Aguiar-Moya, et al., 2009) found that for ± 3 standard deviation from the mean thickness (HMA thickness = 1.5 inch) the fatigue cracking prediction was found to be most affected by 33%.

An in-depth study was conducted by the WIDOT (Mallela, et al., 2008) to understand the effect of input parameters on alligator cracking. Thickness and binder content were found to be most sensitive factor to alligator cracking. These were followed by air void content and AADTT having a moderate effect on alligator cracking. Local calibration guide for Montana DOT (VonQuintus, et al., 2007) specifies to determine the

k_{f1} factor based on voids filled with asphalt (VFA) and then in turn finding k_{f3} based on k_{f1}. The guide also specifies to determine the C_2 based on VFA and leave C_1 and C_4 unchanged.

Table 2.2 Effect of input parameters on alligator cracking in AC layer (NCHRP, 2004)

No	Parameter	Effect on Cracking with change in parameter	Significant effect	Note
1	AC mix stiffness for thin AC layer (1inch thick)	Decrease in stiffness decreases cracking	Yes	Thickness = 1 inch
2	AC mix stiffness for thick AC layer (10 inch thick)	Decrease in stiffness increases cracking.	Yes	Thickness = 10inch
3	AC thickness	AC thickness between 3-5 inches show maximum cracking	Yes (Between 3-5")	To avoid cracking very thin or very thick AC thickness
4	Subgrade Modulus	Increase of subgrade modulus decreases cracking.	No	Sensitivity of subgrade support depends on other parameter like thickness, traffic and site climatic condition.
5	AC mix air voids	Increase in air voids increases cracking	Yes	Air voids in the AC mix are an important parameter to influence cracking.
6	Effective bitumen content	Increase in bitumen content decreases cracking	Yes	Amount of binder content directly influences the amount fatigue cracking.
7	Depth of ground water table (GWT)	Decrease in GWT depth increases cracking	No	Depends on the subgrade encountered. At depths greater than 5 to 7 feet influence of GWT is very low.
8	Traffic Volume (AADTT)	Increase in AADTT increases cracking	Yes	Extremely sensitive parameter to alligator cracking.
9	Traffic speed	For low thickness (1 inch) increases cracking. For higher thickness (8 inches) does not have much effect.	No	Dependent on the thickness of AC layer. Not very significant effect over a broad range of layer thickness
10	Traffic analysis level	Use of level 1 traffic approach yields higher level of cracking compared to 18 kip ESAL's.	Yes	Difference of 3 -7 % was observed between level 1 traffic and ESAL's.
11	Mean annual air temperature (MAAT)	Increase in MAAT results in increase in cracking	Yes	Independent of thickness of AC layer with increase in MAAT alligator cracking increases.
12	Bed rock depth	Closer the bed rock to subgrade interface lesser cracking	No	Critical bedrock depth depends on various cross section properties.

2.9 *Calibration study done in other States*:

The calibration study done by other states was carried out according to the guidelines specified within the Design Guide for calibration purposes. The calibration process done in the Midwest (Kang, et al., 2007), which included Michigan, Ohio and Wisconsin calibrated the fatigue cracking model by calibrating the β_{f2} and β_{f3} factors based on the values suggested in the Design Guide. Another study performed in Wisconsin (Mallela, et al., 2008) found that alligator cracking prediction was reasonably correct for low cracking. However, due to insufficient data for high percentage of cracking the prediction was not verified. Table 2.3 lists the values from both calibration efforts. The calibration process carried out in North Carolina (Muthadi, et al., 2008) calibrated C_1 and C_2 in the transfer function. Calibration carried out in Washington State (Li, et al., 2009) recommended the change in β values as well as C_1 values.

Table 2.3 Values of local calibration effort

States	Values Before calibration					Values After Local Calibration				
	β_{f1}	β_{f2}	β_{f3}	C_1	C_2	β_{f1}	β_{f2}	β_{f3}	C_1	C_2
North Carolina (Muthadi, et al., 2008)	1.0	1.0	1.0	1.0	1.0	1.0	1.0	1.0	0.4371	0.150594
Wisconsin (Kang, et al., 2007)	1.0	1.0	1.0	1.0	1.0	1.0	1.2	1.5	1.0	1.0
Wisconsin (Mallela, et al., 2008)	1.0	1.0	1.0	1.0	1.0	1.0	1.0	1.0	1.0	1.0
Washington (Li, et al., 2009)	1.0	1.0	1.0	1.0	1.0	0.96	0.97	1.03	1.07	1.0

2.10 NCHRP Guidelines for Local Calibration

The local calibration process involves three important steps (NCHRP, 2007) for calibrating MEPDG to local conditions and materials.

Step 1: For selected pavement sections verify the calibration factors developed during the national calibration process.

Step 2: If difference exists between predicted and measured cracking, then calibration of these models coefficients is required to eliminate the bias and to minimize the error between predicted and measured data.

Step 3: Once the calibration is done, it is required to validate the new values with independent sections to check the reasonableness of the predicted performance.

The methodology adopted in this study was based on the NCHRP calibration procedure as well as the local calibration carried out by other researchers across the country. The following section presents the summary of the NCHRP 1-40B project which deals with local calibration guidelines for M-EPDG (Von Quintus, et al., 2009).

2.11 NCHRP 1-40B report

The NCHRP 1-40B report was prepared to validate or revise the M-EPDG global calibration factors (Von Quintus, et al., 2009). The revisions carried out in this study were done so as to account for local conditions and materials that were not considered in the global calibration process during the calibration process of the Design Guide. The report included both rigid and flexible pavements. As this study deals exclusively with alligator cracking occurring in flexible pavements, literature review with respect to rigid was not carried out. Also the literature review for other distresses except alligator cracking were not looked into much detail. The following sections explains in brief the recommendation provided for selecting the level of input, sample size, extraction of data that was provided in the study (Von Quintus, et al., 2009) using pavement sections from Kansas Department of Transportation (KSDOT).

2.11.1 Recommendation for input level to be used

Von Quintus, et al. recommends caibration of fexlible pavement based on pavement management system (PMS) and LTPP datasets. Calibration of flexible pavement was carried out using sixteen PMS sections out of which 11 were new construction/ reconstruction and the rest were overlays. Fifty six LTPP section were used in the study, which comprised of 24 SPS-1 sections and thirty two SPS-5 sections. The LTPP sections were taken from Kansas, Nebraska, Oklahoma, Iowa, Colorado, Missouri and Texas. The report clearly states for validation and calibration process the hierarchical input level of the Design Guide should be consistent with state agency database. As all the input parameters required in the Design Guide are not easily available in the PMS data sets, the calibration process should be carried out with input level 2 and 3, mostly at level 3 input. For LTPP datasets as more detailed information was available, the input data were mostly level 2.

2.11.2 Recommended sample size and data points

The study (Von Quintus, et al., 2009) was carried out on Kansas Department of Transportation (KDOT) sections. The study recommends including HMA design strategies and materials commonly observed in the state. For Kansas, the different type of HMA mixture type included conventional neat HMA mixtures, Superpave mixtures, and polymer modified asphalt (PMA) mixtures. All the different type of mixtures mentioned above was included in the calibration process. The different type of mix present in the LTPP data included conventional flexible pavement, full-depth & deep strength, mix without recycled asphalt pavement (RAP) and mix with RAP.

The study recommends 90 percent level of confidence for estimating the sample size. Sample size is defined as the total number of roadway segment or projects. Thus if the design criteria for fatigue cracking was kept at 20 percent then the minimum number of projects required for 90 percent level of confidence was found to be 8 with 32 observations in total. Equation 2.21 gives the number of project required for a given level of confidence. The tolerable bias selected in the study was 2.5. The value of bias

was estimated from the levels that are expected to trigger rehabilitation process which is a agency dependent value.

$$N = \left(\frac{Z_a * S_y}{e_t}\right)^2 \quad (2.21)$$

Where

N =Minimum number of samples

Z_a =1.282 for 90 percent confidence interval

S_y =Standard deviation of the maximum true or observed value (agency dependent)

e_t =Tolerable bias

The study also recommends evenly spread observation point for all the segments that are being used in the calibration process. For example, to have ten observations points over 10 years for one segment while the other segment only having two or three observations for the same period of 10 years was not recommended. This is because the segment with one observation per year would have more influence on the calibration-validation process as compared to the other segment. The number of observations per year for the 16 PMS segments selected varied from 1.0 observation per year for new construction to 0.75 observation for overlay projects.

2.11.3 Recommendation for extracting and evaluating distress data

KSDOT measures fatigue cracking in the wheel path at every 100 foot and ranks it by crack severity (Von Quintus, et al., 2009). Different types of crack like alligator cracking and longitudinal cracking in the wheel path were not differentiated. This practice is also carried out by other state agencies as was observed in the calibration study conducted in North Carolina (Muthadi, et al., 2008).

The study provides an equation (Equation 2.22) that converted all load related cracking to a single value. The M-EPDG prediction for load related cracking were also combined to a single value for PMS datasets. This was done by simply adding the length of longitudinal crack and reflection crack for HMA overlays, multiplying by 1.0 ft,

dividing that product by the area of the lane and then adding the value of alligator cracking predicted by the MEPDG. Equation 2.22 was developed for KSDOT section and might differ for other State depending on the data collection method adopted by the PMS unit of the particular state agency.

$$FC = \left(\frac{FCR_1(0.5)+FCR_2(1.0)+FCR_3(1.5)+FCR_4(2.0)}{8.0}\right) \quad (2.22)$$

Where
FC_n = Different types of fatigue cracking

One of the important observations of the data used in the calibration-validation was that few of the PMS segments had any measured fatigue cracking, thus confirming that fatigue cracking global calibration value was unlikely. The study also lists the probability of the measured data to exceed the design criteria. As the observed values for fatigue cracking were so low the expected probability of the measured data for the KSDOT PMS data were listed as 0 percent. The maximum area of fatigue cracking measured was less than 3 percent. The study points out the fact that to validate and determine the calibration factor for local condition these values were too low since the design criteria was 20 percent. Thus, alligator cracking might not be the reason for rehabilitation. Hence calibrating the alligator cracking calibration factor becomes more difficult.

For LTPP datasets the average maximum value of fatigue cracking was 13.3 percent while the probability of exceeding the design value was 37.1 percent. This value as compared to the value observed for PMS datasets were on the higher side. The explanation provided in the study for the higher value in the LTPP dataset as compared to PMS dataset were due to the experimental factor designed into LTPP experiments while the same design procedure and material specification were used for all PMS segments.

2.11.4 Recommendations for verification of input data

Important points with respect to input data to be used are listed below.

1. The study suggests initial IRI should be determined from measured values within one or two years after construction as very low values are recorded for the first couple of years.
2. As built plans should be used when dealing with PMS segments to determine material type and thickness. Construction date for full depth pavement and overlays can also be determined from as built plans.
3. The traffic open month can be assumed one month from the construction date.
4. ESAL's from the state agency database can be used to determine the average growth factors.
5. For unavailable data like dynamic modulus, creep compliance and indirect tensile strength for HMA mixtures level 3 or default values from the Design Guide can be assumed.

2.11.5 Recommendation to find the local bias from global calibration factor

The PMS segments were executed with default global calibration factors to find the bias in the predicted performance. A null hypothesis was then formed for the entire sampling matrix. The null hypothesis accepted in the study (Von Quintus, et al., 2009) was that the average residual error or bias was zero for a specified confidence level (90 percent confidence level was used in this study). For determining the null hypothesis Equation 2.23 can be used.

$$H_0: \sum_{i=1}^{n} \left(y_{measured} - x_{predicted}\right)_i = 0 \qquad (2.23)$$

Where

H_0 = Null Hypotheiss

$Y_{measured}$ = Measured value

$X_{predicted}$ = Predicted value

As the PMS segment showed zero to very little fatigue cracking, the hypothesis based on Equation 2.22 was selected for the transfer function. Another model that was used in the reference study included estimating the bias – the intercept (b_o) and slope (m) estimators using linear fitted regression model (Equation 2.24) between the measured (y_i) and predicted (x_i) values. The bias for fatigue cracking based on Equation 2.24 was relatively low, due to low measured and predicted values. One of the important observations that came out of this study was that M-EPDG constantly under predicted the measured fatigue cracking for those PMS segments exhibiting fatigue cracks.

$$\hat{y}_i = b_o + m(x_i) \tag{2.24}$$

The study also suggest that the bias can be due to three reasons

1. The precision of the prediction model is reasonable but accuracy with respect to measured data for a particular section is poor. For this case local calibration coefficient is used to reduce the bias.
2. The bias is low and relatively constant with the number or time of loading cycles but the residual error have a wide dispersion varying from positive to negative values. In this case the coefficient of the prediction equation is used to reduce the bias but the value of local calibration is dependent on some site feature, material property and/ or design feature included in the sampling template.
3. Precision of the predicted model is poor and the accuracy is time or number of cycles dependent. This condition requires highest level of effort and many runs to reduce bias and dispersion.

Thus it becomes necessary to find which of the above three reasons lead to the observed bias and select the appropriate method to eliminate the bias. For the Kansas PMS segment, it was found that the bias was based on the third condition stated above. For some of the KDOT PMS segments which did show little fatigue cracking, the local calibration coefficient (β_{f1}) was used to reduce the bias to the minimum value possible. The final value was found to be mixture dependent for full depth pavements. The calibrated values for PMS segment are listed in Table 2.4.

Table 2.4 Calibrated values of calibration Coefficient β_{f1} for KDOT sections

Type of section	Mix type	Original value of coefficient	Calibrated values
New construction	Conventional Dense-Graded HMA mixtures	1	0.05
	Polymer Modified Dense-Graded Mixtures	1	0.005
	Superpave Dense-Graded Mixtures	1	0.0005
Overlay	All mixture type	1	0.05

For LTPP section it was found that second and third condition were the reasons for bias in the predicted value. β_{f1} value of 0.005 was used for the LTPP section to reduce the bias that was observed.

2.11.6 Recommendation for assessing standard error

Standard error for estimate (SEE) value based on the local calibration were lower than the values determined from the global calibration process for alligator cracking for KSDOT sections. However, as the amount of alligator cracking observed was too low as compared to the design criteria a valid relationship was not developed successfully.

2.12 Summary of NCHRP 1-40B

The summary of the local calibration process provided in the NCHRP 1-40B project report (Von Quintus, et al., 2009) is as follows

1. Select input level depending on the segment, if PMS segment are present mostly level 2 and 3. For LTPP section level 2 inputs should be used.
2. Develop a sampling template to include local conditions, policies, and materials.
3. Estimate the sample size with respect to number of segments such that the desired level of confidence can be achieved. The bias and precision depend on the sample size, thus the size of the sample should be calculated carefully.
4. Select roadway segment to obtain maximum benefit of existing information and data.

5. Extract and evaluate the distress data. If possible all the distress data should be collected in the LTPP format (FHWA, 2003). If different collection and measurement are used for PMS sections then all those datasets should be converted such that they can be compared directly to the output obtained from the Design Guide.
6. All the input data should be checked for consistency and accuracy.
7. The predicted and the measured values should be compared to determine the bias and the standard error for each of the prediction model for local conditions using global calibration values.
8. Eliminate the local bias of distress by first indentifying the cause of bias and then selecting appropriate method to correct that bias.
9. Assess the standard from the sampling template by evaluating the null hypothesis. If the standard error is too large it will result in conservative design.
10. The local standard error of the estimate should be evaluated to determine the impact on the resulting designs at different reliability levels.

The next section summarizes the important points and findings related to alligator cracking and its calibration in the Design Guide which were discussed in the literature above.

2.13 Summary of literature review

1. AI method was the one of the first methods that gave a M-E approach to predict fatigue cracking. However, only crack initiation was predicted by this model, while crack propagation to the surface and its longitudinal spread was not accounted for.
2. The model provided in the design guide accounted for all the three stages of cracking.
3. The model was calibrated using a national database. To get accurate predictions for particular regions, there is a need to validate and possibly recalibrate the model.

4. The alligator cracking model is sensitive to a variety of factors. The factors which have the greatest effect on the cracking prediction are traffic volume, air voids and binder content.
5. The Design Guide internally calculates the time and temperature dependency of the stiffness of the HMA mix by plotting the master curve and calculating the shift factors by utilizing the principle of superposition.
6. Local factors were incorporated in the model with the help of local and global calibration factors. For the purpose of calibrating the alligator cracking model for a specific region these factors were altered to reduce the error and the bias in the predicted data with respect to the measured data.
7. To eliminate the bias, β_{f1} and C_1 should be changed. To reduce error β_{f2}, β_{f3} and C_2 should be changed.
8. NCHRP 1-40B report serves as a guideline for local calibration of the Design Guide.

Chapter 3 DATA

3.1 Introduction

This chapter discusses the input data that was collected and analyzed in this study. Different input data that is required by the Design Guide includes thickness of various layers, annual average daily traffic (AADT), traffic class distribution, binder content, mix type and the location of the section with respect to latitude and longitude to obtain the climate data.

3.2 Reliability of datasets

All the input datasets were compared from multiple sources to confirm the reliability of the datasets. All the long term pavement performance (LTPP) sections data (9 out of 29 sections) were taken from previous study (Siraj, 2008). The reliability of the LTPP datasets was confirmed by the previous researcher using various sources. For traffic input weigh in motion (W.I.M), PaveView (New Jersey Department of Transportation (NJDOT) internal database), vehicles miles travelled (VMT) and as built plans were used in the previous study. Thickness data were collected from LTPP database for LTPP sections while for non-LTPP sections data was obtained from as built plans and core data from the NJDOT material database.

Similar procedure was adopted in this study, for non-LTPP sections the traffic data was confirmed using all the four sources whenever possible (WIM, PaveView, VMT, as-built plan) while for structural data as-built plans and core data was used. For the mix and binder property NJDOT officials in the material bureau were contacted and information regarding the particular project was obtained which was utilized in the analysis.

3.3 Assumptions

Material properties for the entire layer were unavailable for some of the sections. In such cases the material property was assumed. The assumption that was made were then checked for consistency with previous study done by other researchers and specification issued by NJDOT (NJDOT, 2007). The assumptions that were made were done in accordance to the following source of information.

1. Quality control data of NJDOT which contained the percent air void, binder content and mix gradation for similar asphalt concrete layer.
2. Gradation and modulus value for the base and subbase was assumed based on the research report by Bennert, et al., (2005).
3. Assumptions made for gradation of base and subbase was also checked with NJDOT standard specification (NJDOT, 2007)

3.4 Sections

The calibration of the alligator cracking model done in this study was a continuation of the previous study done at Rowan University (Siraj, 2008). It was found in that study, for some of the sections (7 out of 25 sections) measured alligator cracking was not reasonably close enough to the predicted cracking. Thus in this study this sections were analyzed first. For all the analysis purpose level 2 traffic and level 3 material input data was used. This was in accordance with the NCHRP recommendation for local calibration (Von Quintus, et al., 2009).

Twenty nine sections were evaluated in this study, out of which nine sections were LTPP sections from across the state. Table 3.1 lists all the sections analyzed during this study along with the AADTT, milepost and the location of the section with respect to the region. The division of regions with in the State of New Jersey was selected as specified by NJDOT (NJDOT, 2009). The next section describes how each input data were obtained from different sources.

Table 3.1 Sections with respect to region, milepost and AADTT.

Section	Region	Milepost	AADTT*
Route 183 S	North	1.3 -1.8	365
Route 94		21.8 – 22.3	550
Route 124 E		4.0 – 4.2	625
Route 159		0.1 – 0.3	728
Route 15 N (LTPP 1003)		10	1463
Route 23 S (LTPP 1030)		23.9	875
Route 139 W		0.4 – 1.1	2170
Route 64 S	Central	0.0 – 0.2	409
Route I-195 W (LTPP 0508)		10.8	3300
Route I-195 E (LTPP 1011)		10.2	2868
Route 202 S (LTPP 1033)		4.1	626
Route 95 S (LTPP 6057)		1.2	4740
Route 70 W		55.8 – 57.9	739
Route 35 S		21.4 – 21.7	1182
Route 31 S		8.7 – 9.4	1746
Route 31 S		5.9 – 6.3	1883
Route 29 N		17 – 17.8	1500
Route 29 N		17.8 – 18.1	1500
Route 29 S		17 – 17.95	1500
Route 29 S		17.95 – 18.11	1500
Route 55 S (LTPP 1034)	South	58.5	2050
Route 55 N (LTPP 1638)		57.5	2050
Route 55 N (LTPP 1031)		36.4	2860
Route 9 S		45.4 – 48.1	201
Route 322 W		37.0 – 37.2	532
Route 322 W		37.3 – 40.8	532
Route 49 W		3.3 – 5.1	666
Route 70 E		12.4 – 12.6	1780
Route 40 E		47.4 – 47.5	2150

AADTT*= Annual Average Daily Truck Traffic

3.5 Input data

As discussed above the input data consists of traffic, material and climate data. Information with regards to the pavement construction and overlay date are also required as an input in the Design Guide. The following section describes how the information was obtained for this study.

3.5.1 Traffic data

As mentioned earlier, level 2 traffic data was used in this study. The level 2 inputs with respect to traffic data includes site specific initial two way annual average daily truck traffic (AADTT), growth factor, number of lane in each direction, percent of truck in design direction, percent of truck in design lane and vehicle class distribution for that specific region.

W.I.M database (NJDOT, 2009) which contains more than fifteen years of data for most of the road section in New Jersey was used to obtain the AADTT and AADT. The W.I.M data also contains traffic class distribution which is required as an input in the Design Guide. AADT and AADTT for LTPP section 1030 is summarized in Table 3.2. Table 3.3 gives the vehicle class distribution for LTPP section 1030 from W.I.M database (NJDOT, 2009).

Table 3.2 Summary of AADT and AADTT for LTPP section 1030 (Route 23)

Year	AADT*	AADTT**
1993	24665	823
1994	25421	911
1995	25034	852
1996	25516	856
1997	24485	875
1998	24370	832
1999	25980	1042
2000	26313	1263
2001	27342	1081
2002	No data available	
2003		
2004		
2005	28232	1002
2006	27379	998
2007	27019	811
2008	26063	1065

AADT*= Annual average daily traffic
AADTT**= Annual average daily truck traffic

Table 3.3 Vehicle class distribution for north region (LTPP 1030)

Year	1993	1994	1995	1996	1997	1998	1999	2000	2001	2005	2006	2007	2008	Overall Average
% of Truck Traffic														
Class 4	1.70	1.43	2.00	2.34	1.60	0.96	1.73	1.11	1.57	4.99	4.51	3.70	2.91	2.35
Class 5	52.61	57.74	61.97	62.97	69.37	68.75	61.13	73.71	68.09	50.80	52.71	50.18	57.56	60.58
Class 6	19.08	17.67	15.14	12.73	11.09	16.11	15.93	11.40	12.77	16.37	16.93	19.11	17.00	15.49
Class 7	0.49	1.43	1.06	1.52	1.94	0.48	3.74	2.30	3.33	6.89	7.31	9.12	9.58	3.78
Class 8	4.37	3.62	3.76	5.26	4.00	3.37	4.03	2.61	3.70	7.19	6.61	2.84	1.60	4.07
Class 9	21.26	17.67	15.49	14.14	11.66	10.10	12.96	8.55	10.18	13.27	11.72	14.80	10.89	13.28
Class 10	0.49	0.44	0.59	1.05	0.34	0.24	0.38	0.32	0.37	0.50	0.20	0.25	0.47	0.43
Class 11	0.00	0.00	0.00	0.00	0.00	0.00	0.10	0.00	0.00	0.00	0.00	0.00	0.00	0.01
Class 12	0.00	0.00	0.00	0.00	0.00	0.00	0.00	0.00	0.00	0.00	0.00	0.00	0.00	0.00
Class 13	0.00	0.00	0.00	0.00	0.00	0.00	0.00	0.00	0.00	0.00	0.00	0.00	0.00	0.00
Sum	100	100	100	100	100	100	100	100	100	100	100	100	100	100

Traffic data for non-LTPP sections were obtained from multiple sources as mentioned before. AADT was available in all the sources, however percent of truck were not available in VMT database and as-built plans obtained from NJDOT. Thus for sections for which truck distribution factor could not be found out, the truck distribution for that region was assumed from W.I.M database. Table 3.4 (Siraj, 2008) list the different sources of AADTT data for Route 183. As the W.I.M data was unavailable for Route 183 the truck distribution factor was assumed based on the other section from north region.

Table 3.4 Different sources of AADTT data for Route 183 (Siraj, 2008)

Route	Year	AADTT Source			
		NJDOT As-built plan	PaveView	VMT	W.I.M
Non-LTPP Route 183 (Traffic open month, July 2002)	2000	270	290	290	No data available
	2001	280	152	330	
	2002	295	212	365	
	2003	310	212	400	
	2005	320	216	425	

3.5.2 Climate data

Climate information data were collected from online sources (Google, 2009). Climate data includes longitude, latitude, elevation and depth to ground water table for the section. The climate was found using township and county information with respect to the particular section.

3.5.3 Structure data

LTPP database (LTPP, 2008) contains all the information with respect to thickness and information about different layers present for all the LTPP section across the United States. The information that can be obtained from the LTPP database includes material property e.g. binder property, percent air void and gradation. Distress data can also be obtained from LTPP database. Figure 3.1 shows the layer thickness information obtained from LTPP database for LTPP section 1030. For non-LTPP sections structure

data was obtained from as-built plans and core summary data obtained from NJDOT material section as shown in Figure 3.2.

Figure 3.1 Information of Layers and Thickness for LTPP section 1030 (LTPP, 2008).

NEW JERSEY DEPARTMENT OF TRANSPORTATION
BUREAU OF MATERIALS ENGINEERING AND TESTING
BITUMINOUS CORE SUMMARY

02/20/02

LOT NO. : 1 PROJECT : ROUTE 183 Sec. 1B

CORE NO.	LOCATION	STATION	LANE	OFFSET (M)	THICKNESS (mm) SURFACE	Intermediate	BASE	% VOIDS SURFACE	Intermediate	BASE
1	Rt 183	2+100	L1, R1	6.5	54.0			7.7		
2	Rt 183	2+293	L1, R1	1.4	55.0			5.7		
3	Rt 183	2+438	L1, R1	6.3	60.0			5.9		
4	Rt 183	2+722	L1, R1	4.0	64.0			4.2		
5	Rt 183	2+835	L1, R1	0.4	59.0			4.8		

LOT NO.	COURSE	AIR VOIDS AVERAGE	CONTROL	LOT SIZE (S.M.)	kg/S.M./mm	AVG. THICK (mm)	PD	PAY ADJUSTMENT PERCENT	Megagram
1	SURFACE	5.7	2 - 8	9262	2.373	58.4	0.12	1.0	13
	Intermediate		2 - 8						
	BASE		2 - 8						

LOT NO. : 2

CORE NO.	LOCATION	STATION	LANE	OFFSET (M)	THICKNESS (mm) SURFACE	Intermediate	BASE	% VOIDS SURFACE	Intermediate	BASE
6	RT 183	2+072	NB SHLD	0.5	70.0			9.8		
7	RT 183	2+733	NB SHLD	1.8	64.0			4.5		
8	RT 183	2+967	NB SHLD	0.6	89.0			4.3		
9	RT 183	2+370	SB SHLD	1.6	67.0			9.0		
10	RT 183	2+923	SB SHLD	1.4	65.0			5.4		

LOT NO.	COURSE	AIR VOIDS AVERAGE	CONTROL	LOT SIZE (S.M.)	kg/S.M./mm	AVG. THICK (mm)	PD	PAY ADJUSTMENT PERCENT	Megagram
2	SURFACE	6.6	2 - 8	5653	2.375	71.0	31.14	-2.1	-20
	Intermediate		2 - 8						
	BASE		2 - 8						

Figure 3.2 Bituminous Core Summary for Route 183 (Siraj, 2008)

3.5.4 Material data

Material data for LTPP section was obtained from LTPP database (LTPP, 2008). LTPP database includes material property for the HMA surface, base and subbase layer. For non-LTPP section material data was obtained from the quality control data which was obtained from NJDOT material section. For section where some of the data was missing, appropriate assumptions were made based on Section 3.3 above. Quality control data contains the gradation, binder content, percent air void of the HMA mix. Figure 3.3 shows the quality control data obtained from NJDOT material division for Route 183.

NEW JERSEY DEPARTMENT OF TRANSPORTATION

BITUMINOUS CONCRETE - LOT DATA

Mix No.	I - 4 HD
Lot No.	1 - A
Serial No.	R1C0350

PRODUCER: Tilcon Mt. Hope Asphalt LOCATION: Mt Hope NJ

LOT STARTED: 10/15/01 (DATE) ENDED: 01/08/02 (DATE) EXACT SIZE: 2946.45 (TONS)

	PROJECT SHIPPED TO	CONTRACTOR	TONS SHIPPED
1	Rt. 183 Sec. 1B	Tilcon Paving	999.27
2	Mansfield Village Square	Union Paving	1947.18
3			
4			
		TOTAL	2946.45

LOT PORTION	A	B	C	D	E	5 SAMPLES		JOB MIX REQUIREMENTS FOR 5 SAMPLES		
Date Sampled	10/15	10/15	11/20	11/20	12/12	AVG	RANGE	MIN	MAX	RANGE
* Project Shipped To	1	1	1	1	2					
Inspector's Report No.	15	15	18	18	2					
Technician's Name	Bozza	→	→	→	→					
Inspector's Name	A. Tosto	→	F. Palang	→	W. Beck					
SIEVE SIZE PASSING	**COMPOSITION ANALYSIS**									
2" %										
1 1/2" %										
1" %	100	100	100	100	100	100		100		
3/4" %	95	99	98	97	98	97		96	100	
1/2" %	87	92	86	88	92	89		75	95	
3/8" %	75	76	73	72	83	76		65	85	
No. 4 %	47	47	49	49	53	49		35	65	
No. 8 %	35.0	33.5	33.0	33.0	37.0	34.5	4.0	30.0	38.0	13.0
No. 16 %	25	24	25	26	27	26		15	35	
No. 30 %	18	18	21	20	21	20		10	30	
No. 50 %	11	11	15	16	15	13		8	25	
No. 100 %										
No. 200 %	3.5	3.9	4.4	4.2	4.2	4.1	0.6	3.6	6.4	4.8
Asphalt %	4.75	4.80	4.90	4.85	4.85	4.85	0.15	4.45	5.35	1.5
TEST PROPERTY	**MARSHALL TEST RESULTS**							MIN.		MAX.
Stability, Lbs.	3150	2980	2795	2780	3350	3007		1500		
Flow, .01"	13.0	12.5	15.0	14.5	13.0	13.5		5		16
Air Voids, %	4.5	4.7	3.5	3.3	4.4	4.1				

* IDENTIFY PROJECT BY LINE NUMBER

REMARKS: Lot Close -- End of the Year

Ignition Oven Method [✓] Correction Factor = 0.14 Temp.= 535

Lot 1✓) Conforms ( ) Fails to Conform with Job Mix Requirements

Central File (Bituminous) / Reg. North Matls / Res. Engr. / Supplier / File / M. Calderon — U Park, Horticas

Prepared by: [signature] 2/4/02 — Engineering Tech. Materials, Date

Approved by: [signature] 2/4/02

Figure 3.3 Quality control data of Route 183 (Siraj, 2008)

Subgrade material properties were based on the study (Bennert, 2000) which tested and classified the subgrade of six road section across New Jersey. The location of this road sections were identified by different region across New Jersey. The subgrade soil properties were then categorized using AASHTO classification based on the above

mentioned study. Based on the region under which the section to be analyzed was present the AASHTO classification based on the study (Bennert, 2000) was selected.

3.6 Distress data

Measured distress data was obtained from PaveView for non-LTPP sections. For LTPP sections the measured distress data was obtained from LTPP database as well as from Pave View. Alligator cracking data was obtained from LTPP data base for LTPP section 1030 is as shown in Table 3.5.

Table 3.6 summarizes the alligator cracking data for LTPP section 1030 obtained from PaveView. For PaveView data correction had to be applied for mechanical load related cracking (Siraj, 2008) as during data collection non load related cracking were also included under load related which resulted in high percentage of cracking. Alligator cracking was calculated by subtracting the non mechanical load related cracking. Table 3.7 summarizes the alligator cracking for Route 183 obtained from PaveView.

Table 3.5 Alligator cracking data from LTPP database for LTPP section 1030

SURVEY_DATE	Month	Alligator Cracking %
5/11/1999	20	0
9/26/2001	48	3.93855
11/10/2005	98	34.4124

3.7 Summary

The above section discussed the input data that was used in the study. Different sources from which these data were obtained were also described in the section. Distress data for both LTPP and non-LTPP section were also presented in the above section. The next section deals with the analysis for these data for calibrating the alligator cracking model for the State of New Jersey.

Table 3.6 Alligator cracking information from PaveView for LTPP section 1030

Start M.P	End M.P	Date	Measured Cracking
23.3	23.4	11/27/2001	0
23.4	23.5	11/27/2001	0
23.5	23.6	11/27/2001	0
23.6	23.7	11/27/2001	0
23.7	23.8	11/27/2001	0
23.8	23.9	11/27/2001	0
23.9	24	11/27/2001	0
24	24.1	11/27/2001	0
24.1	24.2	11/27/2001	0
24.2	24.3	11/27/2001	0
23.3	23.4	3/23/2004	0
23.4	23.5	3/23/2004	0
23.5	23.6	3/23/2004	0
23.6	23.7	3/23/2004	0
23.7	23.8	3/23/2004	0
23.8	23.9	3/23/2004	0
23.9	24	3/23/2004	0
24	24.1	3/23/2004	0
24.1	24.2	3/23/2004	0
24.2	24.3	3/23/2004	0
23.3	23.4	7/14/2005	0
23.4	23.5	7/14/2005	0
23.5	23.6	7/14/2005	0
23.6	23.7	7/14/2005	0
23.7	23.8	7/14/2005	0
23.8	23.9	7/14/2005	0
23.9	24	7/14/2005	0
24	24.1	7/14/2005	0
24.1	24.2	7/14/2005	0
24.2	24.3	7/14/2005	0
23.3	23.4	12/6/2006	0
23.4	23.5	12/6/2006	0
23.5	23.6	12/6/2006	0
23.6	23.7	12/6/2006	0
23.7	23.8	12/6/2006	2.4
23.8	23.9	12/6/2006	0
23.9	24	12/6/2006	0
24	24.1	12/6/2006	0

Table 3.7 Alligator cracking data from PaveView for Route 183 (Siraj, 2008)

MP From	MP to	Date	AC Ld Mul Slight (%)	AC Ld Mul Moderate (%)	AC Ld Mul Severe (%)
1.30	1.40	5/4/2004	0.00	0.00	0.00
1.40	1.50	5/4/2004	0.00	0.00	0.00
1.50	1.60	5/4/2004	0.00	0.00	0.00
1.60	1.70	5/4/2004	0.00	0.00	0.00
1.70	1.80	5/4/2004	0.00	0.00	0.00
1.80	1.90	5/4/2004	0.00	0.00	0.00
1.90	2.00	5/4/2004	0.00	0.00	0.00

Chapter 4 Simulation of Design Guide

4.1 Introduction

This chapter deals with the simulation process by which various distress are predicted in the Design Guide with the help of a Microsoft Excel worksheet. The Design Guide takes several inputs, explained in previous chapters, and internally calculates various parameters like stress, strain and material properties like the dynamic modulus. These values are then used to predict the pavement distress for the specified design life. Different sections in this chapter deals with calculating the dynamic modulus, tensile strain at various locations and axle load spectra similar to the way it was calculated in the Design Guide and an attempt was made to predict distress. The next section gives a brief overview on the procedure adopted to simulate the process that takes place in the Design Guide. The Design Guide was simulated to facilitate better understanding of the algorithms used to predict distress.

4.2 Methodology adopted

The methodology that was adopted to simulate the process that takes place in the Design Guide was as detailed as possible to encompass all the minute details that went into the Design Guide for calculation of various distresses. Figure 4.1 shows flowchart depicting the process of simulating Design Guide. The first step in the approach was to validate the dynamic modulus equation that was used in the Design Guide. Once this dynamic modulus equation was validated the dynamic modulus obtained from the equation or the output obtained directly from the Design Guide could be used to plot the master curve. Once the master curve with respect to time and temperature was plotted, strain for particular time of loading at a specific temperature could be found out. After the master curve was plotted pavement response in the form of tensile strain was calculated for a particular loading with the help of forward calculation software

(KENPAVE was used in this study). The process of calculating the pavement response has to be done for all the loads that are expected on the pavement. Once the responses for all the loads are calculated, then the responses have to combined to find the cumulative effect of the load on the pavement at the end of the specified design life using alligator cracking model.

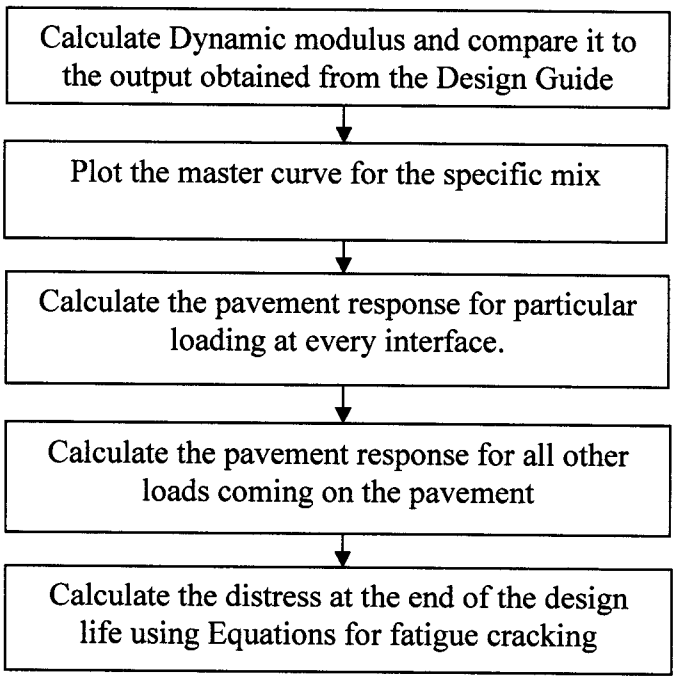

Figure 4.1 Flowchart depicting the process of simulating Design Guide in Microsoft Excel

4.3 Calculation of dynamic modulus

Dynamic modulus in the Design Guide was calculated using of Equations 2.12 – 2.16. The same equations were used in this study to calculate the dynamic modulus. The dynamic modulus was calculated at five different temperatures ranging from 10°F to 130°F. The different temperatures at which the modulus was calculated were 10°F, 40°F, 70°F, 100°F and 130°F. The dynamic modulus was also calculated at five different frequencies ranging from 0.1 Hz to 25 Hz for each temperature value. The A and VTS values were obtained from the Design Guide manual (NCHRP, 2004).

Table 4.1 gives the input values that were used in Equations 2.12 -2.16 to calculate the dynamic modulus at 70°F for LTPP section 1003. Table 4.2 lists the final value obtained after using the Equations 2.12 -2.16 along with the final dynamic modulus. The calculations at other temperatures for LTPP section 1003 are shown in Appendix A. Once the dynamic modulus is calculated it was compared to the output obtained from the Design Guide. If the values obtained from the equations were within a reasonable range to those obtained using the Design Guide then either value could be used in the next step. If the values calculated were different from the values obtained directly from Design Guide then the reason for the discrepancy were indentified. Dynamic modulus values listed in Table 4.2 were very close to the values obtained as an output. After calculating the dynamic modulus, the next step in the process was to plot the master curve for the mix.

Table 4.1 Dynamic modulus calculation table for LTPP 1033 Input table

Temperature	Frequency	Time (tr)	$P_{3/4}$ [1]	$P_{3/8}$ [2]	P_4 [3]	P_{200} [4]	V_b [5]	V_a [6]	A	VTS	Viscosity
°F	Hz	Sec	%	%	%	%	%	%			10^6Poise
70	0.1	10	0	2	31	7	11.6	5	10.7709	-3.6017	13.1
	0.5	2	0	2	31	7	11.6	5	10.7709	-3.6017	13.1
	1	1	0	2	31	7	11.6	5	10.7709	-3.6017	13.1
	5	0.2	0	2	31	7	11.6	5	10.7709	-3.6017	13.1
	10	0.1	0	2	31	7	11.6	5	10.7709	-3.6017	13.1
	25	0.04	0	2	31	7	11.6	5	10.7709	-3.6017	13.1

[1] $\rho_{3/8}$ = cumulative % retained on the 3/8 in sieve
[2] $\rho_{3/4}$ = cumulative % retained on the 3/4 in sieve
[3] ρ_4 = cumulative %retained on the No. 4 sieve
[4] ρ_{200} = %passing the No. 200 sieve
[5] V_{beff} = effective bitumen content, % by volume
[6] V_a = air void content, %

Table 4.2 Output obtained for LTPP section 1003 after using Equations 12-16

δ^1	α^2	β^3	γ^4	C^5	Log t_r [6]	t^7	Log `E*	E* [8]
								Psi (10^5)
2.9	3.8	-1.0	0.3	1.3	1.0	10.0	5.5	3.2
2.9	3.8	-1.0	0.3	1.3	0.3	2.0	5.7	4.8
2.9	3.8	-1.0	0.3	1.3	0.0	1.0	5.8	5.6
2.9	3.8	-1.0	0.3	1.3	-0.7	0.2	5.9	8.0
2.9	3.8	-1.0	0.3	1.3	-1.0	0.1	6.0	9.2
2.9	3.8	-1.0	0.3	1.3	-1.4	0.0	6.0	11

[1]δ = Using Equation 13
[2]α = Using Equation 14
[3]β = Using Equation 15
[4]γ = Using Equation 16
[5]C= constant
[6]t_r = time loading at reference temperature, sec
[7]t = time of loading at a given temperature, sec
[8]E* = Dynamic modulus, psi

4.4 Master Curve

The master curve was plotted for the binder grade AC-20 that was used in LTPP section 1003. The reference temperature in the Design Guide was 70°F. Thus, the stiffness at all other temperatures was shifted to 70°F using Equation 2.16. Figure 4.2 shows the master curve for AC 20 used in LTPP section 1003. Figure 4.2 shows the master curve in which the variation of stiffness with respect to time is shown. Once this curve was plotted and knowing the loading and rest period of the load coming on the pavement the strain and the stress in the pavement can be calculated at any temperature. The next step in the simulation process was to calculate the strain at different depths along the pavement thickness for a particular load that was expected to come on the pavement.

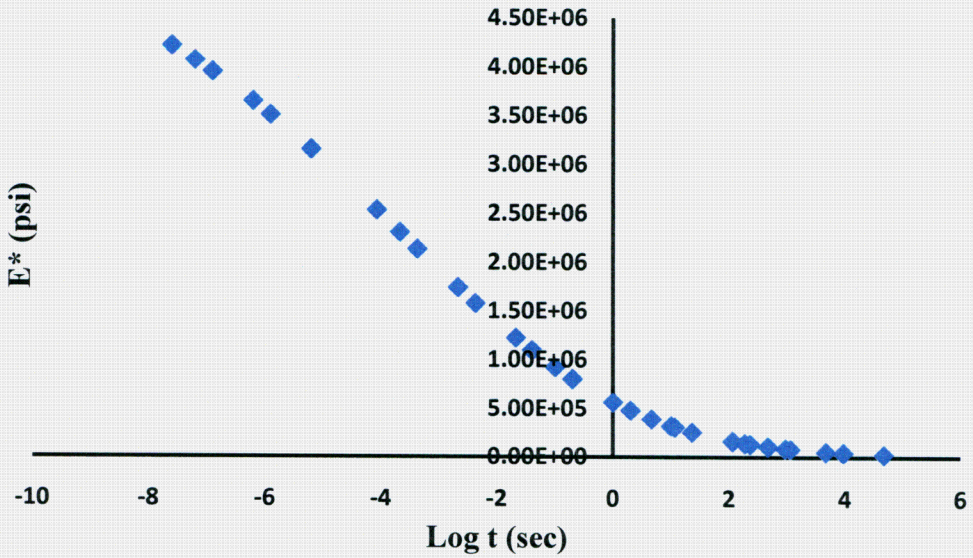

Figure 4.2 Master curve for LTPP section 1033, Log of time plotted against stiffness

4.5 Strain calculation

Strain was calculated using the stiffness value that was obtained as an output from the Design Guide. The main purpose of the simulation process was to depict the output that was obtained in the design guide. Once that was done, then the effect of each input parameter on the predicted output can be estimated accurately. Design guide specifies that there is no such fixed position of critical strain that results in cracking. The location of critical strain is dependent on pavement structure, material properties, climate and loading. Thus at the first attempt, strain at each interface was calculated for all the five temperatures for a particular loading. Different combination of stiffness and strain value were tried, to match the calculated cracking from the Excel worksheet to the predicted cracking from the Design Guide.

As the predicted cracking was very close to zero, the loading spectra were changed until the Design Guide predicted considerable cracking. For LTPP section 1003, vehicle class distribution was changed from 0% for class 13 to 100%. The corresponding alligator cracking in the pavement was observed to change from 0% to 12.5%. Also the

AADTT was changed to 24000 and the number of axle was reduced to zero for all other vehicle class except class 13. It was assumed that only single axle of class 13 trucks with number of single axle in each truck equal to five (refer Table 4.3) were coming on the pavement. Axle load configuration acting on the pavement was changed so that only 41 kip were coming on the pavement in place of the default axle load configuration for level 3. Only single axle was assumed so that the strain calculation could be done accurately. If multiple loads were assumed to come on the pavement one after the other then the strain induced due to each load and their cumulative effect would be very difficult to calculate accurately. Therefore the Excel Worksheet could not be effectively used to predict the strain accumulation at the end of the design life. Since the purpose of simulation was to understand the algorithm of predicting distress and not superposition of multiple loads, the single load coming on the pavement at a time helped in better understanding the manner by which distress was predicted in the Design Guide. Table 4.3 shows the comparison between the actual data for LTPP section 1003 and the changes that were made so that cracking was predicted.

For the purpose of strain calculation, the dynamic modulus value which was obtained as an output from the Design Guide at 70°F was selected (as it was the reference temperature). Table 4.4 shows the stiffness value obtained from the Design Guide that was used to calculate the tensile strain. The combined E value is the value that was obtained by combining the entire asphalt concrete layer. The combined stiffness value was calculated using Equation 4.1 (Huang, 2004). The critical tensile strain below each interface as recommended by the Design Guide (refer Figure 2.5) was calculated using KENPAVE which are listed in Table 4.5. The stiffness and thickness values from Table 4.4 were used to calculate the strain. The pressure at which these values were calculated was 120 psi which was equal to the tire pressure that was used for distress prediction in the Design Guide. The next section deals with comparison of the calculated cracking from the Excel worksheet and the predicted cracking from Design Guide.

$$E = \left[\frac{h_1(E_1)^{1/3}+h_2(E_2)^{1/3}}{h_1+h_2}\right]^3 \quad (4.1)$$

Where

E = Equivalent modulus of the combined layer, psi
E_1 = Modulus of the first layer, psi
E_2 = Modulus of the second layer, psi
h_1 = Thickness of first layer, inches
h_2 = Thickness of second layer, inches

Table 4.3 Comparison between actual data for LTPP 1003 and modified data to show cracking.

Properties	Original					Modified				
AADTT	1463					24000				
Vehicles class distribution	Class 4 = 4%					Class 4 = 0%				
	Class 5 = 61%					Class 5 = 0%				
	Class 6 = 11.2%					Class 6 = 0%				
	Class 7 = 1.8%					Class 7 = 0%				
	Class 8 = 4%					Class 8 = 0%				
	Class 9 = 17.4%					Class 9 = 0%				
	Class 10 = 0.4%					Class 10 = 0%				
	Class 11 = 0.2%					Class 11 = 0%				
	Class 12 = 0%					Class 12 = 0%				
	Class 13 = 0%					Class 13 = 100%				
Number of axles per truck	Vehicle Class	Single Axle	Tandem Axle	Tridem Axle	Quad Axle	Vehicle Class	Single Axle	Tandem Axle	Tridem Axle	Quad Axle
	4	1.62	0.39	0.00	0.00	4	0.00	0.00	0.00	0.00
	5	2.00	0.00	0.00	0.00	5	0.00	0.00	0.00	0.00
	6	1.02	0.99	0.00	0.00	6	0.00	0.00	0.00	0.00
	7	1.00	0.26	0.83	0.00	7	0.00	0.00	0.00	0.00
	8	2.38	0.67	0.00	0.00	8	0.00	0.00	0.00	0.00
	9	1.13	1.93	0.00	0.00	9	0.00	0.00	0.00	0.00
	10	1.19	1.09	0.89	0.00	10	0.00	0.00	0.00	0.00
	11	4.29	0.26	0.06	0.00	11	0.00	0.00	0.00	0.00
	12	3.52	1.14	0.06	0.00	12	0.00	0.00	0.00	0.00
	13	2.15	2.13	0.35	0.00	13	**5.00**	0.00	0.00	0.00
Axle load (kip)	3000 – 41000					41000				
Material Properties	Same									
Climate										

Table 4.4 Stiffness value at 70°F for LTPP section 1003 obtained from Design Guide.

	Thickness (in)									
Month	**0.5**	**0.5**	**1.2**	**1**	**1**	**3.5**	**7.7**	**24.9**	**Infinite**	**Combined E**
	Stiffness (10^6 psi) below the specified thickness									
May	2.4	2.0	1.7	0.9	0.9	0.8	0.03	0.05	0.01	0.95
June	1.4	1.7	1.0	0.4	0.4	0.4	0.03	0.05	0.01	0.50
July	1.1	0.9	0.8	0.3	0.3	0.3	0.03	0.05	0.01	0.40
August	1.3	1.1	0.9	0.4	0.4	0.3	0.03	0.05	0.01	0.45
September	2.0	1.7	1.4	0.7	0.6	0.6	0.03	0.05	0.01	0.72
October	3.5	3.2	2.8	1.5	1.5	1.5	0.03	0.05	0.01	1.60
November	3.6	3.5	3.4	1.5	1.5	1.5	0.03	0.05	0.01	1.67
December	3.6	3.5	3.4	1.5	1.5	1.5	0.05	0.05	0.01	1.67
January	3.6	3.5	3.4	1.5	1.5	1.5	0.02	0.05	0.01	1.67
February	3.6	3.5	3.4	1.5	1.5	1.5	1.00	0.08	0.01	1.67
March	3.6	3.5	3.4	1.5	1.5	1.5	0.14	0.03	0.01	1.67
April	3.6	3.5	3.4	1.5	1.5	1.5	0.02	0.03	0.01	1.67

Table 4.5 Critical strain below thickness as specified by Design Guide for LTPP section 1003.

Month			**Thickness (in)**			
	0.5	**1**	**2.2**	**3.2**	**4.2**	**7.7**
	Critical Tensile Strain (microstrains) below the specified thickness					
May	140	107	33	-16	-63	-250
June	191	142	32	-36	-100	-355
July	213	157	30	-45	-117	-396
August	195	142	22	-51	-119	-381
September	154	115	26	-30	-85	-295
October	102	79	28	-6	-40	-174
November	97	75	23	-10	-43	-175
December	91	70	23	-8	-38	-158
January	100	77	23	-11	-45	-182
February	50	41	22	10	1	-30
March	88	69	25	-3	-31	-137
April	111	85	26	-13	-52	-205

Note: - = Tensile strain, + = compressive strain

4.6 *Comparing predicted cracking obtained from the Design Guide to calculated cracking from Excel sheet*

The strain calculated in Table 4.5 was used to calculate the cracking using the constants already embedded in the alligator cracking model. For the purpose of calculating cracking, an Excel worksheet was created which included all the input that were in the alligator cracking model in the Design Guide along with the calibration constant and other coefficients. Table 4.6 shows the different combinations that were tried for LTTP 1003. Table 4.7 shows the input data that was used to calculate cracking. The stiffness that was used was the combined value determined from Equation 4.1 for the entire asphalt concrete layer. Table 4.8 and 4.9 show the output obtained from excel worksheet created to simulate Design Guide prediction and the output directly obtained from the Design Guide respectively.

The combination shown in Table 4.9 were the best results achieved after trying various combinations of stiffness and strain. The various combinations included, trying each stiffness value with the corresponding strain and thickness of that particular layer. The combined stiffness value was also tried with all the thickness and strain values till the closest possible match was achieved. In all about eighteen combinations for the modified data listed in Table 4.6 were carried out. Figure 4.3 shows comparison between calculated alligator cracking for LTPP section 1003 for design life of 240 along with the percent difference between predicted and calculated cracking. It can be observed that even for the closest match the percent difference between the predicted and calculated cracking was close to 90%. The next section of this chapter gives possible reasons for the difference between the predicted and calculated cracking.

Table 4.6 Combinations tried to obtain the best results for the Excel Sheet Developed

Stiffness	Strain	Thickness
E_1	ε_1	H_1
E_2	ε_2	H_2
E_3	ε_3	H_3
E_4	ε_4	H_4
E_5	ε_5	H_5
E_6	ε_6	H_6
E_C	ε_1	H_1
	ε_2	H_2
	ε_3	H_3
	ε_4	H_4
	ε_5	H_5
	ε_6	H_6
	ε_1	H_T
	ε_2	
	ε_3	
	ε_4	
	ε_5	
	ε_6	

Note:
$E_{n(1-6)}$ = Stiffness of layer, psi
$\varepsilon_{n(1-6)}$ = Strain beneath each layer, microstrains
$H_{n(1-6)}$ = Thickness of each layer, inches
E_C = Combined stiffness of all the layers, psi
H_T = Combined thickness of all the layers, inches

Table 4.7 Input sheet for the Excel sheet created to simulate the cracking prediction done by the Design Guide for first twelve months

Months	H_{HMA}	E_{HMA}	ε_t 10^-6	V_{be}	V_a	n	k_{f1}	k_{f2}	k_{f3}	M	C	C_H	C_2^*	C_1^*	C_4
	in	psi	Radial Strain	%	%										
1	7.7	953640.8	6.32E-05	8.8	5	8.45E+05	0.007566	3.9492	1.281	0.25322	0.558183	250	2.49116	4.982326	6000
2	7.7	503292	1.00E-04	8.8	5	8.45E+05	0.007566	3.9492	1.281	0.25322	0.558183	250	2.49116	4.982326	6000
3	7.7	404274.3	1.17E-04	8.8	5	8.45E+05	0.007566	3.9492	1.281	0.25322	0.558183	250	2.49116	4.982326	6000
4	7.7	448798.8	1.19E-04	8.8	5	8.45E+05	0.007566	3.9492	1.281	0.25322	0.558183	250	2.49116	4.982326	6000
5	7.7	717965.6	8.45E-05	8.8	5	8.45E+05	0.007566	3.9492	1.281	0.25322	0.558183	250	2.49116	4.982326	6000
6	7.7	1604442	4.01E-05	8.8	5	8.45E+05	0.007566	3.9492	1.281	0.25322	0.558183	250	2.49116	4.982326	6000
7	7.7	1671127	4.33E-05	8.8	5	8.45E+05	0.007566	3.9492	1.281	0.25322	0.558183	250	2.49116	4.982326	6000
8	7.7	1671092	3.85E-05	8.8	5	8.45E+05	0.007566	3.9492	1.281	0.25322	0.558183	250	2.49116	4.982326	6000
9	7.7	1671092	4.54E-05	8.8	5	8.45E+05	0.007566	3.9492	1.281	0.25322	0.558183	250	2.49116	4.982326	6000
10	7.7	1671050	1.00E-06	8.8	5	8.45E+05	0.007566	3.9492	1.281	0.25322	0.558183	250	2.49116	4.982326	6000
11	7.7	1671008	3.09E-05	8.8	5	8.45E+05	0.007566	3.9492	1.281	0.25322	0.558183	250	2.49116	4.982326	6000
12	7.7	1671050	5.18E-05	8.8	5	8.45E+05	0.007566	3.9492	1.281	0.25322	0.558183	250	2.49116	4.982326	6000

Table 4.8 Output obtained from the worksheet developed for the first and last twelve months

Month	$N_{f\text{-}HMA}$	DI_{Bottom}	Cracking at bottom of asphalt layer
	$(*10^{8})$	$(*10^{-3})$	%
1	8.9	9.5	0.1
2	3.3	3.6	0.2
3	2.3	7.2	0.5
4	1.9	11.6	0.8
5	4.1	13.7	0.9
6	2.7	14.0	0.9
7	19.3	14.5	1.0
8	30.7	14.7	1.0
9	15.9	15.3	1.1
10	15.9	15.8	1.1
11	72.8	15.9	1.1
12	9.5	16.8	1.1
229	8.9	320	22.6
230	3.3	323	22.8
231	2.3	326	23
232	1.9	331	23.2
233	4.1	333	23.3
234	2.7	333	23.4
235	1.9	334	23.4
236	3.1	334	23.4
237	15.9	334	23.4
238	15.9	335	23.5
239	72.8	335	23.5
240	9.5	336	23.5

Table 4.9 Output obtained from Design Guide for LTPP section 1003

Month	DI_{Bottom}	Cracking at bottom of asphalt layer
		%
1	0.02	0.01
2	0.12	0.07
3	0.27	0.17
4	0.37	0.23
5	0.40	0.26
6	0.41	0.26
7	0.41	0.26
8	0.41	0.26
9	0.41	0.26
10	0.41	0.26
11	0.41	0.26
12	0.41	0.26
229	15.8	11.9
230	16	12.1
231	16.2	12.3
232	16.4	12.4
233	16.5	12.5
234	16.5	12.5
235	16.5	12.5
236	16.5	12.5
237	16.5	12.5
238	16.5	12.5
239	16.5	12.5
240	16.5	12.5

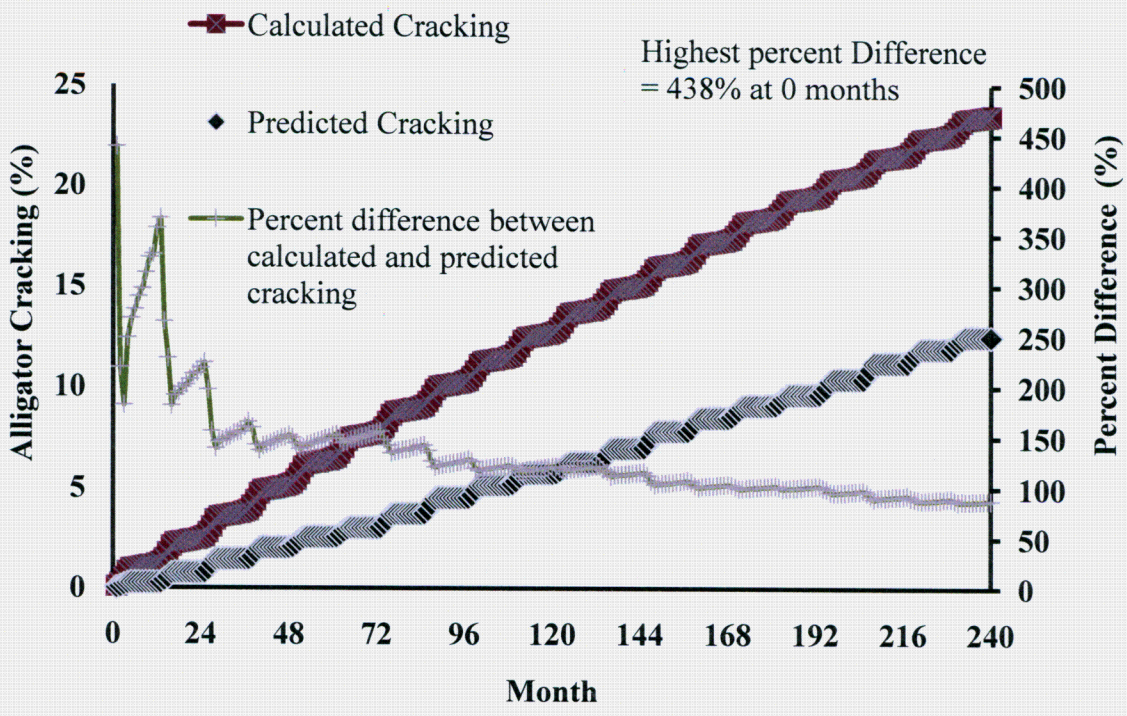

Figure 4.3 Comparison between predicted and calculated alligator cracking for LTPP section 1003 for the design life of 240 months.

4.7 Causes for difference between predicted and calculated cracking

The comparison of predicted and calculated cracking as discussed above was done for only one vehicle class distribution and single axle load coming on the pavement. The error of about 90% was found to be present for the given conditions. It was also observed that a constant error of about 95% was present in the damage index calculation. To confirm the reasons for the high difference in predicted and calculated cracking the damage index which was obtained as one of the output from the Design Guide was used to calculate the cracking. Figure 4.4 shows the comparison of predicted and calculated cracking when the damage index obtained from the Design Guide was used. It can be observed that the difference between the predicted and calculated cracking is minimal with the maximum percentage difference of 3%. Thus it can be stated that the error that was previously observed was due to error in damage index calculation. Damage index

calculation as stated previously (in section 2.3.4) calculates the number of repetition to failure. Damage index calculation takes into account various factors including the axle load, class distribution, monthly distribution of vehicles with respect to the number of axles coming on to the pavement. The loading and the rest period is internally calculated in the Design Guide for all the different types of load coming on the pavement. Also the strain corresponding to each load and at each interface is calculated and the cumulative strain is used to calculate the damage index and finally the cracking. Thus if the cumulative strain was used above in place of the individual strain value the calculated cracking would be even higher and the percent difference between calculated and predicted would be even more.

Effort was made to include all the corresponding strain value with their respective stiffness value for each loading. However to simulate such a process in an Excel worksheet to get a reasonable output was found to be difficult. A considerable time and effort was spent in creating the excel worksheet and trying various combination so that the calculated and predicted cracking matched. However these efforts were not successful and the focus of the study was then shifted to recalibrating the alligator cracking model for the State of New Jersey.

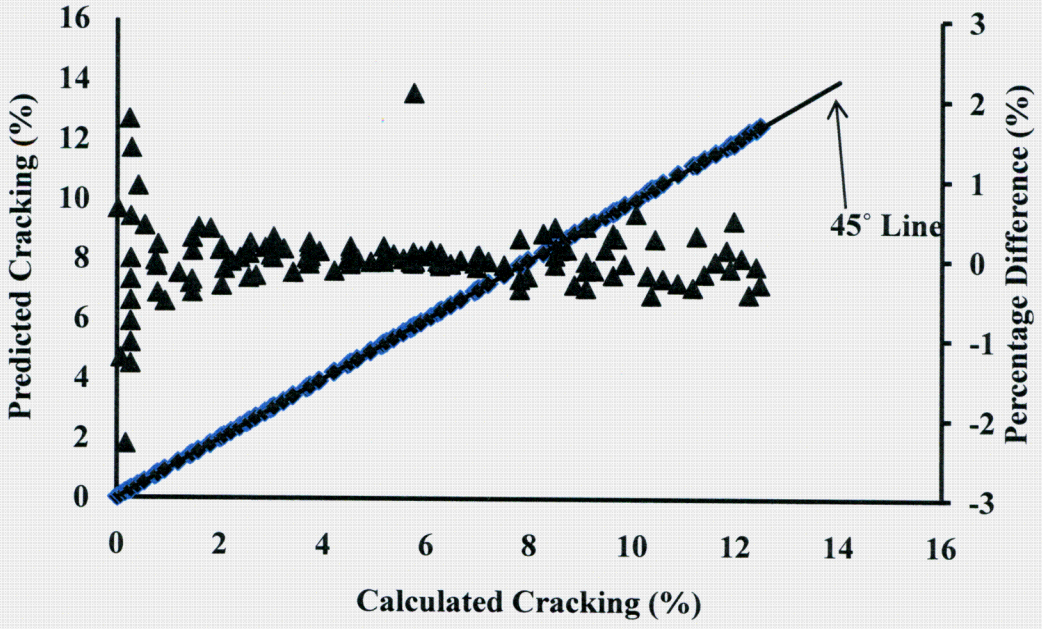

Figure 4.4 Comparison between Predicted and calculated cracking when Damage Index from Design Guide was used for LTPP section 1003.

4.8 Summary

The above chapter showed the attempt that was made to simulate the process that takes place in the Design Guide in predicting alligator cracking with the help of an Excel Worksheet. The algorithm that was used in the Design Guide was too complex to recreate from start to finish using a spread sheet. However various part of the calculation was recreated using the spreadsheet. The main reason behind the simulation was to understand the algorithm that was used to predict cracking and the effect of each input parameter on cracking prediction. This knowledge was then used in the next part of this study, where focus of the study shifts from simulation of the Design Guide to calibrating the model for the State of New Jersey. These aspects are discussed in detail in the next chapter.

Chapter 5 Calibration and validation of the alligator cracking model

5.1 Introduction

The following chapter deals with the calibration of the alligator cracking model using regional data for the State of New Jersey. The calibration was done in accordance with the guidelines specified by NCHRP (refer section 2.10 and 2.11 above). Also at various stages during the calibration process, previous studies done by other researchers for calibration of alligator cracking for other states are referenced (as mentioned in section 2.9). Calibration of the alligator cracking involved trying various combinations of the beta values until a reasonable match between the predicted and measured values were obtained. The results obtained from each of these combinations are not listed here, but overviews as to what combinations were tried before the final values were chosen are described in section below. Calibration of the alligator cracking model was achieved by calibrating the beta values which are embedded in the equation used for predicting the number of axles to failure (Equation 2.5). The reasons and the process by which beta values were calibrated are described in the next section in detail.

5.2 Why Beta values?

The beta factors (β_{fi}) present in Equation 2.5 were introduced to eliminate the bias and scatter in predictions that arose from the global calibration factor K (k_{fi}). All the three beta factors provided in the equation were related to different pavement properties and response as listed in Table 5.1. The K factors were determined through laboratory testing of material properties while the beta factors were introduced to reduce the scatter and bias once all the values were compared on a national scale. The discrepancy between the predicted and measured data for some regions might be more as compared to other

regions, depending on how much the measured data was scattered when it was compared to the national average cracking values. The above stated reason leads to the need for recalibration of these beta values, as the first step towards calibration of the prediction model for any particular State before recalibrating any other parameter in the model.

Table 5.1 Relationship of beta values with pavement properties and response affected

Pavement property or response	Beta values	Default value
AC thickness	β_{f1}	1
Tensile strain	β_{f2}	1
Material stiffness	β_{f3}	1

Table 5.1 shows which beta values were used during the national calibration process to reduce the scatter and bias in prediction of the pavement response and/or properties along with the default value of these beta values. The effect of each parameter or property on cracking prediction is explained below.

The thickness of pavement varies depending on the type of roads (major highways, urban roads, local roads) and also from state to state. The thickness correction factor (C_H) which was already embedded in prediction equation was included mainly for sections with higher thickness. However, β_{f1} was included for thickness that differed from average national values. The tensile strain induced is dependent on the load coming on the pavement as well as the rest and loading period. As the cracking model was developed on the national scale the default truck distribution might differ greatly for some state. The default class 13 truck embedded in Design Guide was 13% while that for New Jersey was close to 0%. Thus, the strain induced for traffic level present in New Jersey would differ greatly when compared to strain induced for default national values. To get the strain values for States like New Jersey close to the national values, β_{f2} was introduced. The material stiffness is one of the factors that play an important role in

determining the fatigue life of the pavement. As the stiffness of asphalt concrete is dependent on variety of factors, β_{f3} was introduced to eliminate the bias and scatter caused due to the difference in prediction caused due to the stiffness of the material present.

Moreover, the Design Guide manual (NCHRP, 2004) specifies that for calibration of fatigue model it is these beta factors (B_{fi}) that should be calibrated as the first step towards calibration of the fatigue cracking model. Based on all the above stated reasons and after reviewing studies (Refer Section 2.9) done in other states it was decided to recalibrate the beta values as part of calibrating the alligator cracking model for the State of New Jersey. The next section deals with sections that were used for calibration and validation.

5.3 Sections

Of the total of twenty nine sections that were evaluated in this study, fourteen were used for calibrating the model while the remaining fifteen sections were used for validating the new values. The sections were divided equally based on the region as shown in Table 5.2 (refer Chapter 3). Also LTPP sections were divided equally between calibration and validation as these sections showed considerably more cracking as compared to other sections. In all, there were 120 measured data points to be matched with predicted data for the calibration of alligator cracking model.

Table 5.2 Calibration and validation section.

Region	Section	Milepost	Annual Average Daily Truck Traffic	Max. Alligator Cracking (%) / Months after construction	Calibration/ Validation
North	183 S	1.3 – 1.8	365	0/48	C
	94	21.8 – 22.3	550	0/129	C
	124 E	4.0 – 4.2	625	0/88	V
	159	0.1 – 0.3	728	0/144	V
	15 N (LTPP 1003)	10	1463	56.15/138	V
	23 S (LTPP 1030)	23.9	875	34.41/102	C
	139 W	0.4 – 1. 1	2170	0/159	C
Central	64 S	0.0 – 0.2	409	0/159	V
	I-195 W (LTPP 0508)	10.8	3300	3.5/139	C
	I-195 E (LTPP 1011)	10.2	2868	0/16	V
	202 S (LTPP 1033)	4.1	626	50.95/70	C
	95 S (LTPP 6057)	1.2	4740	9.7/162	V
	70 W	55.8 – 57.9	739	0/64	V
	35 S	21.4 – 21.7	1182	0/35	C
	31 S	8.7 – 9.4	1746	0/121	C
	31 S	5.9 – 6.3	1883	0/126	V
	29 N	17 – 17.8	1500	0/103	C
	29 N	17.8 – 18.1	1500	0/103	V
	29 S	17 – 17.95	1500	0/103	C
	29 S	17.95 – 18.11	1500	0/103	V
South	55 S (LTPP 1034)	58.5	2050	20.8/180	V
	55 N (LTPP 1638)	57.5	2050	17.09/200	C
	55 N (LTPP 1031)	36.4	2860	0.78/115	C
	9 S	45.4 – 48.1	201	0/139	V
	322 W	37.0 – 37.2	532	0/167	C
	322 W	37.3 – 40.8	532	0/167	V
	49 W	3.3 – 5.1	666	0/132	C
	70 E	12.4 – 12.6	1780	0/37	V
	40 E	47.4 – 47.5	2150	0/64	V

The minimum number of section required based on the NCHRP 1-40B report was eight as calculated using Equation 2.21 (refer section 2.11.2). The minimum sample size required based on Equation 21 for 95% confidence interval with tolerable bias of 2.5 is 16. Thus the total number of sample present in this study (29 with 164 data point) satisfies the condition. The next section shows the how the calibration of the alligator cracking model was carried out.

5.4 Calibration

The original values that were used in the calibration of the fatigue model for β_{f2} were 0.8, 1.0 and 1.2 while that for β_{f3} were 0.8, 1.5 and 1.2, respectively. These values acted as a starting point for this calibration study. As the interval between the original values were too large the combinations tried in this study focused on reducing the interval and then comparing the predicted output to measured data. The initial combination focused on increasing the interval by 0.02 for both β_{f2} and β_{f3} as listed in Table 5.3. However it was soon realized that the difference between the measured and the predicted cracking was still large. The next step was including β_{f1} also as part of the calibration process. As the range for β_{f1} was not provided in the Design Guide, the values provided in studies conducted in other states were selected as a starting point and then changed accordingly (Section 2.9). The total numbers of combinations after the above mentioned interval were applied to the beta values yielded a total of 3528 combinations. These combinations were tried as part of the first attempt to calibrate the alligator cracking model. On an average, it would take about 20 minutes for one combination to run. Thus, for 3528 combination an estimated 1100 hours was required. After obtaining the output from the Design Guide, each of the predicted output had to be compared to measured field data. This was done to calculate the difference between predicted and the measured data. After conducting these first set of 3528 runs the values were narrowed down and a new range of beta values were established.

As the number of combination was so large, only one section was calibrated and once the predicted and measured started giving a reasonable match then those values were tried for calibration of other sections. After running the first trial of 3528

combination, it was seen that the range of beta values for which predicted values was closer to measured data was within a comparatively smaller range as compared to the initial assumed range as listed in Table 5.3. The new ranges of beta values are listed in Table 5.4. As the range got closer the interval was reduced from 0.02 for β_{f1} and β_{f2} to 0.01 while that for β_{f3} was reduced from 0.5 to 0.05.

Table 5.3 Combination of Beta values tried for calibration

β_{f1}	β_{f2}	β_{f3}
0.8	0.8 – 1.2 (with 0.02 increment)	0.8 - 2.5 (with 0.5 increment)
0.82		
0.84		
0.86		
0.88		
0.9		
0.92		
0.94		
0.96		
0.98		
1		
1.02		
1.04		
1.06		
1.08		
1.1		
1.12		
1.14		
1.16		
1.18		
1.2		

Table 5.4 Revised range of beta values after first trial

β_{f1}	β_{f2}	β_{f3}
0.8	0.9 – 1.0 (with an increment of 0.01)	1 – 1.5 (with an increment of 0.05)
0.81		
0.82		
0.83		
0.84		
0.85		
0.86		
0.87		
0.88		
0.89		
0.90		

The revised range of beta values was used for calibration of multiple sections. They were analyzed to see the effect of new beta values on the predicted output. As the LTPP sections showed considerable cracking as compared to other sections they were calibrated first. LTPP sections 1033, 1031, 1638 and 0508 were tried with second set of beta values. After comparing results for the four sections the best possible match that was obtained was using beta values of 0.81, 0.94 and 1.2 for β_{f1}, β_{f2} and β_{f3} respectively. This combination of beta value was then tried with the remaining calibration sections. The comparison of predicted and measured data for Route 202 S (LTPP section 1033), I-195 W (LTPP section 0508), Route 23 S (LTPP section 1030) and Route 23 S are as shown in Figure 5.1, 5.2, 5.3 and 5.4 respectively. The comparisons of other calibration section are present in Appendix B.

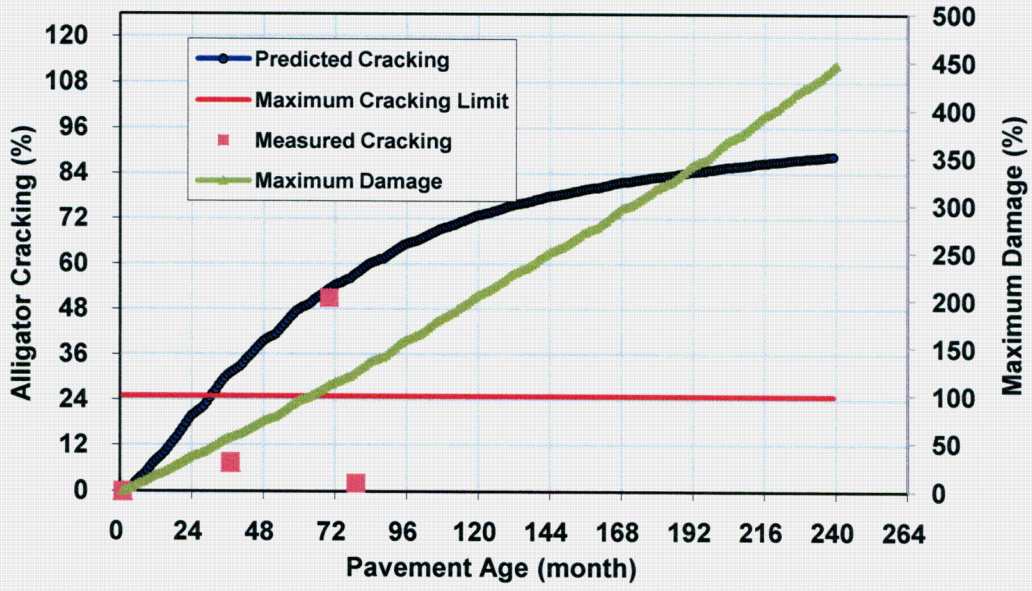

Figure 5.1 Comparison for Route 202 S (LTPP section 1033) for beta value 0.81, 0.94 and 1.2

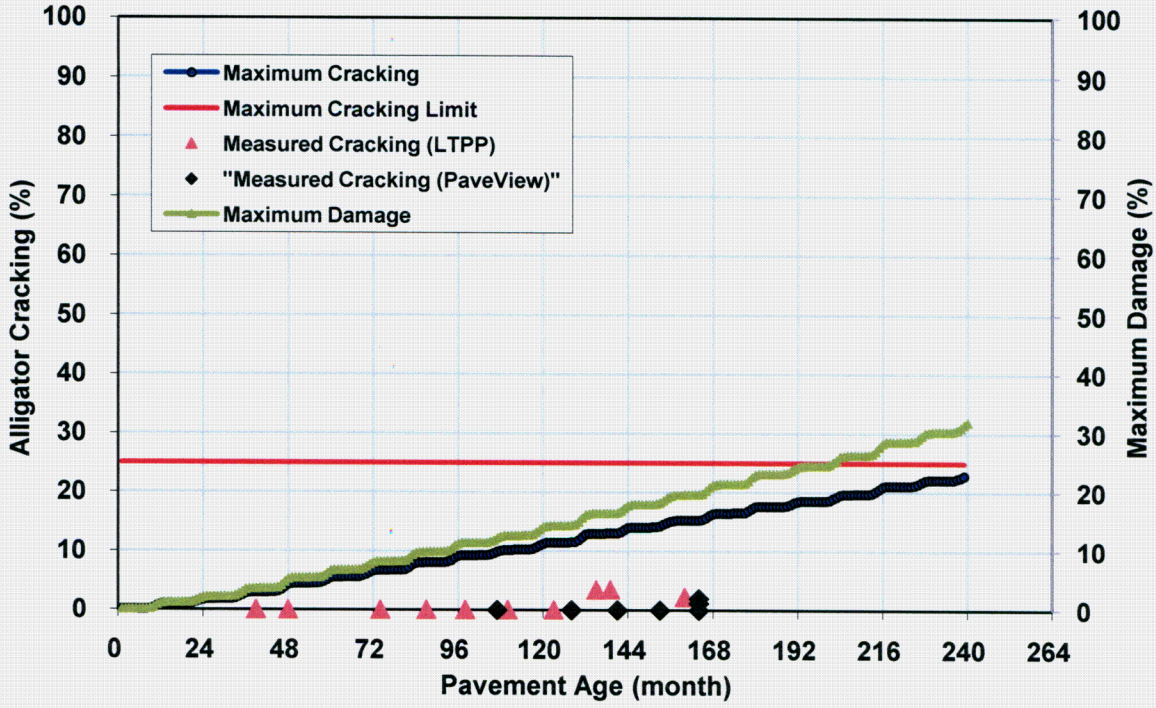

Figure 5.2 Comparison for Route I-195 W (LTPP section 0508) for beta value 0.81, 0.94 and 1.2.

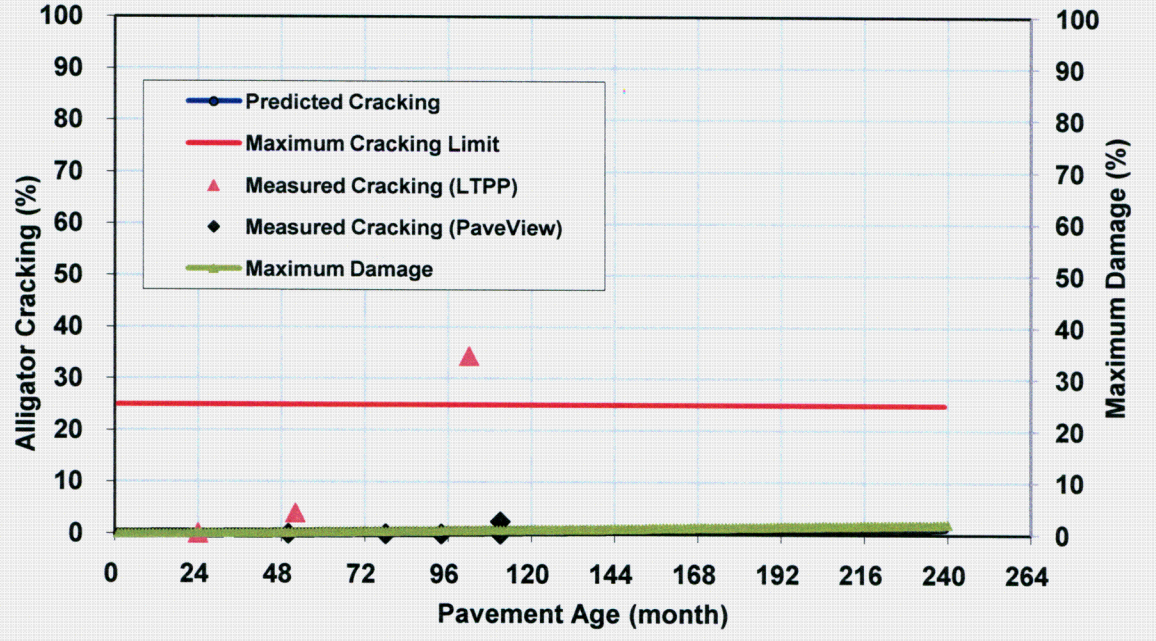

Figure 5.3 Comparison for Route 23 S (LTPP section 1030) for beta value 0.81, 0.94 and 1.2.

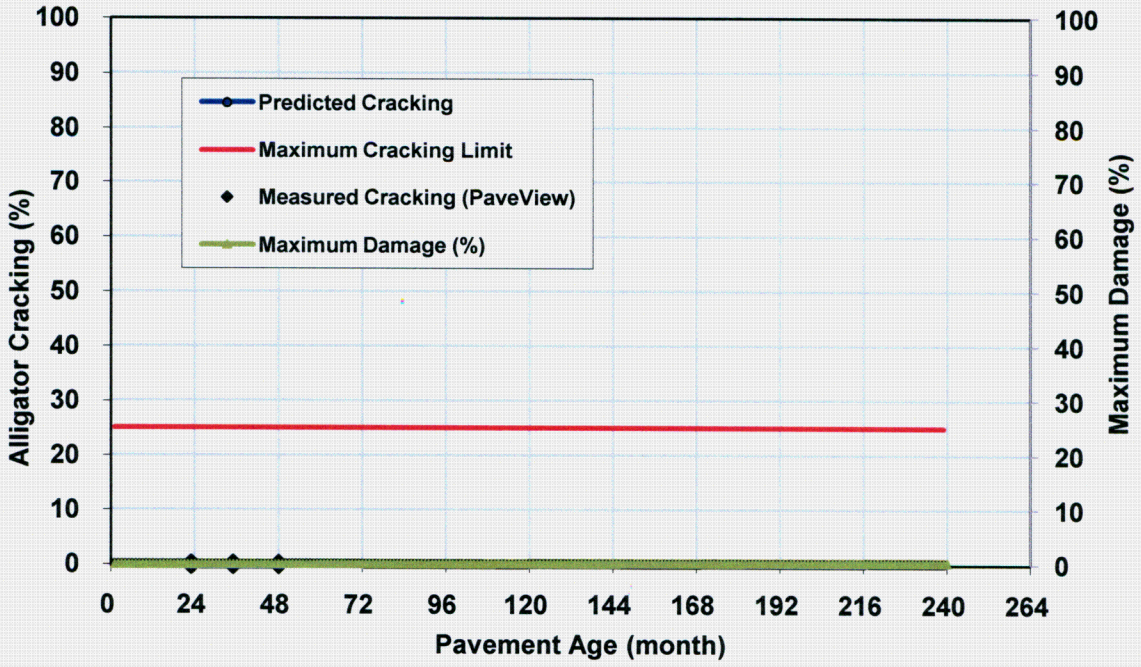

Figure 5.4 Comparison for Route 183 S for beta value 0.81, 0.94 and 1.2

Figure 5.1 shows that route 202 S (LTPP section 1033) showed considerable cracking as compared to other sections. The measured cracking increases and then drops. This drop might be due to resurfacing or other rehabilitation work carried out. The prediction shows a good match with the measured data until the drop in the measured cracking was observed. Presently the prediction of rehabilitation work carried out in middle of the design period specified in the Design Guide is not possible. Thus, the drop in the measured cracking that was observed was not captured in the predicted trend. The measured PaveView cracking has a value equal to zero which was observed for almost all the sections. During the calibration process if LTPP data was present then the prediction was tried to match it with the LTPP measured data as Design Guide was originally calibrated with this data set. However for section with only PaveView dataset the calibration was carried to match those values with the predicted data.

On comparing Figure 5.1and 5.2, it is evident that I-195 W (LTPP section 0508) cracked less than Route 202 S. The measured cracking for this section shows cracking around 135 months and then drops around 160 months. The cracking observed was around 3.5% at 140 months while the predicted cracking was 13% at the same pavement age. This difference was considered to be reasonable taking into account that input data

was concentrated between level 2 and 3. Figure 5.3 shows (Route 23 S - LTPP section 1030) considerable cracking which was not predicted by the Design Guide for these particular beta values. The predicted cracking did predict similar cracking for other set of beta values (0.8, 0.84, and 1.2). However, these beta values predicted high cracking for all the section even when the measured cracking was close to 0%. It was expected that few sections predictions might differ from the measured values. When all the calibration sections were looked at together and if the comparison of measured and predicted values where within reasonable range for the given set of beta values, those values were selected which were 0.81, 0.94 and 1.2. Figure 5.4 shows route 183 S, the predicted as well as the measured cracking show a very good match which was close to 0%. The next section explains the validation effort carried out to validate the new beta values that were found as part of the calibration process.

5.5 Validation

Validation effort not only concentrated on the validation section but all the sections studies were included to find the overall error present. The validation consisted of testing the beta values established during the calibration process (0.81, 0.94 and 1.2) on the sections as listed in Table 5. Figure 5.5, 5.6 and 5.7 shows three typical sections showing considerably "good" match for "high" crack, "not so good" match for "high" crack and "good" match for "low" crack, respectively. The cracking prediction (Figure 5.5) shows considerably good match before a reduction in the measured data was observed. The rehabilitation work is not captured by the Design Guide prediction. Figure 5.6 shows a section for which the prediction was very low as compared to measured data. Similar to 23 S (LTPP section 1030) the beta values that showed cracking similar to measured cracking were 0.8, 0.84 and 1.2. The only difference from Route 23 S was β_1 value of 0.81. Comparisons of predicted and measured cracking data for other sections are listed in Appendix B. For validating these new beta values all the section were compared together to find the average error as well to compare the overall difference and similarity in the predicted and measured value.

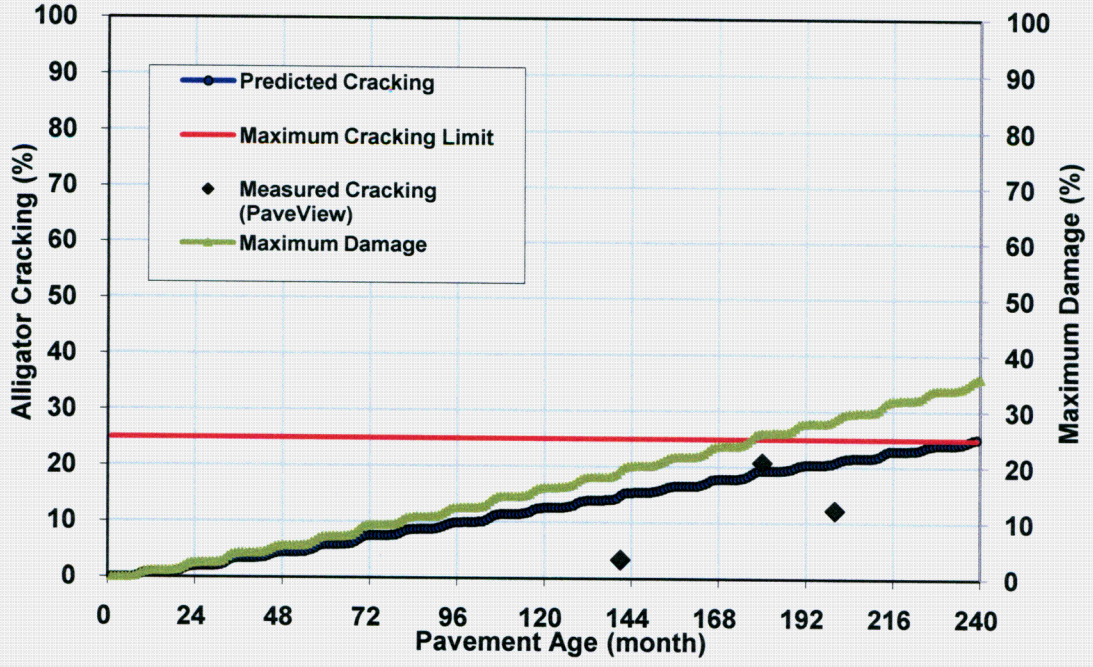

Figure 5.5 Comparison for Route 55 S (LTPP section 1034) for beta value 0.81, 0.94 and 1.2.

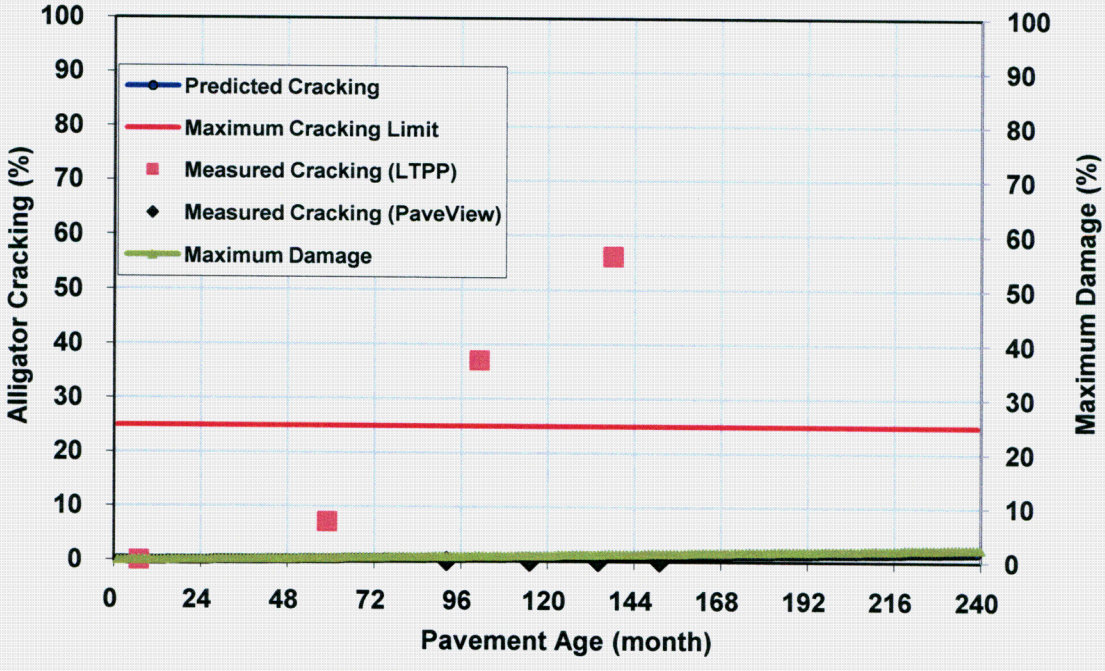

Figure 5.6 Comparison for Route 15 N (LTPP section 1003) for beta value 0.81, 0.94 and 1.2.

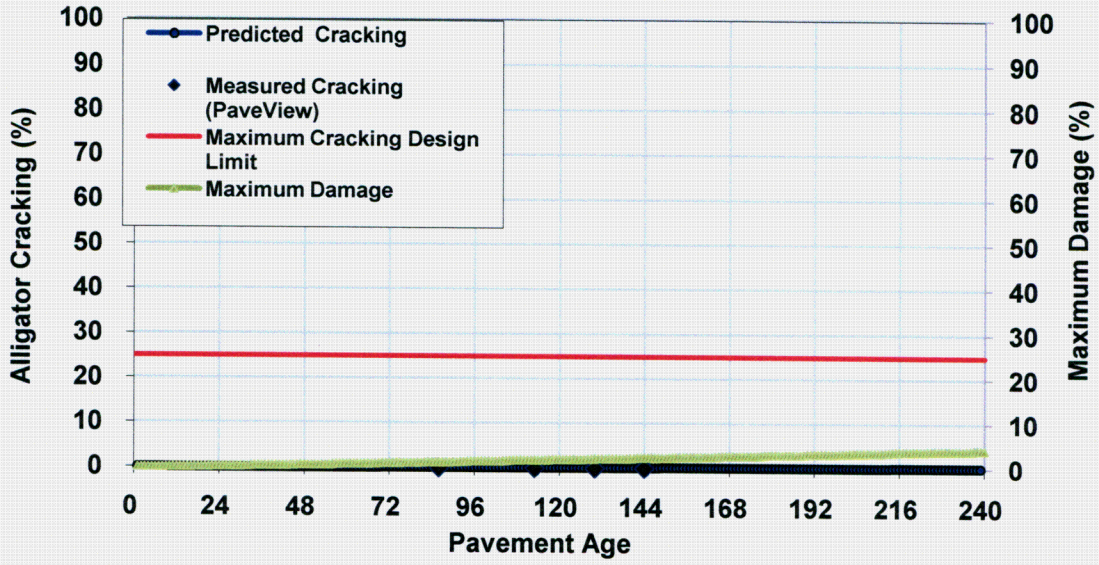

Figure 5.7 Comparison for Route 159 for beta value 0.81, 0.94 and 1.2.

Table 5.5 shows the comparison of the measured and predicted cracking for the 29 sections evaluated in this study. It can be observed that the standard deviation for both measured as well as predicted cracking were on the higher side. This was due to the fact that LTPP data showed considerable cracking while non-LTPP section showed very litle to no cracking. It can also be observed that the average cracking for both measured as well as predicted are considerably low if compared to the default design limit of 25%. The average cracking for measured data was 2.579% while that for predicted data was 5.97%. Figure 5.8 shows the graphical comparison of the measured and predicted cracking. The bar above each crack represents the 95% confidence interval. It can be observed from Figure 5.8 a reasonable overlap exist between the predicted and measured cracking considering the input level were level 2 and 3. The comparison of predicted and measured cracking for all the data points can be observed in Figure 5.9. The number of data points that showed large difference between predicted and measured cracking are listed in Table 5.6.

Table 5.5 Comparison between measured and predicted cracking for 29 Sections with 120 data points

	Average Cracking (%)	Standard Deviation	Standard Error
Measured Cracking	2.579	8.791	0.802
Predicted Cracking	5.97	14.6	1.33

Table 5.6 Data points showing considerable difference between predicted and measured cracking for total 120 data points.

Percent Difference between measured and predicted	Number of data points	Percent of sections exceeding
Greater than 15 %	9	7.5
10 – 15%	6	5
5 – 10%	14	11.7
Less than 5%	91	75.8

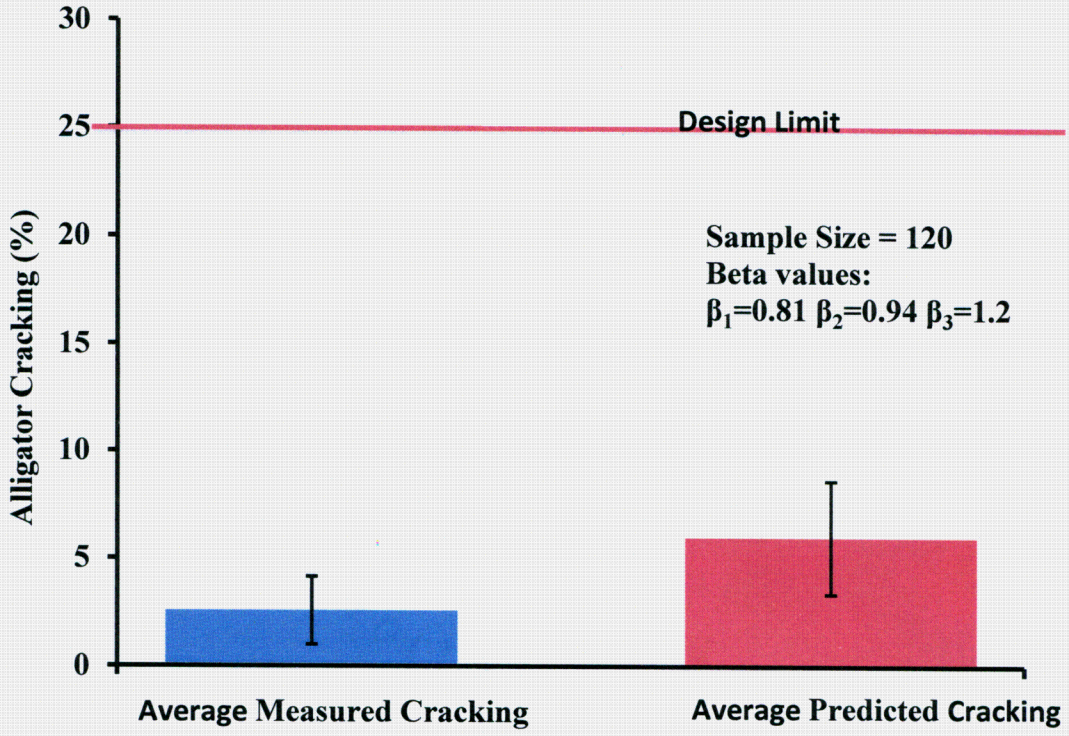

Figure 5.8 Comparison of Measured and predicted cracking for 29 sections with 120 data points.

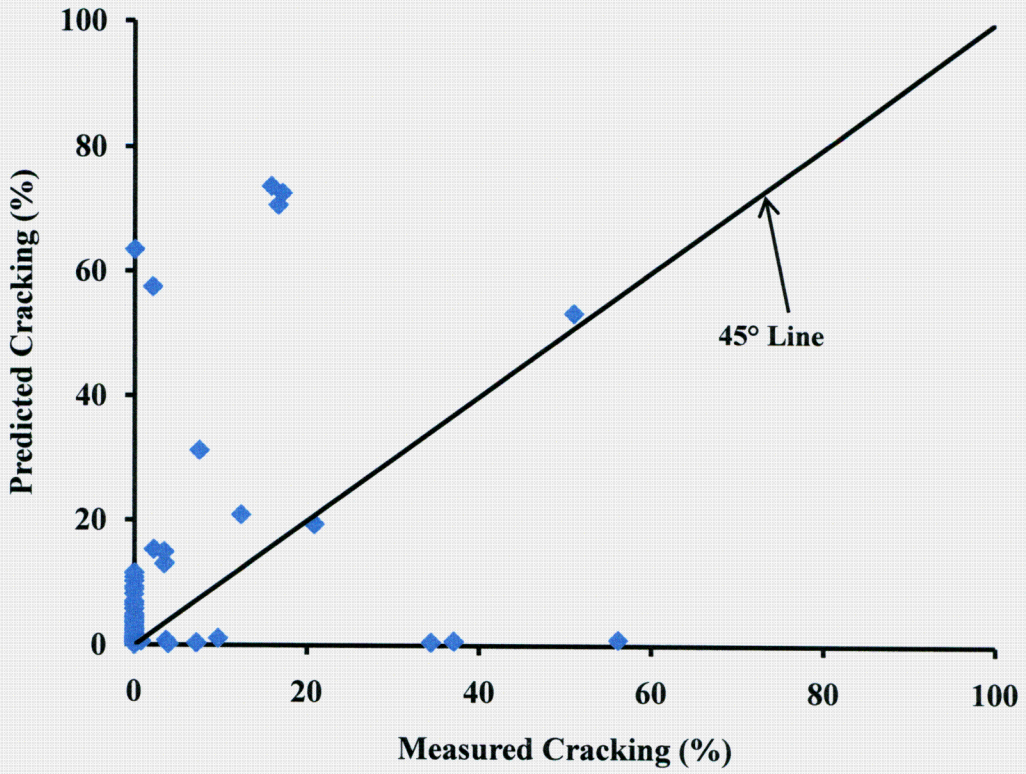

Figure 5.9 Comparison of predicted and measured cracking

Only 9 data points out of total of 120 shows a difference of more than 15% between measured and predicted cracking while 15 sections show a difference of more than 10% and 29 sections show more than 5% difference. Thus considering the input level of level 2 and 3 with 95 sections (80% of the sections) showing difference between measured and predicted cracking less than 5%, it proved to be satisfactory to take beta value of 0.81, 0.94 and 1.2 as the final values. The next section gives the summary of the work described in this chapter.

5.6 Summary

The above factors focused on the calibration and the validation of the alligator cracking model for the State of New Jersey. The study took into account twenty nine sections out of which nine sections were LTPP sections. The calibration effort focused on calibrating the beta values present in the alligator cracking model as it was these beta values that were used during the national calibration process to calibrate the model. The

initial values were selected based on the literature review which consisted of calibration carried out in other states as well as the Design Guide manual.

Initially, the range of beta values were established which were then reduced until a considerable match was obtained for majority of the sections. The beta value that was selected at the end of the calibration effort were 0.81, 0.94 and 1.2 while the default values were 1, 1 and1. Few of the sections did not show a good match for these particular beta values but showed reasonable match for other set of values. However when those values were tried on other sections it did not yield a good match. The final values were selected based on all the 29 sections. The combination of 0.81, 0.94 and 1.2 yielded better match between the predicted and measured cracking with only 15 data points showing difference more than 10% and 29 section showing difference more than 5%. The next chapter provides the summary of findings, conclusions and recommendations that were established during this research.

Chapter 6 Summary of Findings, Conclusions, and Recommendations

This study calibrated the alligator cracking model in the Design Guide based on twenty nine section spread across the State of New Jersey. Important findings, conclusion and recommendation that came out based on this study are listed below.

6.1 Summary

Summary of major task conducted:

1. The calibration study conducted in other regions calibrated the beta values and the transfer regression constants C_1 and C_2 to calibrate the model for the particular region.
2. Twenty nine sections were evaluated in this study which included nine LTPP sections.
3. The sections where divided into south, central and north regions, based on the subgrade encountered across the State.
4. The level of input data was between level 2 and 3.
5. Input data were verified from multiple sources to confirm the accuracy of the data inputted.
6. Excel sheet to simulate the Design Guide was created to understand the algorithm behind prediction process.
7. For calculating the dynamic modulus for the mix, master curve was plotted at reference temperature of 70°F.
8. Strain was calculated at various interfaces, these interfaces were based on predefined location as stated in Design Guide Manual.
9. The result from this study were compared to other studies are shown in Table 6.1.

Summary of finding:

1. Fatigue cracking is affected by variety of factors which include stiffness of the mix, strain induced due to the incoming load, thickness of the pavement, load coming on the pavement, binder content in the mix, air void present in the mix and the age of the binder.
2. The final beta values selected after analyzing twenty nine section was β_{f1} =0.81, β_{f2} =0.94 and β_{f3}=1.2.

Table 6.1 Comparison with other Studies

States	Values Before calibration					Values After Local Calibration				
	β_{f1}	β_{f2}	β_{f3}	C_1	C_2	β_{f1}	β_{f2}	β_{f3}	C_1	C_2
North Carolina (Muthadi, et al., 2008)	1.0	1.0	1.0	1.0	1.0	1.0	1.0	1.0	0.4371	0.150594
Wisconsin (Kang, et al., 2007)	1.0	1.0	1.0	1.0	1.0	1.0	1.2	1.5	1.0	1.0
Wisconsin (Mallela, et al., 2008)	1.0	1.0	1.0	1.0	1.0	1.0	1.0	1.0	1.0	1.0
Washington (Li, et al., 2009)	1.0	1.0	1.0	1.0	1.0	0.96	0.97	1.03	1.07	1.0
New Jersey (Our Study)	1.0	1.0	1.0	1.0	1.0	0.81	0.94	1.2	1	1

6.2 Conclusions

The model for predicting alligator cracking in the Design Guide did not predict any cracking when it was compared to measured data showing considerable cracking for default beta values (Siraj, 2008). In this study the model was calibrated to predict

alligator cracking closer to measured data for the state of New Jersey based on twenty nine sections across the state for level 2 and 3 input. A total of 120 data points were present for the twenty nine section evaluated in this study. When average predicted cracking was compared to average measured cracking a reasonable approach was found to exist between the two. The final beta values selected after the analyzing the twenty nine sections were β_{f1} =0.81, β_{f2} =0.94 and β_{f3}=1.2. 76% of measured and predicted values had a difference of less than 5%.

6.3 Recommendations

The recommendations of the study are as follows:

1. Input values used for calibration should be verified from multiple sources. If significant differences are present for same input value then the discrepancy in the data is to be sorted out before using for calibration process
2. Proper factors should be established to convert the measured distresses into Design Guide format for non LTPP sections.
3. Thorough literature review should be conducted before starting the calibration process to find out which constants or coefficients should be calibrated to achieve the closest match between measured and predicted distress.
4. Location of critical strain along with its value if obtained as an output in the Design Guide would help enormously in understanding the algorithm behind fatigue cracking prediction.
5. Detail information with respect to the master curve for the bituminous concrete layer should be provided as an output. This would help in assessing the change of stiffness on distress prediction and will also help in calculation of distress if strain is also provided as an output.
6. The measured and predicted cracking should be compared at regular interval to determine the difference between the two to establish the efficiency of the calibrated beta values.
7. More sections should be included in the calibration process to ensure that the calibrated values are applicable to the whole state.

Bibliography

Aguiar-Moya, J., Banerjee, A., & Prozzi, J. (2009). Sensitivity Analysis of the M-E PDG Using Measured Probability Distributions of Pavement Layer Thickness. *2009 Annual Meeting Transportation Research Board.* Washington DC.

Baladi, G. (1987). Fatigue Life and Permanent Deformation Characteristics of Asphalt Concrete Mixes. *Transportation Research Record 1227* (Washington DC).

Bennert, T. M. (2000). *Resilient Modulus Properties of New Jersey Subgrade Soils. Report No. FHWA 2000-01.* Washington DC: FHWA.

Bennert, T., & Maher, A. (2005). *The Development of a performance Specification for Granualar base and subbase material. Report No. FHWA-NJ-2205-003.* FHWA.

FHWA. (2003). *Distress-Indentification Manual for Long Term Pavement PErformance program (Fourth Revised Edition), Publication No. FHWA-RD-03-031.* Washington DC: Federal Highway Administration.

Finn, F. N., Nair, K., & Hilliard, C. (1973). *Minimizing Premature Cracking of Asphalt Concrete Pavements. NCHRP report 195.* Washington DC: National Cooperative Highway Research Program. National Research Council.

Finn, F. N., Saraf, C. L., Kulkarni, R., Nair, K., Smith, W., & Abduallah, A. (1986). *Development of Pavement Structural Subsystems. NCHRP Report 291.* Washington DC: National Cooperative Highway Research Program. Transportation Research Board. National Research Council.

Google. (2009). *Google Earth*, 5.0. (Google) Retrieved April 7, 2009, from Google Earth: http://earth.google.com/

Huang, Y. (2004). *Pavement Analysis and Design.* Englewood, New Jersey: Prentice Hall.

Jha, V., Mehta, Y., Saridaki, E., & O'Brien, K. (2008). *Evaluation of Pavement Cracking Performance for The State of Rhode Island Based on Critical Strain Value.*

Kang, M., & Adams, T. M. (2007). Local Calibration for Fatigue Cracking Models Used in the Mechanistic-Empirical Pavement Design Guide. *Proceedings of the 2007 Mid-Continent Transportation Research Symposium.* Ames, Iowa.

Li, J., Pierce, L., & Uhlmeyer, J. (2009). Calibration of the Flexible Pavement Portion of the Mechanistic-Empirical Pavement Design Guide for the Washington State Department of Transportation. Washington D.C.: 88th Annual Meeting Transportation Research Board.

LTPP. (2008, January). *LTPP DataPave Online*, 22. Retrieved April 7, 2009, from http://www.ltppproducts.com/DataPave/visualization/DetailedReport.asp?STATE_CODE=34-1030-G-1

Mallela, J., Titus-Glover, L., Von Qunitus, H., Darter, M. I., & Bahia, H. (2008). *Implementation of mechanistic-empirical pavement design guide in Wisconsin.* Wisconsin Department of Transportation.

Maupin, G. J., & Freeman, J. J. (1976). *Sample Procedure for fatigue Characterization of Bituminous Concrete. Report No. FHWA-RD-76-102.* Washington DC: Federal Highway Administration.

Muthadi, N., & Kim, Y. (2008). LOCAL CALIBRATION OF THE MEPDG FOR FLEXIBLE PAVEMENT DESIGN. *2008 TRB Annual Meeting Transportation Research Board.*

NCHRP. (2004). *2002 Design Guide: Design of New and Rehabilitated Pavement Structures.Draft Final Report NCHRP Study 1-37A.* Washington DC: National Cooperative Highway Research Program and Applied Research Associates Inc.

NCHRP. (2004). *Guide for Mechanistic-Empirical Design of New & Rehabilitated Pavement Structures. Appendix RR Finite Element Procedure for Flexible Pavement Analysis.* Washington D.C: NCHRP.

NCHRP. (2004). *Guide for Mechanistic-Empirical Design of New and Rehabilitated Pavement Structures, Appendix II-2.* National Cooperative Highway Research Program and Applied Research Associates Inc.

NCHRP. (2007). *Local Calibration Guidance for the Recommended Guide for Mechanistic-Empirical Design of New and Rehabilitated Pavement Structures.* Round Rock, TX: National Cooperative Highway Research Program and Applied Research Associates Inc.

NCHRP. (2004). *Part 2 Chapter 2 Material Characterization.* National Cooperative Highway Research Program and Applied Research Associates Inc.

NJDOT. (2007). *New Jersey Department of Transportation, 2007.Standards Specifications: Road and Bridge Construction.* Retrieved 3 19, 2009, from http://www.state.nj.us/transportation/eng/specs/2007/Division.shtml.

NJDOT. (2009). *NJDOT* . Retrieved 3 19, 2009, from http://www.state.nj.us/transportation/about/directory/centralregion.shtm

NJDOT. (2009, March 19). *NJDOT W.I.M database*. Retrieved April 07, 2009, from http://www.state.nj.us/transportation/refdata/roadway/truckwt.shtm

Powell, W. D., Potter, J. F., Mayhew, H. C., & Nunn, M. E. (1984). *The Structural Design of Bituminous Pavements. TRRL Laboratory Report 1132.* United Kingdom: Transportation and Research Research Laboratory.

Rauhut, J. B., Lytton, R. L., & Darter, M. I. (1984a). *Pavement Damage Functions for Cost Allocation Vol.1. Report No. FHWA/RD-84/018.* Washington DC: Fedral Highway Administration.

Rauhut, J. B., Lytton, R. L., & Darter, M. I. (1984b). *Pavement Damage Functions for Cost Allocation Vol.2-Description of Detailed Studies. Report No. FHWA/RD-84/019.* Washington DC: Federal Highway Administration.

Santucci, L. (1998). *The Role of Compaction in the Fatigue Resistance.*

Shell. (1978). *Shell Pavement Design Manual- Asphalt Pavements and Overlays for Road Traffic.* London, England. United Kingdom: Shell International Petroleum.

Siraj, N. (2008). *Verification of Asphalt Concrete Performance Prediction Using Level 2 and Level 3 Inputs of Mechanistic-Empirical design Guide for Flexible Pavements of The State of New Jersey.*

Thompson, M. R. (1987). ILLI-PAVE Based Full-Depth Asphalt Concrete Pavement Design Procedure . *6th International Conference on Structural Design of Asphalt Pavements, 6th.* University of Michigan. Ann Arbor, MI.

Von Quintus, H. L., Scherocman, J. A., Hughes, C. S., & Kennedy, T. W. (1991). *Asphalt-Aggregate Mixture Analysis System (AAMAS). NCHRP Project No. 338.* Washington DC: National Cooperative Highway Research Program. Transportation Research Board. National Research Council.

Von Quintus, H., & Moulthrop, J. (2007). *Mechanistic-Empirical Pavement Design Guide Flexible Pavement Performance Prediction Models Volume II Reference Manual.* Montana Department of Transportation.

Von Quintus, H., Dater, M., & Mallela, J. (2009). *NCHRP 1-40B Local Claibration guidance for the Recommended Guide for Mechanistic Empirical Design of New and Rehabilitated Pavement Sturctures.* Washington D.C and Round Rock: National Cooperative Highway Research Program and Applied Research Associates INC.

VonQuintus, H., & Moulthrop, J. (2007). *Mechanistic-Empirical Pavement Design Pavement Performance Prediction Models For Montana: Volume III Field Guide.* Montana Department of Transportation.

Walubita, L., Martin, A., Jung, S., Glover, C., Park, E., Chowdhury, A., et al. (2005). *Comparison of Fatigue Analysis Approaches for Two Hot Mix Asphalt Concrete (HMAC) Mixtures.* Techincal Report.

Wang, H., & Al-Qadi, I. (2008). Full-depth Flexible Pavement Fatigue Response under Various Tire and Axle Load Configurations. *88th Transportation Research Board Annual meeting.*

WSDOT. (2009, 03 02). *Washington Department of Transportation mix design methods.* Retrieved 03 02, 2009, from Washington Department of Transportation mix design methods: http://training.ce.washington.edu/wsdot/Modules/05_mix_design/05-2_body.htm

Appendix A

Calculation of Dynamic Modulus

Table A 1 Calculation of Dynamic modulus for LTPP section 1003 at 10°F

Temperature	frequency	time(tr)	$P_{3/4}$	$P_{3/8}$	P_4	P_{200}	V_b	V_a	A	VTS	Viscosity
°F	Hz	Sec	%	%	%	%	%	%			Poise (10^6)
10	0.1	10	0	2	31	7	11.6	5	10.77	-3.602	1.1
	0.5	2	0	2	31	7	11.6	5	10.77	-3.602	1.1
	1	1	0	2	31	7	11.6	5	10.77	-3.602	1.1
	5	0.2	0	2	31	7	11.6	5	10.77	-3.602	1.1
	10	0.1	0	2	31	7	11.6	5	10.77	-3.602	1.1
	25	0.04	0	2	31	7	11.6	5	10.77	-3.602	1.1

δ	α	β	γ	C	Log t_r	t	Log `E*	E*
						(10^{-8})		psi (10^6)
2.9	3.8	-1.0	0.3	1.3	-5.2	625	6.5	3.2
2.9	3.8	-1.0	0.3	1.3	-5.9	125	6.5	3.5
2.9	3.8	-1.0	0.3	1.3	-6.2	62.5	6.5	3.6
2.9	3.8	-1.0	0.3	1.3	-6.9	12.5	6.6	3.9
2.9	3.8	-1.0	0.3	1.3	-7.2	6.25	6.6	4.1
2.9	3.8	-1.0	0.3	1.3	-7.6	2.50	6.6	4.2

Table A 2 Calculation of Dynamic modulus for LTPP section 1003 at 40°F

Temperature	frequency	time(tr)	$P_{3/4}$	$P_{3/8}$	P_4	P_{200}	V_b	V_a	A	VTS	Viscosity
°F	Hz	Sec	%	%	%	%	%	%			Poise (10^3)
40	0.1	10	0	2	31	7	11.6	5	10.77	-3.602	1.77
	0.5	2	0	2	31	7	11.6	5	10.77	-3.602	1.77
	1	1	0	2	31	7	11.6	5	10.77	-3.602	1.77
	5	0.2	0	2	31	7	11.6	5	10.77	-3.602	1.77
	10	0.1	0	2	31	7	11.6	5	10.77	-3.602	1.77
	25	0.04	0	2	31	7	11.6	5	10.77	-3.602	1.77

δ	α	β	γ	C	Log t_r	T	Log `E*	E*
						(10^{-4})		psi (10^6)
2.9	3.8	-1.0	0.3	1.3	-1.7	211	6.1	1.2
2.9	3.8	-1.0	0.3	1.3	-2.4	42.2	6.2	1.5
2.9	3.8	-1.0	0.3	1.3	-2.7	21.1	6.2	1.7
2.9	3.8	-1.0	0.3	1.3	-3.4	4.2	6.3	2.1
2.9	3.8	-1.0	0.3	1.3	-3.7	2.1	6.4	2.3
2.9	3.8	-1.0	0.3	1.3	-4.1	0.8	6.4	2.5

Table A 3 Calculation of Dynamic modulus for LTPP section 1003 at 100°F

Temperature	frequency	time(tr)	$P_{3/4}$	$P_{3/8}$	P_4	P_{200}	V_b	V_a	A	VTS	Viscosity
°F	Hz	Sec	%	%	%	%	%	%			Poise (10^{-1})
100	0.1	10	0	2	31	7	11.6	5	10.77	-3.602	3
	0.5	2	0	2	31	7	11.6	5	10.77	-3.602	3
	1	1	0	2	31	7	11.6	5	10.77	-3.602	3
	5	0.2	0	2	31	7	11.6	5	10.77	-3.602	3
	10	0.1	0	2	31	7	11.6	5	10.77	-3.602	3
	25	0.04	0	2	31	7	11.6	5	10.77	-3.602	3

δ	α	β	γ	C	Log t_r	t	Log `E*	E*
						(10^2)		psi (10^4)
2.9	3.8	-1.0	0.3	1.3	3.1	11	4.9	8.3
2.9	3.8	-1.0	0.3	1.3	2.4	2.3	5.1	13
2.9	3.8	-1.0	0.3	1.3	2.1	1.1	5.2	16
2.9	3.8	-1.0	0.3	1.3	1.4	0.2	5.4	26
2.9	3.8	-1.0	0.3	1.3	1.1	0.1	5.5	31
2.9	3.8	-1.0	0.3	1.3	0.7	0.04	5.6	39

Table A 4 Calculation of Dynamic modulus for LTPP section 1003 at 130°F

Temperature	frequency	time(tr)	$P_{3/4}$	$P_{3/8}$	P_4	P_{200}	V_b	V_a	A	VTS	Viscosity
°F	Hz	Sec	%	%	%	%	%	%			Poise (10^{-2})
130	0.1	10	0	2	31	7	11.6	5	10.77	-3.602	1.6
	0.5	2	0	2	31	7	11.6	5	10.77	-3.602	1.6
	1	1	0	2	31	7	11.6	5	10.77	-3.602	1.6
	5	0.2	0	2	31	7	11.6	5	10.77	-3.602	1.6
	10	0.1	0	2	31	7	11.6	5	10.77	-3.602	1.6
	25	0.04	0	2	31	7	11.6	5	10.77	-3.602	1.6

δ	α	β	γ	C	Log t_r	t	Log `E*	E*
						(10^2)		psi (10^4)
2.9	3.8	-1.0	0.3	1.3	4.7	470	4.4	2.8
2.9	3.8	-1.0	0.3	1.3	4.0	94	4.6	4.4
2.9	3.8	-1.0	0.3	1.3	3.7	47	4.7	5.4
2.9	3.8	-1.0	0.3	1.3	3.0	9.4	4.9	8.8
2.9	3.8	-1.0	0.3	1.3	2.7	4.7	5.0	11
2.9	3.8	-1.0	0.3	1.3	2.3	1.9	5.1	14

Appendix B

Comparison of Beta Values

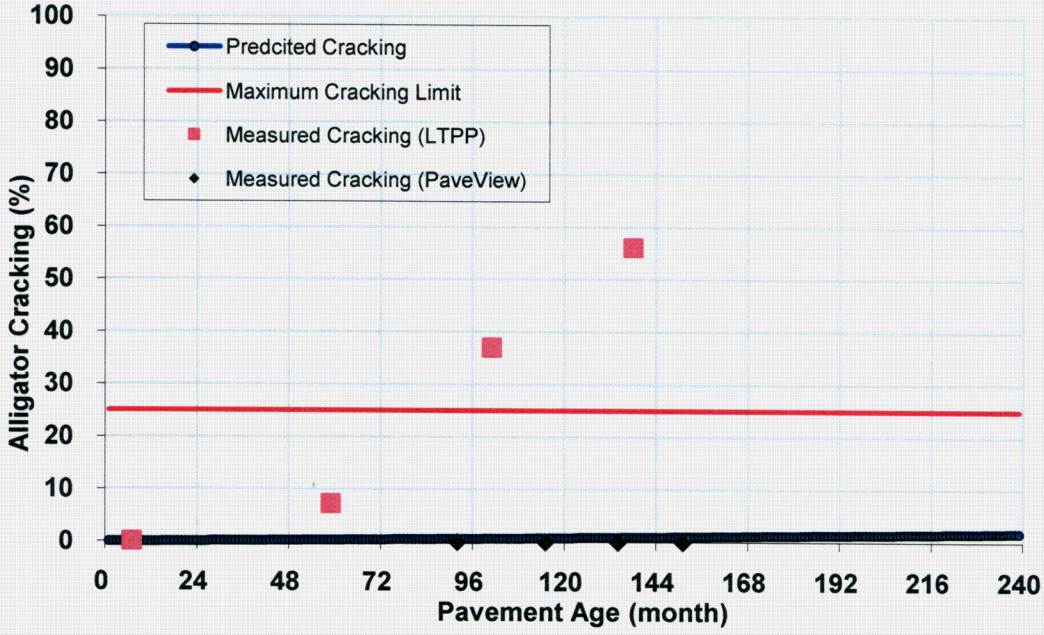

Figure B 1 Comparison for Route I-195 E (LTPP section 1011) for beta value 0.81, 0.94 and 1.2.

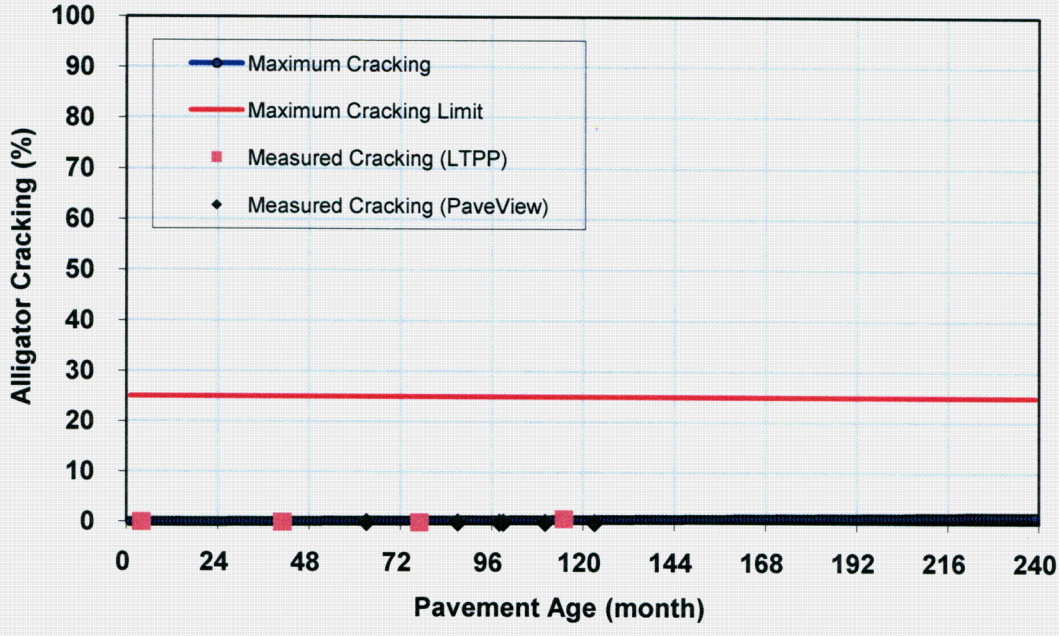

Figure B 2 Comparison for Route 55 N (LTPP section 1031) for beta value 0.81, 0.94 and 1.2.

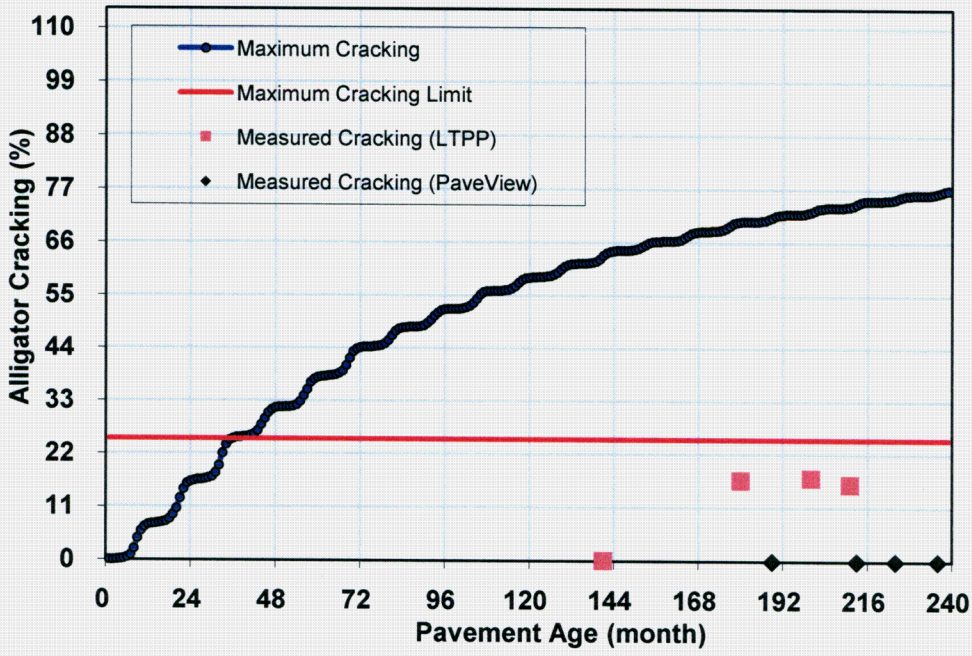

Figure B 3 Comparison for Route 55 N (LTPP section 1638) for beta value 0.81, 0.94 and 1.2.

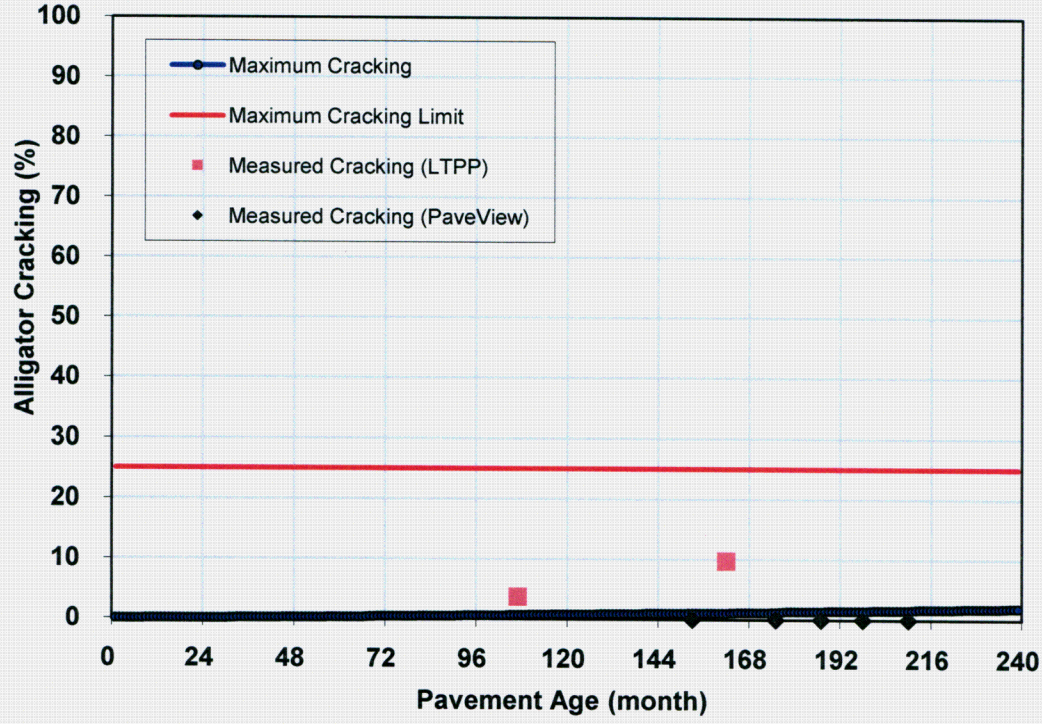

Figure B 4 Comparison for Route 95 S (LTPP section 6057) for beta value 0.81, 0.94 and 1.2.

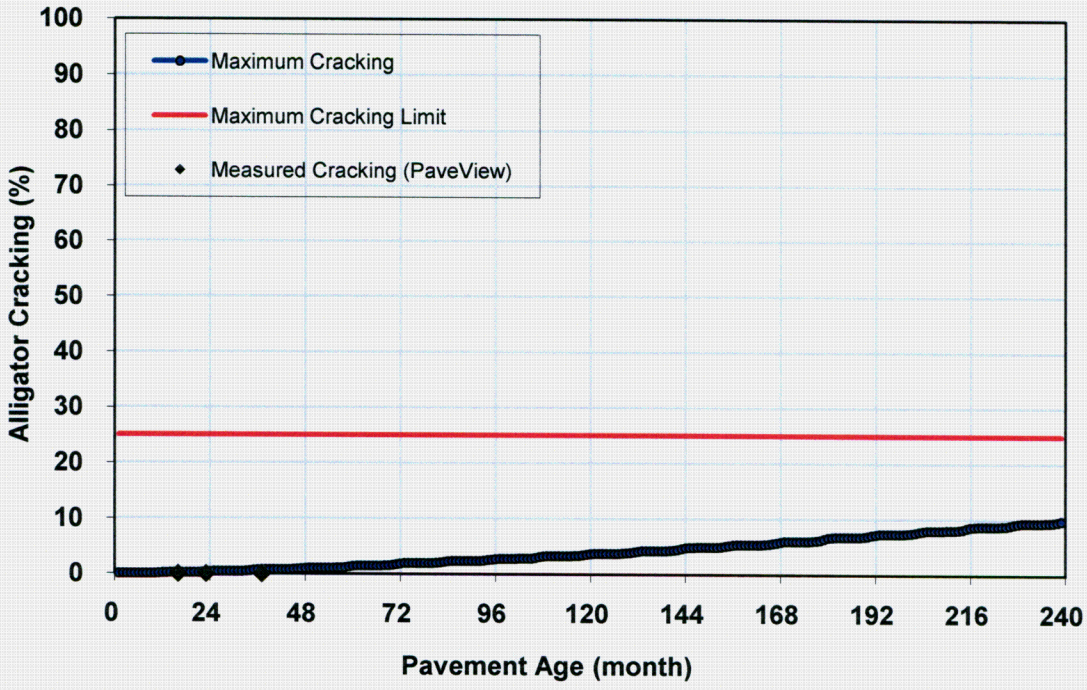

Figure B 5 Comparison for Route 35 for beta value 0.81, 0.94 and 1.2.

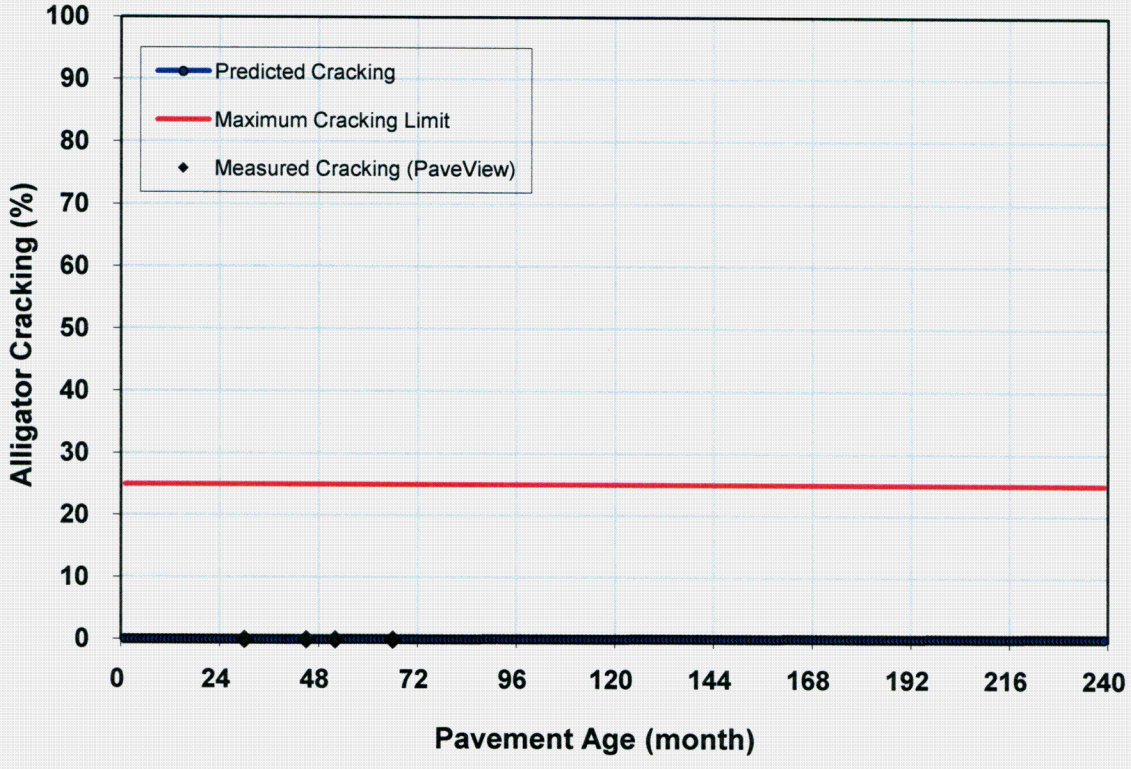

Figure B 6 Comparison for Route 40 for beta value 0.81, 0.94 and 1.2.

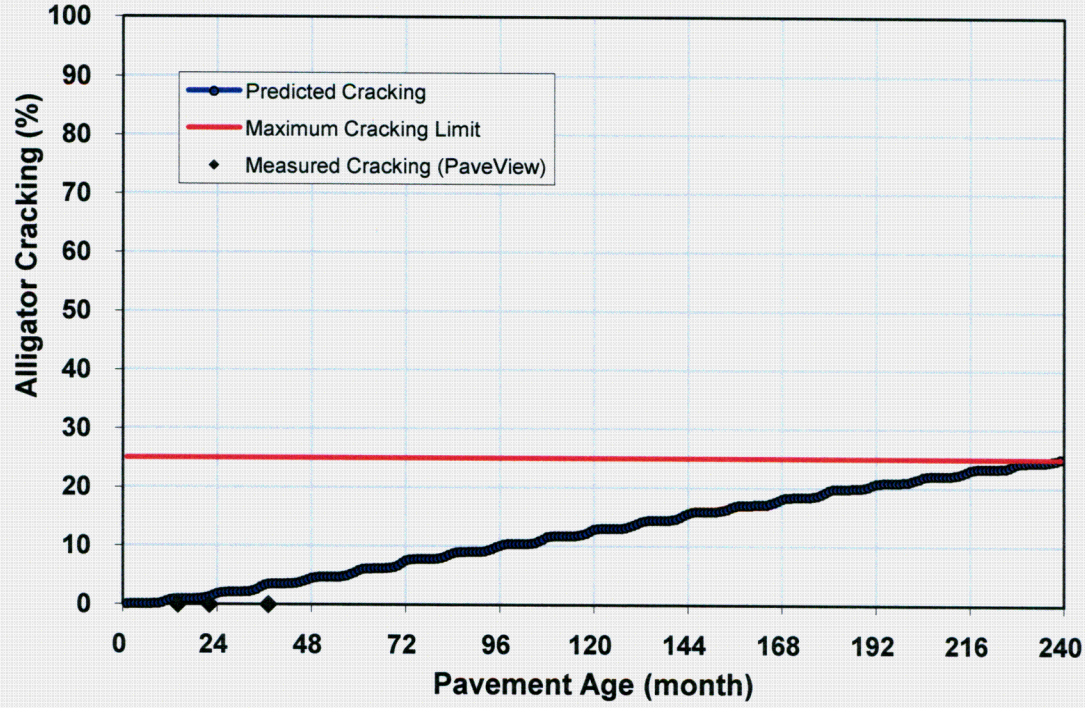

Figure B 7 Comparison for Route 70 (M.P 12-12.6) for beta value 0.81, 0.94 and 1.2.

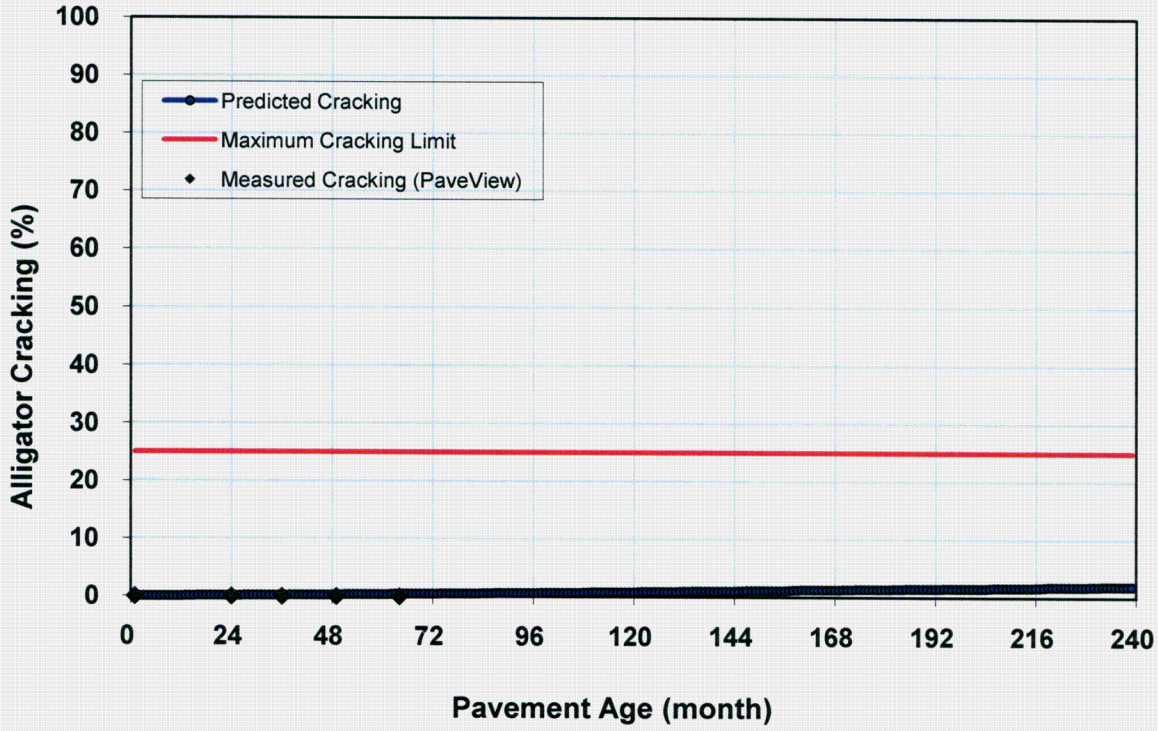

Figure B 8 Comparison for Route 70 (M.P:55.71-58.09) for beta value 0.81, 0.94 and 1.2.

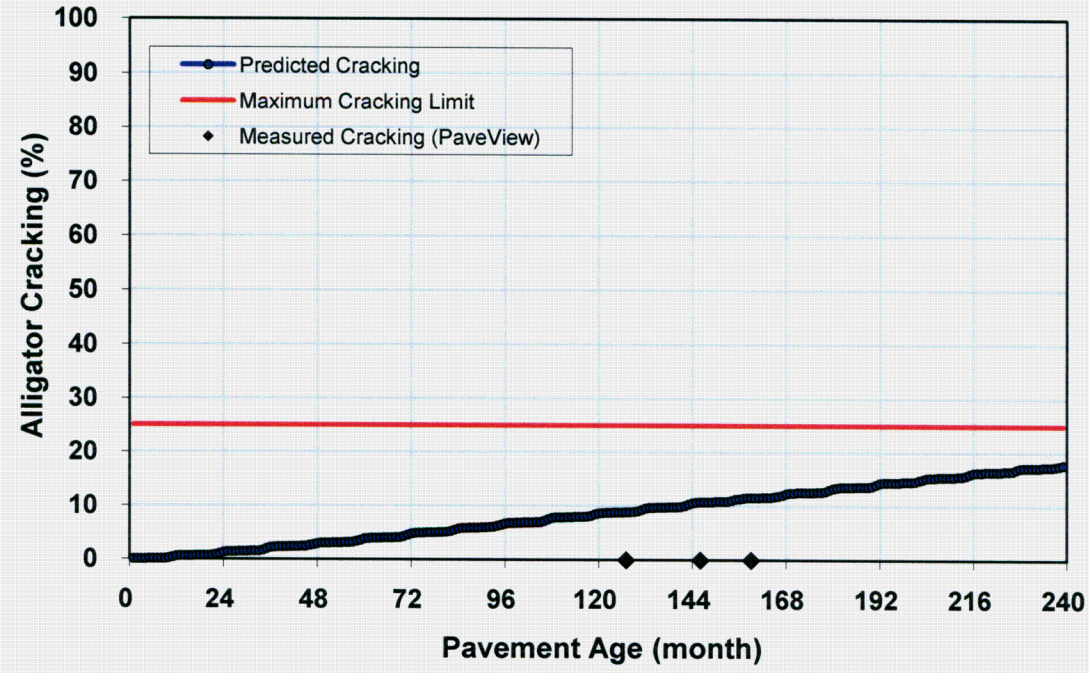

Figure B 9 Comparison for Route 139 L for beta value 0.81, 0.94 and 1.2.

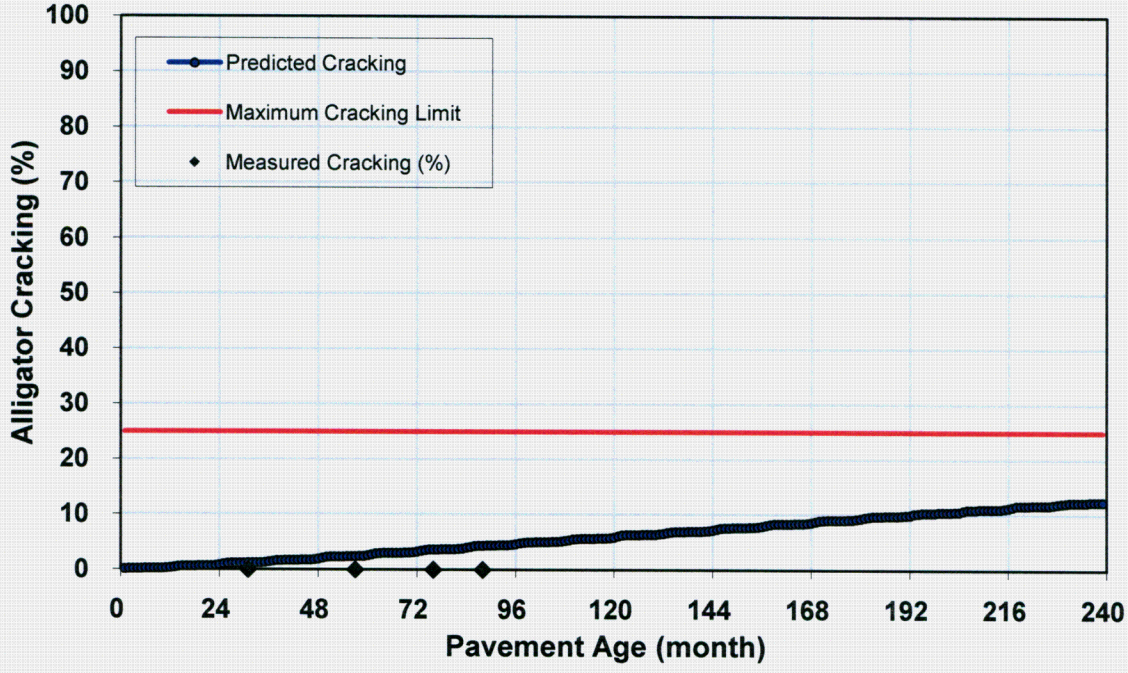

Figure B 10 Comparison for Route 124 for beta value 0.81, 0.94 and 1.2.

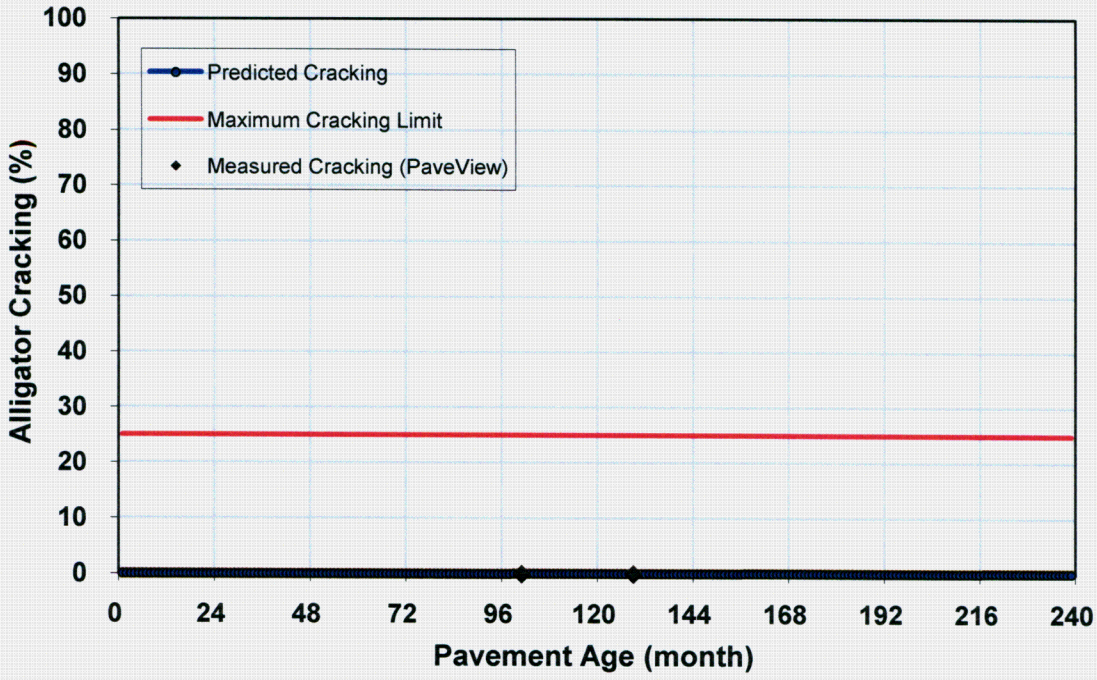

Figure B 11 Comparison for Route 94 for beta value 0.81, 0.94 and 1.2.

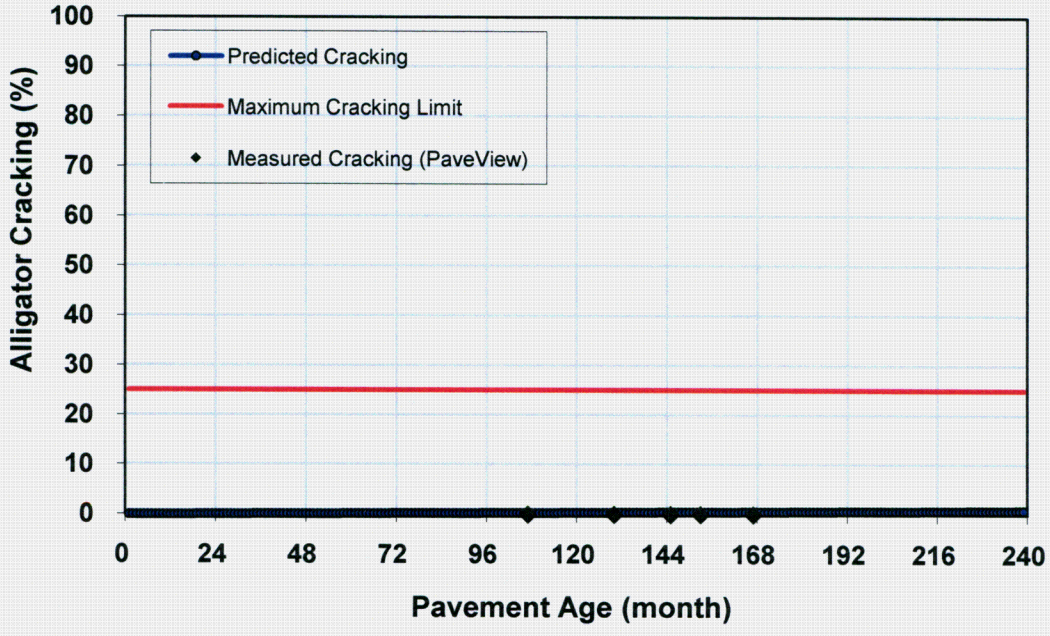

Figure B 12 Comparison for Route 322 (M.P 37-37.2) for beta value 0.81, 0.94 and 1.2.

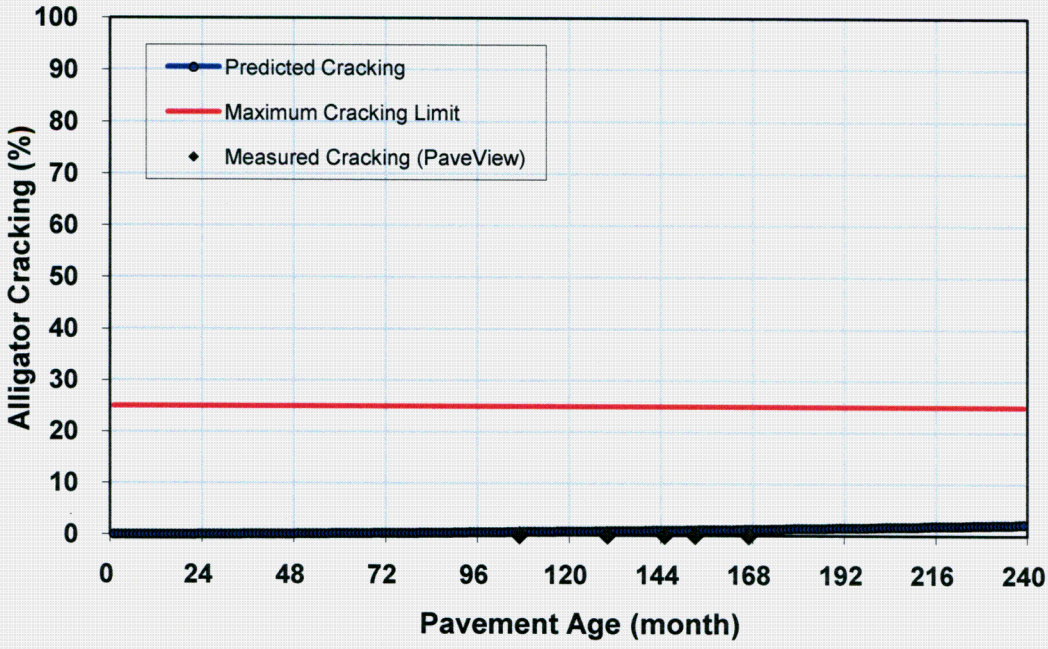

Figure B 13 Comparison for Route 322 (M.P 37.2-41) for beta value 0.81, 0.94 and 1.2.

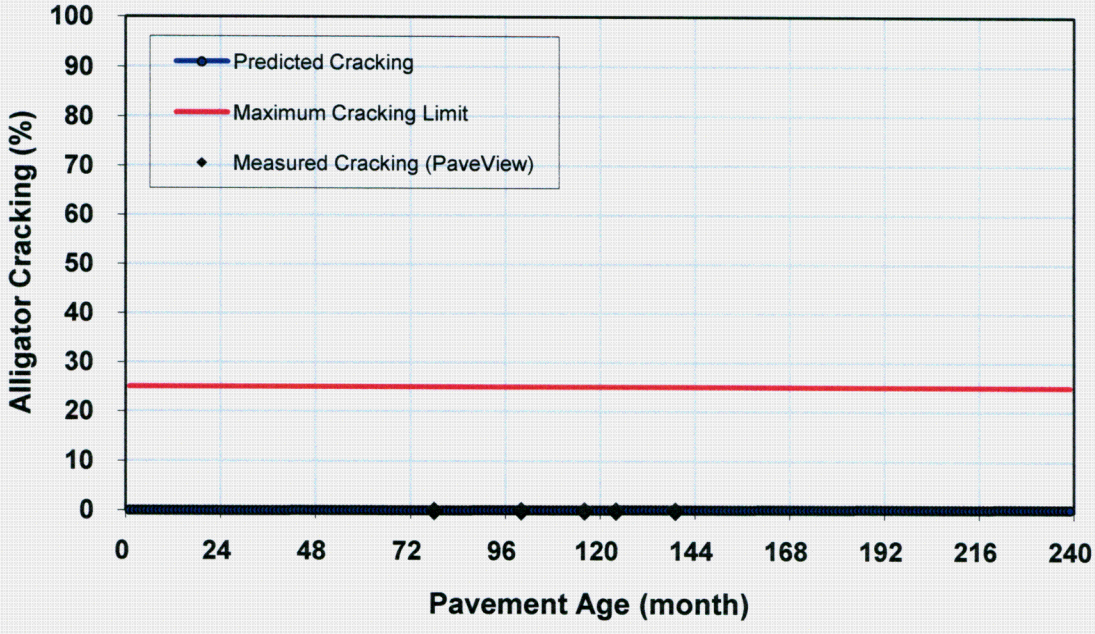

Figure B 14 Comparison for Route 9 for beta value 0.81, 0.94 and 1.2.

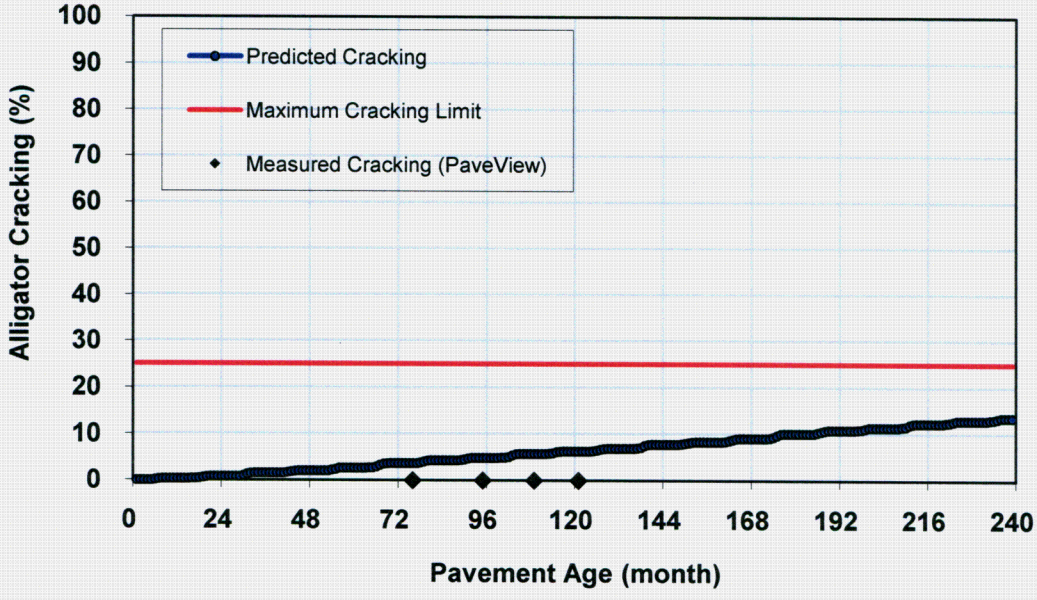

Figure B 15 Comparison for Route 31 (M.P 8-10) for beta value 0.81, 0.94 and 1.2.

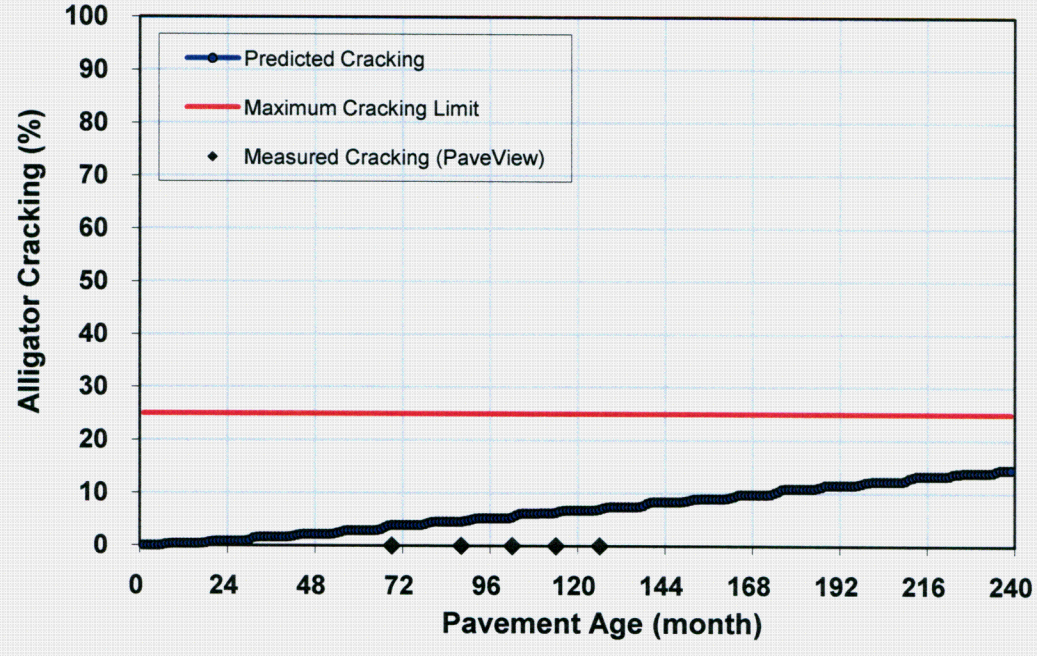

Figure B 16 Comparison for Route 31 (M.P 4-6) for beta value 0.81, 0.94 and 1.2.

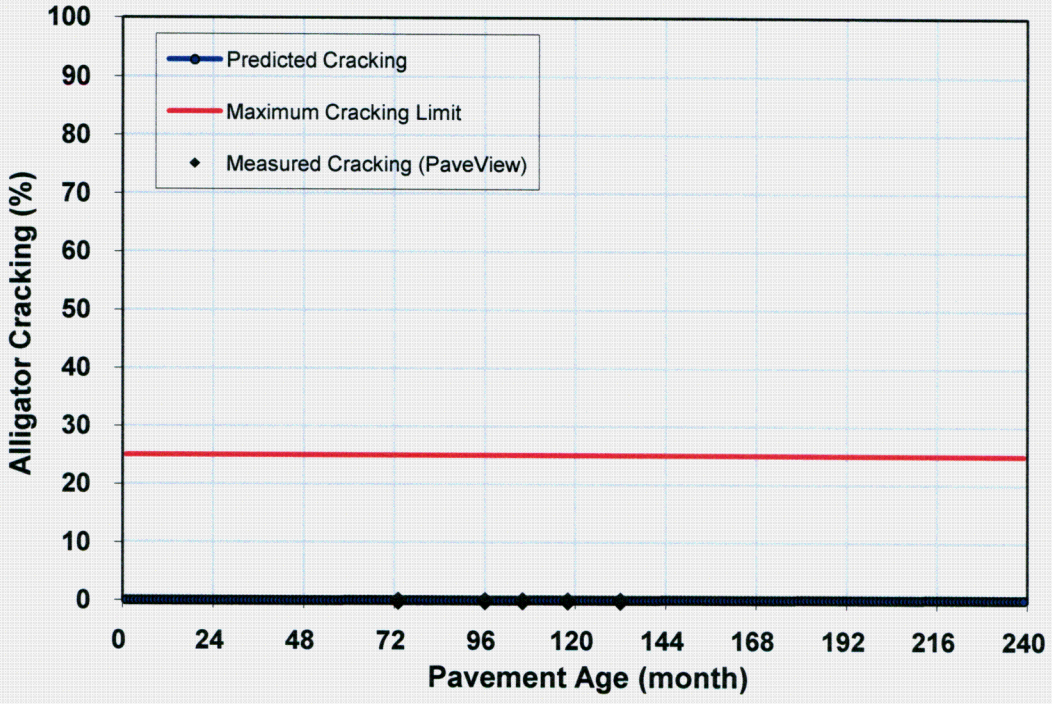

Figure B 17 Comparison for Route 49 for beta value 0.81, 0.94 and 1.2.

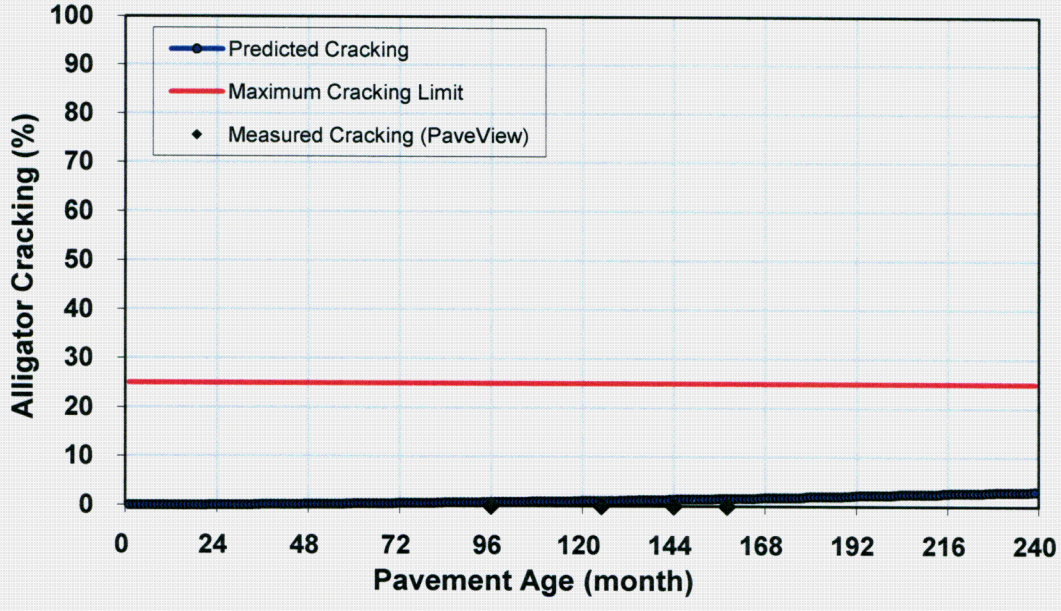

Figure B 18 Comparison for Route 64 for beta value 0.81, 0.94 and 1.2.

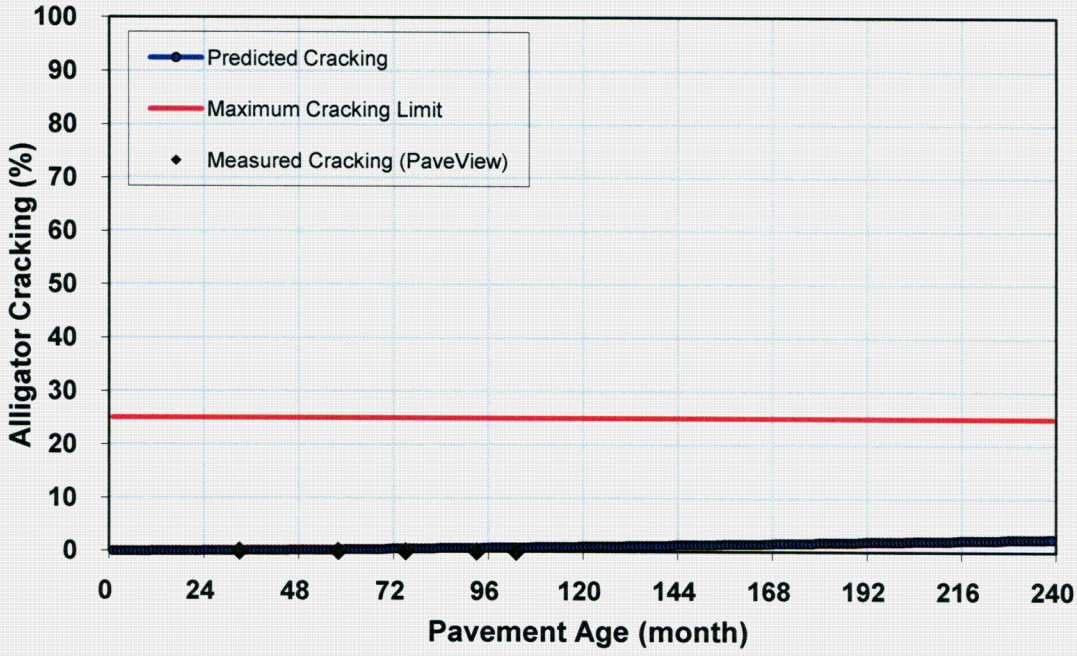

Figure B 19 Comparison for Route 29 NB (M.P 17-17.8) for beta value 0.81, 0.94 and 1.2.

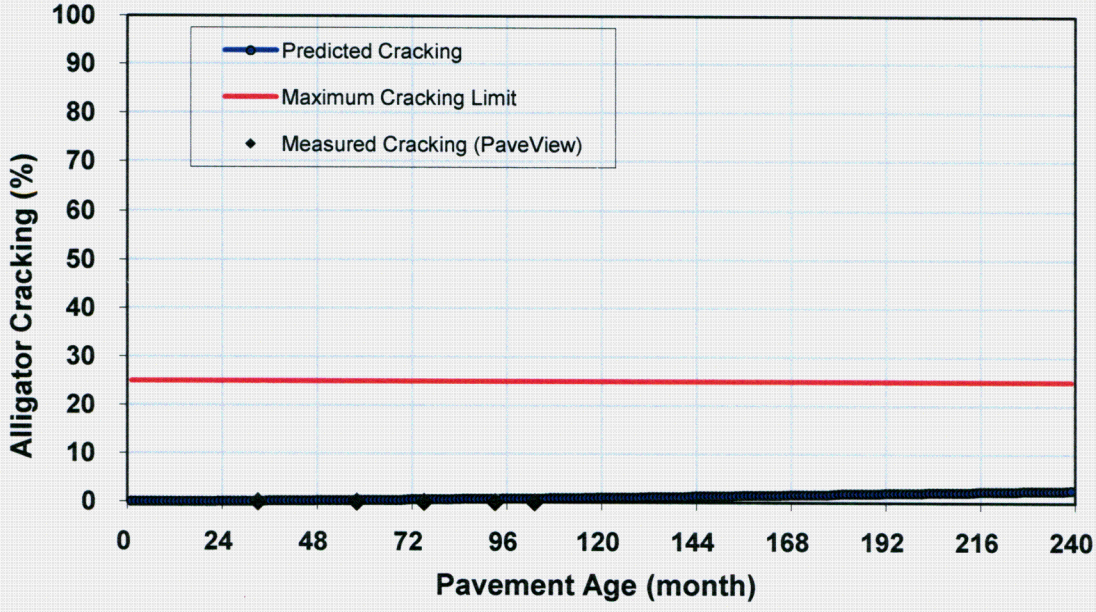

Figure B 20 Comparison for Route 29 NB (M.P 17.8-18.11) for beta value 0.81, 0.94 and 1.2.

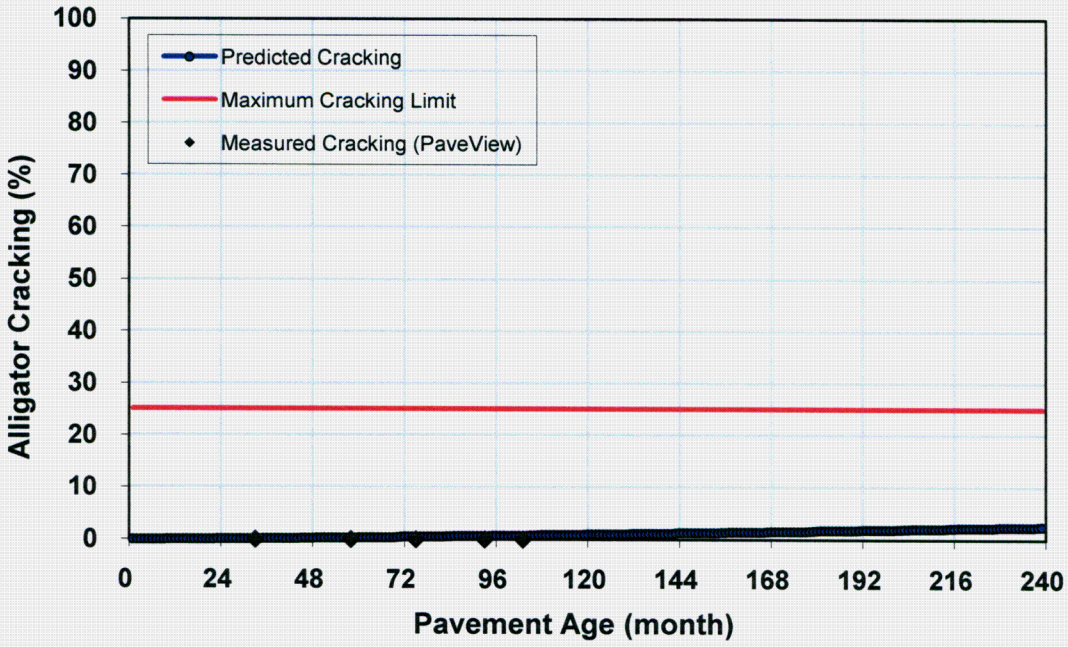

Figure B 21 Comparison for Route 29 SB (MP 17-17.8) for beta value 0.81, 0.94 and 1.2.

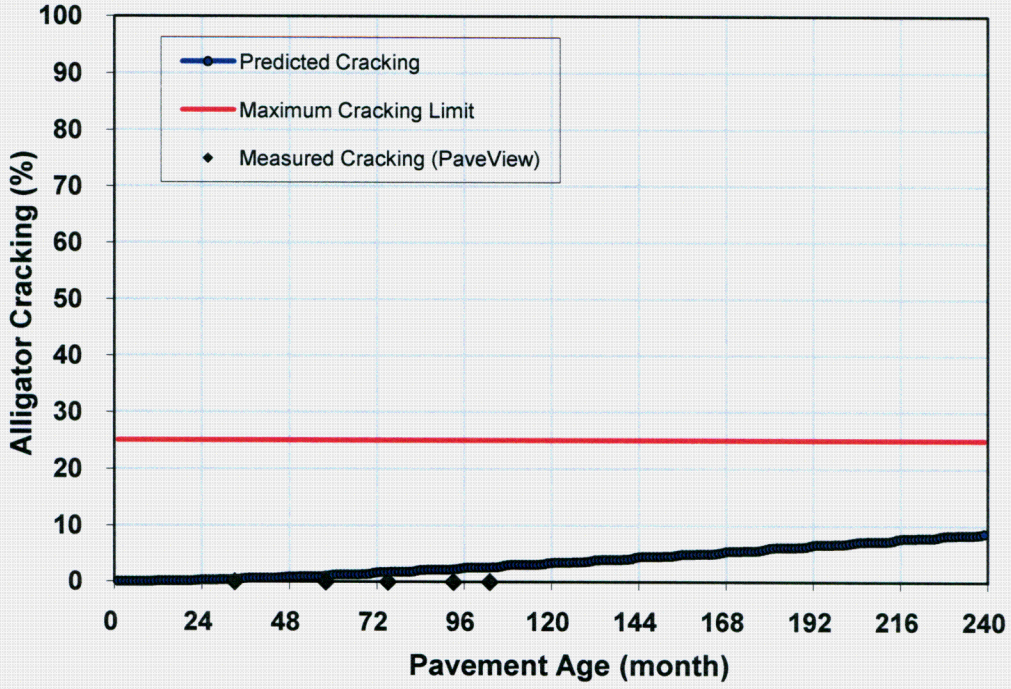

Figure B 22 Comparison for Route 29 SB (M.P 17.8-18.11) for beta value 0.81, 0.94 and 1.2.